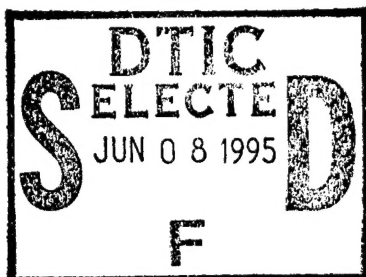


NAVAL POSTGRADUATE SCHOOL MONTEREY, CALIFORNIA



THESIS

**CORRELATION OF BULLET DISPERSION AND
TRANSVERSE BARREL TIP DISPLACEMENT
ON A FIRING PHALANX GUN SYSTEM**

by

David Cela
December, 1994

Thesis Advisor
Second Reader:

Steven R. Baker
David D. Cleary

Approved for public release; distribution is unlimited.

DTIC QUALITY INSPECTED 3

19950606 035

REPORT DOCUMENTATION PAGE

Form Approved OMB No. 0704-0188

Public reporting burden for this collection of information is estimated to average 1 hour per response, including the time for reviewing instruction, searching existing data sources, gathering and maintaining the data needed, and completing and reviewing the collection of information. Send comments regarding this burden estimate or any other aspect of this collection of information, including suggestions for reducing this burden, to Washington Headquarters Services, Directorate for Information Operations and Reports, 1215 Jefferson Davis Highway, Suite 1204, Arlington, VA 22202-4302, and to the Office of Management and Budget, Paperwork Reduction Project (0704-0188) Washington DC 20503.

1. AGENCY USE ONLY (Leave blank)	2. REPORT DATE December 1994	3. REPORT TYPE AND DATES COVERED Master's Thesis	
4. TITLE AND SUBTITLE CORRELATION OF BULLET DISPERSION AND TRANSVERSE BARREL TIP DISPLACEMENT ON A FIRING PHALANX GUN SYSTEM		5. FUNDING NUMBERS	
6. AUTHOR(S) David Cela			
7. PERFORMING ORGANIZATION NAME(S) AND ADDRESS(ES) Naval Postgraduate School Monterey CA 93943-5000		8. PERFORMING ORGANIZATION REPORT NUMBER	
9. SPONSORING/MONITORING AGENCY NAME(S) AND ADDRESS(ES)		10. SPONSORING/MONITORING AGENCY REPORT NUMBER	
11. SUPPLEMENTARY NOTES The views expressed in this thesis are those of the author and do not reflect the official policy or position of the Department of Defense or the U.S. Government.			
12a. DISTRIBUTION/AVAILABILITY STATEMENT Approved for public release; distribution is unlimited.		12b. DISTRIBUTION CODE	
13. ABSTRACT (maximum 200 words) The PHALANX Close-In Weapons System (CIWS) is a very important part of the anti-ship missile defense structure of the U.S. Navy. The PHALANX gun system currently experiences random and variable bullet dispersion which diminishes its ability to destroy its intended targets. The more that is understood about parameters that control PHALANX gun dispersion performance, the more the Navy can increase its performance and hence, ship survivability. The research described in this thesis is an attempt to correlate measured bullet dispersion with transverse barrel tip displacement data derived from measured barrel tip acceleration data taken on a firing PHALANX gun system. The goal of this project is to relate barrel tip vibration, which can be measured on a gun at any location, to bullet dispersion, which can only be measured on a test range. Acceleration measurements were made on a firing PHALANX gun at the Navy Air Weapons Station, China Lake, CA. From these measurements were derived the vertical and horizontal components of gun barrel tip displacement by direct time integration and by a fourier transform procedure. It was found that the resulting displacement time records were contaminated by a large, spurious, low frequency contribution, the source of which is unknown. It is speculated that it is most likely due to the effect of temperature on the accelerometers. A procedure was developed to remove the low frequency trend from the displacement time records using cubic spline smoothing. The resulting horizontal and vertical barrel tip displacement records were compared to bullet dispersion data gathered during the gun firing. Although there was a good correlation between the time of firing obtained from the dispersion data and the time of maximum vertical displacement, correlation between dispersion data and extracted lateral barrel tip displacement was disappointing. Suggestions are made to improve the procedure for extracting the barrel tip lateral displacement from vibration measurements on a firing gun.			
14. SUBJECT TERMS PHALANX Dispersion Analysis, Barrel Tip Acceleration and Displacement. Gun Movement Dispersion and Displacement Correlation.		15. NUMBER OF PAGES 118	
		16. PRICE CODE	
17. SECURITY CLASSIFI- CATION OF REPORT Unclassified	18. SECURITY CLASSIFI- CATION OF THIS PAGE Unclassified	19. SECURITY CLASSIFICA- TION OF ABSTRACT Unclassified	20. LIMITATION OF ABSTRACT UL

Approved for public release; distribution is unlimited.

**CORRELATION OF BULLET DISPERSION AND TRANSVERSE BARREL
TIP DISPLACEMENT ON A FIRING PHALANX GUN SYSTEM**

by

David Cela
Lieutenant, United States Navy
B.S., United States Naval Academy, 1988

Submitted in partial fulfillment
of the requirements for the degree of

MASTER OF SCIENCE IN PHYSICS

from the

NAVAL POSTGRADUATE SCHOOL

December 1994

Author:

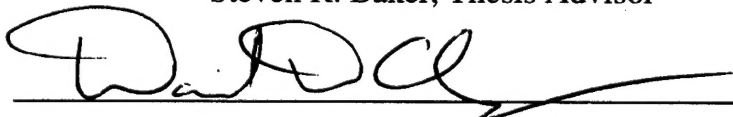


David Cela

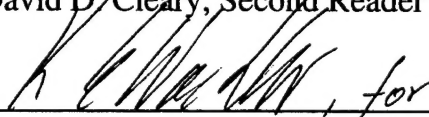
Approved by:



Steven R. Baker, Thesis Advisor



David D. Cleary, Second Reader



William B. Colson, Chairman
Department of Physics

Accession For	
NTIS CRA&I	<input checked="" type="checkbox"/>
DTIC TAB	<input type="checkbox"/>
Unannounced	<input type="checkbox"/>
Justification	
By	
Distribution /	
Availability Codes	
Dist	Avail and/or Special
A-1	

ABSTRACT

The PHALANX Close-In Weapons System (CIWS) is a very important part of the anti-ship missile defense structure of the U.S. Navy. The PHALANX gun system currently experiences random and variable bullet dispersion which diminishes its ability to destroy its intended targets. The more that is understood about parameters that control PHALANX gun dispersion performance, the more the Navy can increase its performance and hence, ship survivability.

The research described in this thesis is an attempt to correlate measured bullet dispersion with transverse barrel tip displacement data derived from measured barrel tip acceleration data taken on a firing PHALANX gun system. The goal of this project is to relate barrel tip vibration, which can be measured on a gun at any location, to bullet dispersion, which can only be measured on a test range.

Acceleration measurements were made on a firing PHALANX gun at the Navy Air Weapons Station, China Lake, CA. From these measurements were derived the vertical and horizontal components of gun barrel tip displacement by direct time integration and by a fourier transform procedure. It was found that the resulting displacement time records were contaminated by a large, spurious, low frequency contribution, the source of which is unknown. It is speculated that it is most likely due to the effect of temperature on the accelerometers. A procedure was developed to remove the low frequency trend from the displacement time records using cubic spline smoothing. The resulting horizontal and vertical barrel tip displacement records were compared to bullet dispersion data gathered

during the gun firing. Although there was a good correlation between the time of firing obtained from the dispersion data and the time of maximum vertical displacement, correlation between dispersion data and extracted lateral barrel tip displacement was disappointing. Suggestions are made to improve the procedure for extracting the barrel tip lateral displacement from vibration measurements on a firing gun.

TABLE OF CONTENTS

I. INTRODUCTION	1
A. PHALANX CLOSE-IN WEAPON SYSTEM	2
1. System Description	2
a. On-Mount Fire Control Assembly	2
b. Gun Assembly	4
c. Mount and Train-Drive Assembly	4
d. Barbette	5
e. Electronics Enclosure	6
f. CIWS MK 149 Round	6
B. MOTIVATION	8
II. DESCRIPTION OF FIELD EXPERIMENTS	9
A. INTRODUCTION	9
1. Equipment setup	9
a. Dynamic Signal Analyzer Model SA 390	11
b. PCB Quartz Shear Mode ICP Accelerometers	11
c. Oehler System 82	13
B. EXPERIMENTAL SETUP FOR 9 MAY 1994	15
C. EXPERIMENTAL SETUP FOR 31 MAY 1994	19
III. DISPERSION DATA ANALYSIS	27
A. DISPERSION DATA	28
1. Firing Rate	28
2. Dispersion	30
IV. ACCELEROMETER DATA ANALYSIS	33
A. DATA CONVERSION	33

B. DATA ANALYSIS	37
1. Determining the Time of the First Round	37
2. Barrel Tip Lateral Displacement from Acceleration	40
a. Displacement from Direct Time Integration	40
b. Displacement from the FFT of the Acceleration	44
c. Comparison of Two Integration Methods	46
d. Removing the Low Frequency Trend	47
(1) Time and Frequency Windowing.	48
(2) Global Polynomial Approximation.	50
(3) Cubic Spline Approximation.	52
C. CORRELATION OF DISPERSION DATA AND BARREL TIP LATERAL DISPLACEMENT	58
V. CONCLUSIONS	63
APPENDIX A. DISPERSION DATA	65
APPENDIX B. CROSS CORRELATION CODE	71
APPENDIX C. GTESTFFT.M	75
APPENDIX D. THRESHOLD.M	81
APPENDIX E. CALIBRATION CERTIFICATES FOR THE QUARTZ SHEAR MODE ICP ACCELEROMETERS USED FOR DATA COLLECTION ON THE PHALANX GUN SYSTEM.	85
APPENDIX F. TIME DOMAIN WINDOW	93

APPENDIX G. FREQUENCY DOMAIN WINDOW	95
APPENDIX H. CUBIC SMOOTHING SPLINES CODE	97
LIST OF REFERENCES	101
INITIAL DISTRIBUTION LIST	103

List Of Figures

Figure 1-1 PHALANX System Components	3
Figure 1-2 Gun Assembly	5
Figure 1-3 PHALANX MK 149 Round	7
Figure 2-1 PHALANX Gun System at China Lake, CA	10
Figure 2-2 Muzzle Restraint Accelerometers	12
Figure 2-3 Mid Housing Accelerometers	12
Figure 2-4 Aft Bearing Accelerometers	13
Figure 2-5 Oehler Frame and Battenboard System at China Lake, CA	14
Figure 2-6 Prototype Muzzle Restraint	15
Figure 2-7 Production Muzzle Restraint	16
Figure 2-8 Firing Signal for the Third Firing 9 May 1994	17
Figure 2-9 Muzzle Restraint Acceleration (Horizontal) for 9 May 1994	18
Figure 2-10 Muzzle Restraint Acceleration (Horizontal) for 31 May 1994	20
Figure 2-11 SA 390 Trace for the Muzzle Restraint Acceleration (Horizontal)	22
Figure 2-12 SA 390 Trace for the Muzzle Restraint Acceleration (Vertical)	22
Figure 2-13 SA 390 Trace for the Mid-House Bearing Acceleration (Horizontal)	23
Figure 2-14 SA 390 Trace for the Mid-House Bearing Acceleration (Vertical)	23
Figure 2-15 SA 390 Trace for the Mid-House Bearing Acceleration (Axial)	24
Figure 2-16 Aft Bearing Acceleration (Horizontal)	24
Figure 2-17 SA 390 Trace for the Aft Bearing Acceleration (Vertical)	25
Figure 2-18 Firing Pin Signal	25
Figure 3-1 Firing Rate for the Second Firing, 31 May 1994	28
Figure 3-2 Firing Rate for the Third Firing, 31 May 1994	29
Figure 3-3 Dispersion Pattern for the Third Firing	31
Figure 4-1 Aft Bearing Acceleration	34
Figure 4-2 Muzzle Restraint Acceleration	35
Figure 4-3 Mid Housing Bearing Acceleration	36
Figure 4-4 Normalized FFT of Muzzle Restraint Acceleration (Horizontal)	37

Figure 4-5 Results of Cross Correlation between acceleration and dispersion	39
Figure 4-6 Muzzle Restraint Acceleration (Horizontal) versus the Best Estimated First Round Time	40
Figure 4-7 Muzzle Restraint Displacement (Horizontal) from Direct Time Integration	42
Figure 4-8 Muzzle Restraint Velocity (Horizontal) from Direct Time Integration	42
Figure 4-9 Detrended Muzzle Restraint Displacement (Horizontal) from Direct Time Integration	43
Figure 4-10 FFT of Muzzle Restraint Displacement (Vertical)	45
Figure 4-11 Muzzle Restraint Displacement (Vertical) from the Inverse FFT	45
Figure 4-12 Comparison of the Two Integration Methods without Detrending	46
Figure 4-13 Comparison of the Two Integration Methods with Detrending.	47
Figure 4-14 Detrended Displacement from 1.216 to 1.413 Seconds	48
Figure 4-15 Window Function	49
Figure 4-16 Time-Windowed Muzzle Restraint Acceleration (Horizontal) From 1.5 to 2 Seconds	49
Figure 4-17 Frequency-Windowed FFT of the Muzzle Restraint Displacement (Horizontal)	50
Figure 4-18 Twelfth Order Polynomial Fit to the Displacement Data	51
Figure 4-19 Barrel Tip Displacement Extracted from Twelfth Order Polynomial Fit to the Displacement Data	51
Figure 4-20 Cubic Spline Smoothing of the Displacement Data	53
Figure 4-21 Zoom of the Cubic Smoothing Approximation. Obtained using CSAPS.m The Smoothing Parameter $p=0.9999999999999418$	54
Figure 4-22 Muzzle Restraint Displacement (Horizontal) Extracted Using Cubic Smoothing of the Displacement Data	54
Figure 4-23 Zoom of the Cubic Smoothing Approximation. Obtained using CSAPS.m. The smoothing parameter $p=0.9999417957207211$	55

Figure 4-24 Muzzle Restraint Displacement (Horizontal) Extracted Using Cubic Smoothing on the Displacement Data	56
Figure 4-25 Muzzle Restraint Displacement (Vertical) Extracted Using Cubic Smoothing on the Displacement Data	56
Figure 4-26 Muzzle Restraint Displacement (Horizontal) From 1.5 to 2 Seconds	57
Figure 4-27 Muzzle Restraint Displacement (Vertical) From 1.5 to 2 Seconds	57
Figure 4-28 Difference Between the Horizontal and Vertical Displacement	58
Figure 4-29 Correlation of Barrel Tip Displacement and Dispersion Data (Vertical) ..	59
Figure 4-30 Correlation of Barrel Tip Displacement and Dispersion (Horizontal)	60
Figure 4-31 Dispersion Correlation (Vertical)	61
Figure 4-32 Dispersion Correlation (Horizontal)	61

List Of Tables

1-1	Characteristics of the PHALANX Gun System	7
2-1	9 May 1994 Accelerometer Set up	13
2-2	9 May Firing runs made with prototype muzzle restraint	18
2-3	9 May Firing runs made with production muzzle restraint	19
2-4	9 May Firing runs made with no muzzle restraint	19
2-5	Firing runs for 31 May 1994 (all using the production muzzle restraint)	21
3-1	Firing Runs for 31 May 1994	30

I. INTRODUCTION

All gun/ammunition systems have a dispersion figure. Dispersion refers to the lateral rms error in putting rounds on a target, usually measured as an angle. If a number of rounds are fired from a weapon against a target there will be dispersion in both the horizontal (X) and vertical (Y) lateral directions. For small caliber weapons, lateral dispersion tends to be small and equal in both directions.¹ It is known that the horizontal and vertical dispersions are normally distributed if the X and Y dispersion figures are equal.² Typically, dispersion is measured in terms of the standard deviation of a Gaussian distribution. It can also be expressed in terms of the radius of a circle which encompasses 80 percent of the rounds in a pattern.

There is a considerable difference in hit-probability between firing a new weapon and one with wear, between firing armour-piercing and high-explosive ammunition, and between firing single-shot and in bursts. When a weapon is fired in bursts, as opposed to single shots, dispersion increases by 50 per cent.³ For the PHALANX gun system the dispersion is quoted to be 1.4 mradians at one sigma. [Ref 1]

Dispersion data for a firing PHALANX gun system were collected at the Naval Air Weapon Station, China Lake, CA. The data were collected in conjunction with accelerometer data. The intent of this research is to correlate bullet dispersion and transverse barrel tip displacement data obtained on a firing PHALANX gun system.

¹ International Defense Review 11/91

² International Defense Review 11/91

³ International Defense Review 11/91

A. PHALANX CLOSE-IN WEAPON SYSTEM

The PHALANX Close-In Weapon System (CIWS) program was initiated in the late 1960's to provide the Navy with close-in autonomous defense against low-altitude Anti-Ship Missiles (ASMs). Low-altitude ASMs were considered the primary threat of the 1970s because they could penetrate the other principal defense systems in the fleet. Since then, there have been significant changes to the ASM threat.

PHALANX was first introduced to the fleet as a Block 0 system. Since then, Block 0 systems have formed the backbone of the Navy's current CIWS defense program. As the program progresses, so does CIWS technology. The PHALANX program has introduced system improvements through upgrades, modifications, and new subsystems supported by an evolving test and integration schedule. Improvements from Block 0 to Block 1 Baseline 2 include pneumatic gun drive to allow higher firing rates with higher reliability, improved search sensitivity through new standing wave planar array search antennas, and the gun muzzle restraint to control gun dispersion. [Ref 2]

1. System Description

The PHALANX gun system is designed as a stand-alone integrated weapon system that encompasses functions usually performed by separate, independent systems. As an integrated package, it carries out search, detection, target declaration, tracking, threat elevation, declaration of engagement, fire control, and target kill assessment. The integrated concept (shown in Figure 1-1) provides the fast reaction time required for the CIWS mission.

PHALANX consists of six major assemblies and components. Five of these are the radar and servo assembly, gun assembly, mount and train drive platform, barrette equipment assembly, and electronics enclosure. The sixth component is made up of the local control panel and the remote control panel.

a. On-Mount Fire Control Assembly

The on-mount fire control assembly performs the following functions: target search, detection and threat declaration, track acquisition, target track and measurement of range, velocity and angle, target prediction, lead angle computation, gun

aiming and firing, projectile detection, measurement of projectile velocity and angle, and gun aim bias correction.

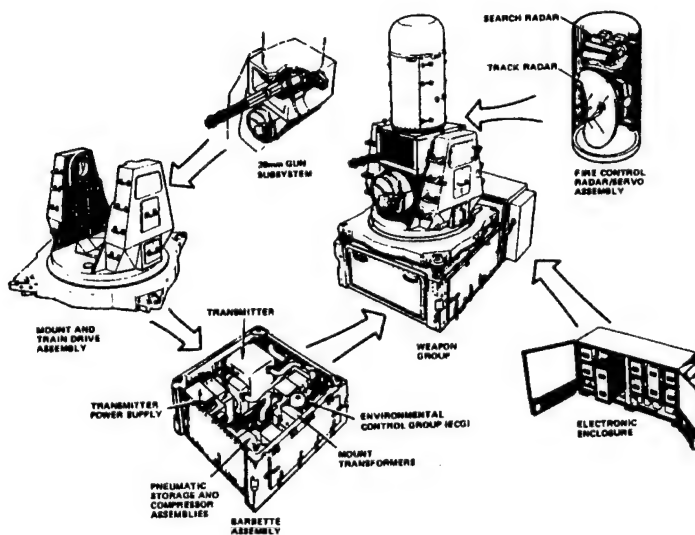


Figure 1-1 PHALANX System Components

Fast reaction times are achieved by using search and track radars along with the weapon control computer to achieve target acquisition. This is accomplished by maintaining the search platform in a horizontally-stabilized position and salved to a vertical gyro so that targets may be sorted and correlated according to range, range rate, and angular position. The track antenna reference system, with its own rate-integrating gyro package, is space-stabilized upon command of the weapon control computer to ensure fast handover and track acquisition.

The search antenna subsystem consists of standing wave antennas mounted to the search platform at specific elevation angles to provide a large elevation coverage. The combination of the track radar, antenna control, fire control computer solution and mount servo defines the engagement control system for the PHALANX system. Using the

antenna position as a reference, the difference between gun position and director solution provides an error signal that generates a gun pointing correction. This technique eliminates the need for independent antenna position measurement and eliminates deck reference with its flexure problems. This technique allows extremely accurate angle error measurement between mount and antenna.

b. Gun Assembly

The heart of the PHALANX weapon system is the versatile M61A1 gatling gun, providing a high rate of fire (variable 3000 or 4500 rounds per minute) with a specifically-designed high kinetic energy round, to provide the necessary lethality. The six-barrel Gatling gun was adopted from the Air Force M61 Vulcan gun series used in several types of aircraft and ground mounted for airfield defense.⁴ The gun assembly (Figure 1-2) is made up of five major sub-assemblies. The gun is electronically controlled and pneumatically driven. The gun consists of a rotating cluster of six barrels with a breech bolt for each barrel. The ammunition subsystem includes all components that store, feed and transport rounds and empty cartridge cases within the system.

c. Mount and Train-Drive Assembly

The mount provides structural support to the gun assembly and the radar servo assembly and houses the servo drive components that provide elevation control of the gun. The train drive assembly is a cast structure that contains the train bearing. This assembly is a combination gear and bearing which serves as the interface between the gun mount and barrette. The train drive gear box is mounted to the platform assembly and provides azimuth drive to the gun mount through the train bearing. An instrument gearbox is also attached to the train drive platform and provides position feedback to the azimuth servo loop system and fire interrupt for no fire sectors.

⁴ The Ships and Aircraft of the U.S. Fleet, Thirteenth edition.

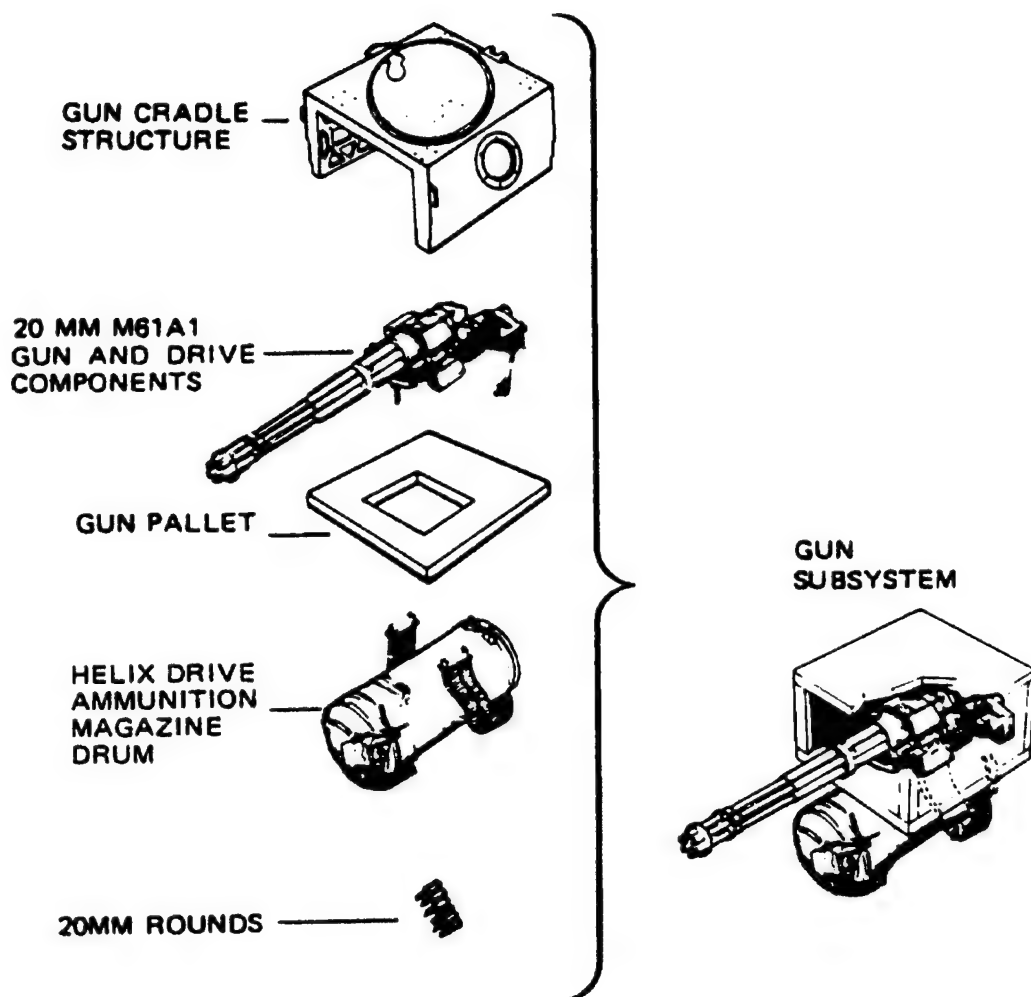


Figure 1-2 Gun Assembly

d. Barbette

The barbette houses the transmitter, transmitter power supply, pneumatic drive power supply, pneumatic electronic control unit, power controller transformer assembly, and the electronic control group (ECG). The PHALANX CIWS provides environmental control for its weapon group equipment, receiving only seawater and electrical power from the ship for this function. The ECG provides air to the system electronics for temperature and condensation control, dry air for waveguide pressurization

and a water/glycol mixture for transmitter cooling.

e. Electronics Enclosure

The electronics enclosure provides weather and electromagnetic interference protection for the rest of the electronics that includes the signal processor, signal generator, gun control unit, mount elevation and train power drives, search and track servo electronics, power supply control group and the weapon control group computer.

f. CIWS MK 149 Round

The PHALANX CIWS utilizes 20 millimeter projectiles that prove to be lethal against an incoming missile. This projectile must have a high muzzle velocity and be capable of penetrating numerous components in a missile forebody. Having penetrated or otherwise exposed the warhead, it must impact the explosive material with the correct relationship of residual velocity and cross-sectional area but also cause a warhead reaction. Development tests have resulted in the MK149 armor piercing discarding sabot round (Figure 1-3), which is a sub-caliber, spin-stabilized tungsten penetrator. At firing, the pusher imparts spin to the projectile and forms a gas seal. After leaving the muzzle, both the lightweight pusher and sabot are discarded leaving the penetrator to intercept the target.

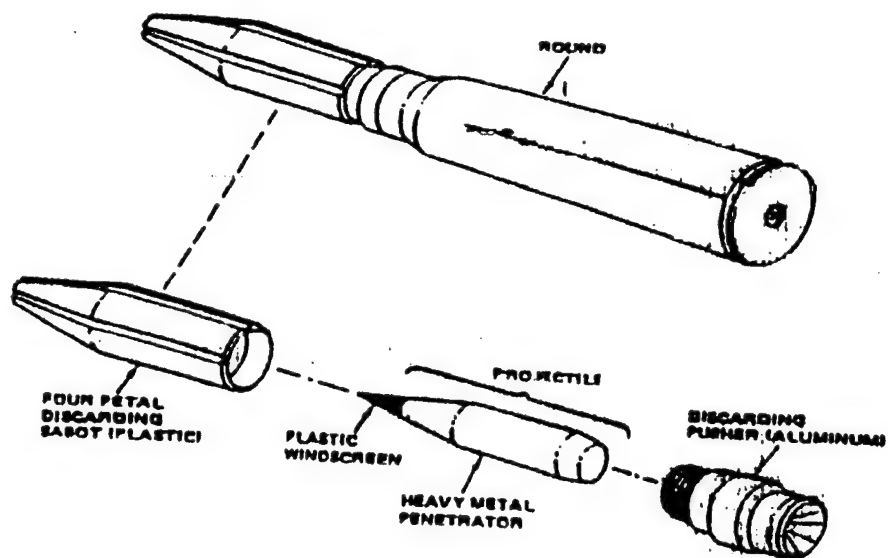


Figure 1-3 PHALANX MK 149 Round

The key characteristics of the gun are defined in Table 1.

PARAMETER	CHARACTERISTIC
GUN	
Fire Rate	3,000 or 4,500 rounds/minute
Ammunition Magazine Capacity	1,556 rounds (including chuting)
Reload Time	< 15 minutes
PAC Burst Length	Continuous, 1.2 seconds or 2.0 seconds
ROUND (MK 149)	
Muzzle Velocity	> 3600 feet/second (1027 m/s)
Velocity Decrease	0.2 feet/second per foot (0.06 m/s per m)
Round Weight	0.6 pounds (0.27 kg)
Penetrator Weight	> 1000 grains
Caliber	20 mm

Table 1-1, Key Characteristics of the PHALANX Gun System

B. MOTIVATION

In today's littoral operating environment the threat is unclear and unpredictable, and Navy ships are in constant threat from anti-surface missiles (ASM's). These missiles are getting faster, smaller, smarter and are available to almost any country in the world. The PHALANX close-in weapon system is a very important part of the anti-ship missile defense structure of the U.S. Navy. The more that is understood about parameters that control PHALANX gun dispersion performance, the more the Navy can increase its performance and therefore ship survivability.

The data collected on a firing PHALANX gun at the Naval Air Weapon Station, China Lake CA, will help in understanding the relationship between the barrel tip movement and dispersion. The objective of this research is to correlate accelerometer data and dispersion data. The ultimate goal is to apply the results of this study to PHALANX systems in the fleet and determine their dispersion value.

This research was conducted in support of the Naval Surface Warfare Center (NSWC), Port Hueneme Division, testing and evaluation of the PHALANX close-in weapon system.

II. DESCRIPTION OF FIELD EXPERIMENTS

A. INTRODUCTION

The Naval Air Weapon Station (NAWS) at China Lake, CA, is one of the Navy's weapons testing facilities. It is used for testing and evaluation of new and current weapon systems. It is at NAWS that the Naval Surface Weapon Center (NSWC) Port Hueneme Division conducts all testing of the PHALANX close-in weapon system. NSWC conducts many performance evaluations of PHALANX. They include performance versus live targets, sonic and subsonic, and tracking exercises versus numerous targets. The facility is also equipped with round dispersion analysis equipment.

1. Equipment setup

Data for dispersion analysis were collected on the PHALANX CIWS system at the NAWS. (Figure 2-1) The CIWS system used was a Block 1 Baseline 2 with HOL (High Order Language). It was part of a CTE (Contractor Testing & Evaluation) evaluation phase of hardware and software testing. During a CTE, the contractor, Hughes Corporation, is allowed to use government facilities for research and development.

Two trips were made to China Lake, the first one on 9 May 1994 and the second one on 31 May 1994. Eleven PAC (Pre-Action Calibration) fires were conducted on each day at low and high firing rates, firing between 100 and 170 rounds, respectively. On each firing, accelerometer data were collected at various positions on the PHALANX gun system. PACs were conducted with the prototype muzzle restraint, production muzzle restraint, and with no muzzle restraint. The accelerometer data were used to determine the gun movement during a firing. Dispersion data were also collected but only on the second trip to China Lake. The dispersion data were taken to correlate against the gun movement, specifically lateral barrel tip deflection with the production muzzle restraint installed.

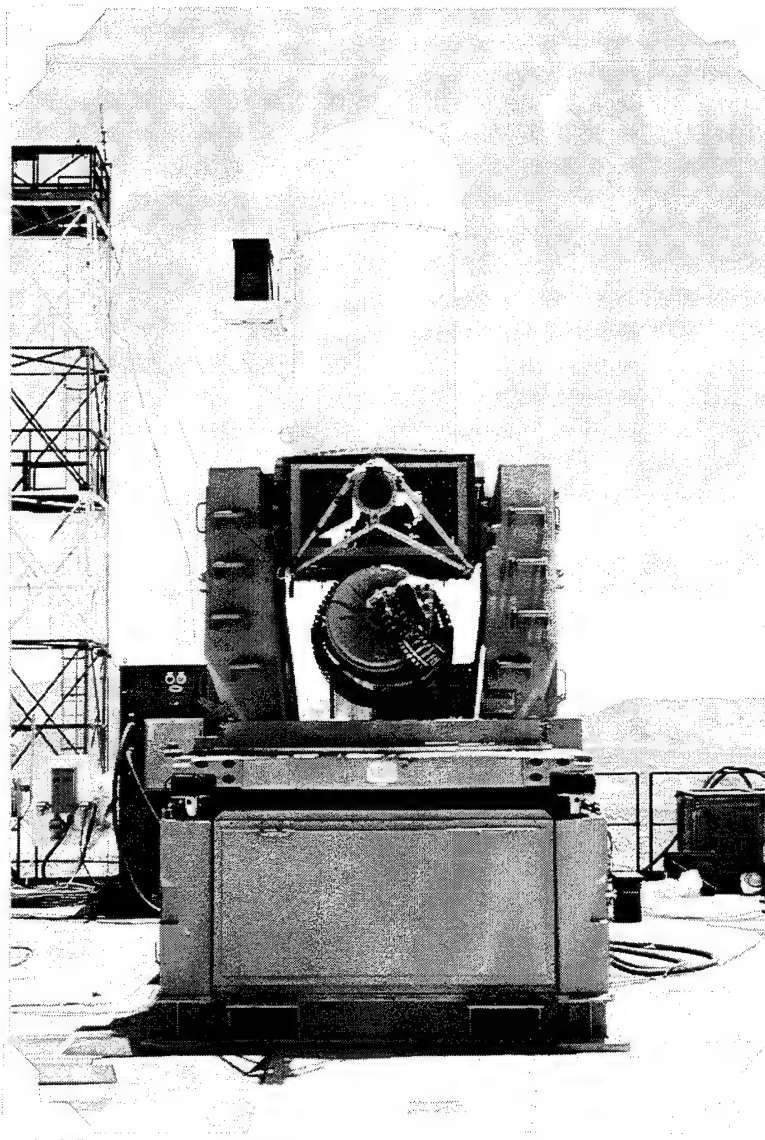


Figure 2-1 PHALANX Gun System at China Lake, CA

a. Dynamic Signal Analyzer Model SA 390

In order to conduct a study and understand the movement of the PHALANX gun system, accelerometer data were collected using the Scientific Atlanta SA 390 Dynamic Signal Analyzer. [Ref 3] The SA 390 was donated to the Naval Postgraduate School by Scientific-Atlanta. The SA 390 is a full-featured 8 channel, 0-100 kHz signal analyzer featuring 16-bit A/D conversion with 32-bit floating point processing for high speed digital signal processing. The SA 390 provides real-time processing of data for which acquisition, processing and display can take place with no loss of data. It has selectable resolution of 200, 400, 800 or 1600 spectral lines. The SA 390 was the signal analyzer of choice because of its eight channels and extended recorder capability.

b. PCB Quartz Shear Mode ICP Accelerometers

The accelerometer data were collected using PCB Quartz Shear Mode ICP Accelerometer Series 353. [Ref 4] The Series 353 accelerometers employ built-in, solid state microelectronics for conditioning the signal generated by the naturally piezoelectric, quartz crystal, sensing element. This type of sensor is designated ICP which stands for Integrated Circuit Piezoelectric. The built-in ICP microelectronics incorporates a MOSFET transistor that requires excitation power. This is supplied by a regulated constant current source of typically 4 milliamps.

In order to conduct a complete study of motion, sets of accelerometers were placed on three key locations on the gun; the muzzle restraint, the mid-house bearing and the aft bearing. They were mounted on tri-axial cubes. The muzzle restraint and aft bearing accelerometers were mounted with their sensitive axis oriented horizontally and vertically. The mid-house accelerometers were mounted along the horizontal, vertical and axial axes. Figures 2-2, 2-3, 2-4 show these mounts.

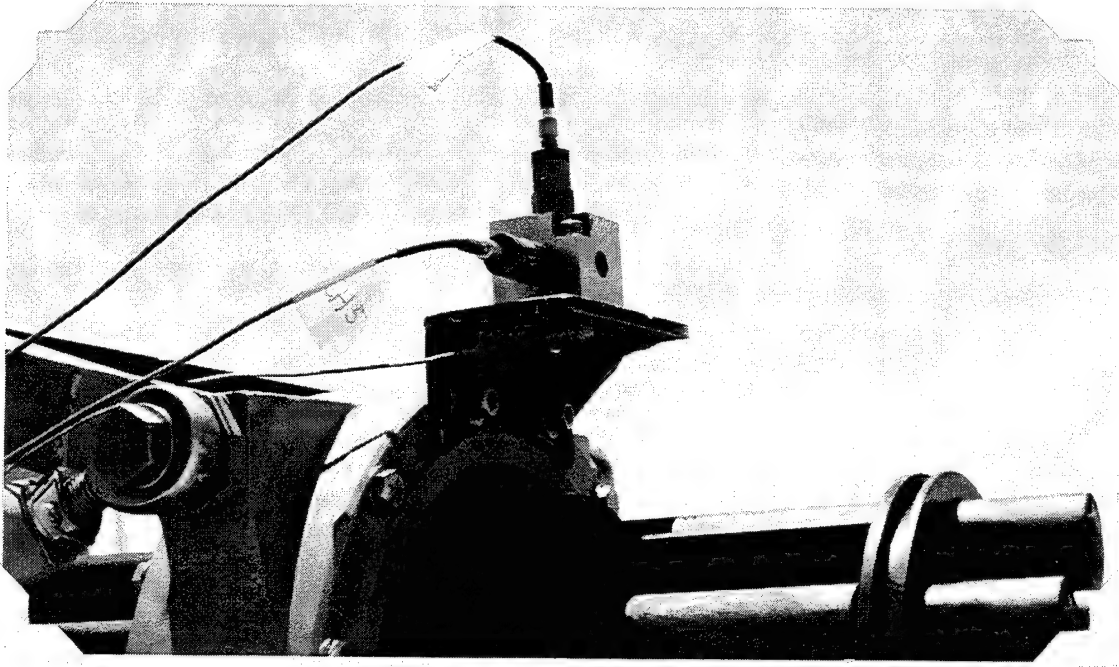


Figure 2-2 Muzzle Restraint Accelerometers

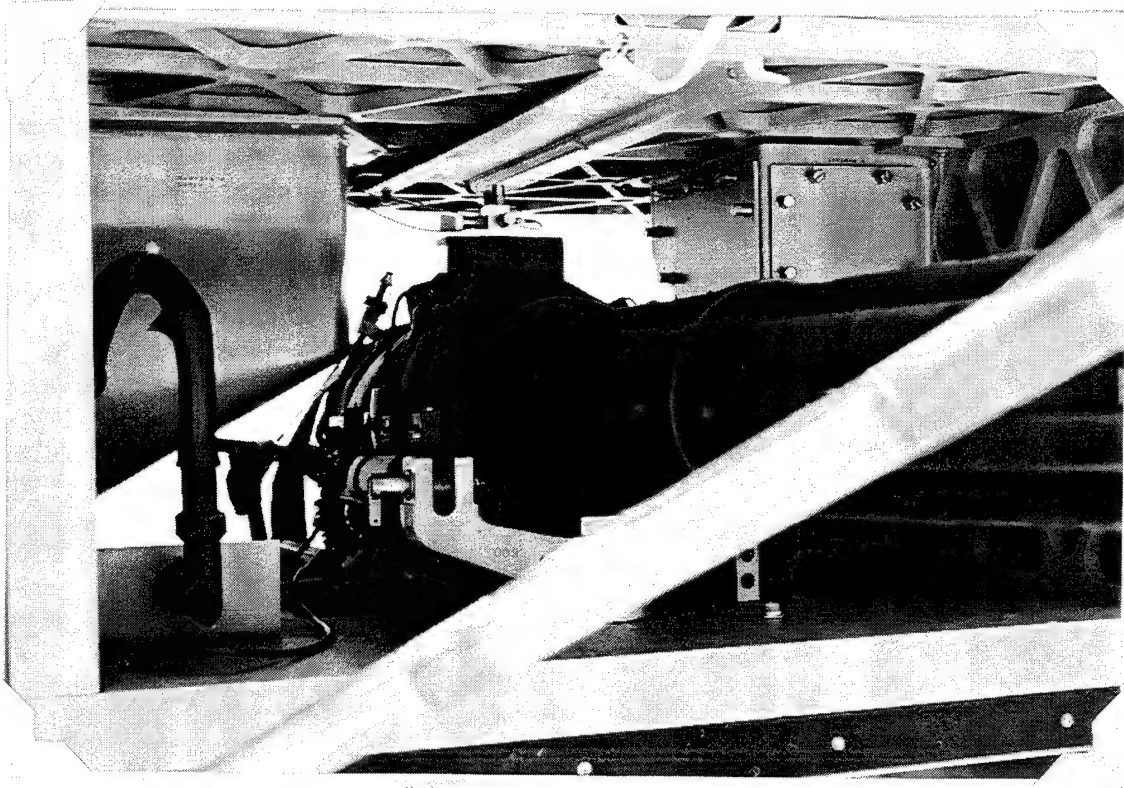


Figure 2-3 Mid Housing Accelerometers

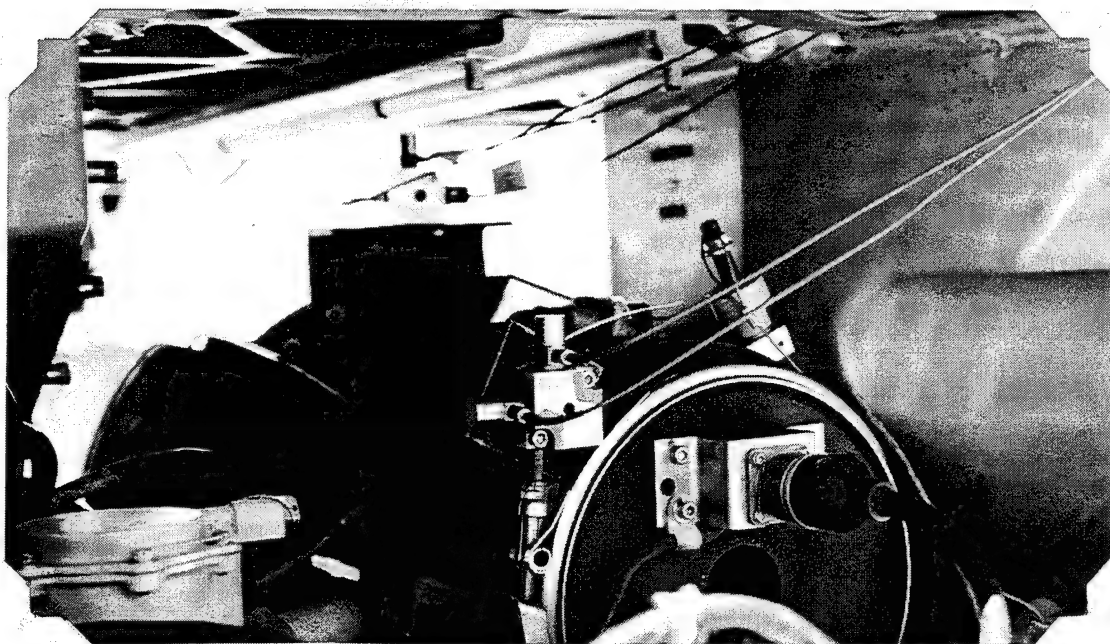


Figure 2-4 Aft Bearing Accelerometers

Table 2-1 summarizes the accelerometer set up for 9 May 1994.

Accelerometer			
Model	Serial Number	Location	Direction
J353B03	SN 5968	Mid Housing	Axial
J353B03	SN 5966	Mid Housing	Vertical
J353B03	SN 5967	Mid Housing	Horizontal
J353B03	SN 5969	Aft Bearing	Horizontal
J353B03	SN 9319	Aft Bearing	Vertical
353B03	SN10267	Muzzle Restraint	Horizontal
353B03	SN10983	Muzzle Restraint	Vertical

Table 2-1, 9 May 1994 Accelerometer Set Up

c. Oehler System 82

The facility at NAWS is equipped with an Oehler System 82. The Oehler system is used to collect dispersion data on a firing gun. It consists of a frame with a microphone at each corner. For a dispersion firing, the PHALANX gun is aimed at the

center of the frame, thus forming an apparent target for the PHALANX supersonic projectiles. The Oehler system detects where within the frame the bullet passed, and with the machine-gun chronograph, it records bullet position and time data. It calculates the rate-of-fire for each round. The Oehler System 82 merges measurement, recording and analytical functions required in ballistic testing into a single integrated system. Oehler dispersion data will be used to correlate the dispersion against the gun movement data obtained from the accelerometers. Figure 2-5 shows the Oehler frame and battenboard system at NAWS China Lake. The frame is six feet in diameter and the system accuracy is typically 0.1 inches. [Ref 5] The battenboard provides an immediate picture of the dispersion. Appendix A contains the output of the Oehler System for the firing three.

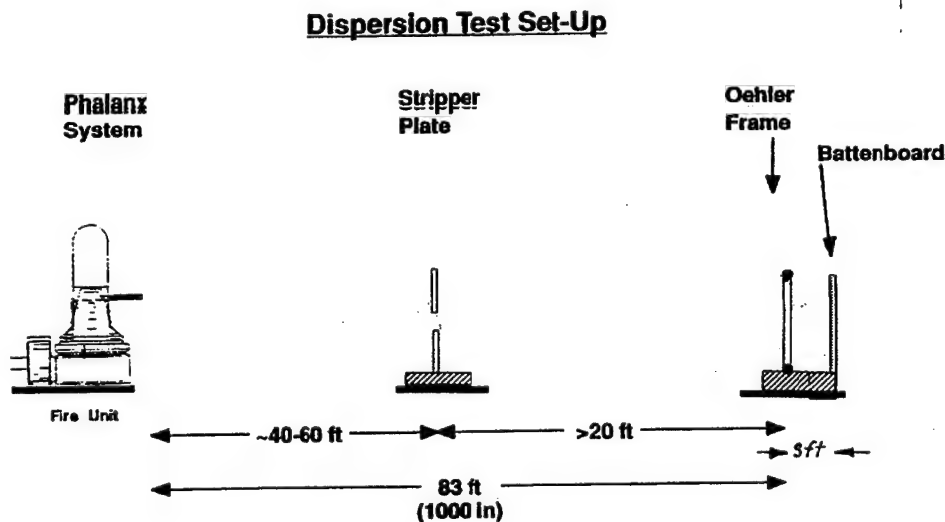


Figure 2-5 Oehler Frame and Battenboard System at China Lake, CA

B. EXPERIMENTAL SETUP FOR 9 MAY 1994

On the first trip to China Lake, accelerometer data were collected on a firing gun with the prototype muzzle restraint (Figure 2-6), the production muzzle restraint (Figure 2-7), and with no muzzle restraint. The muzzle restraints were designed by Hughes as an attempt to control dispersion. The production muzzle restraint is the restraint approved as a system modification for the PHALANX system. It is being produced and provided to the U.S. Navy as an ordnance modification for its close-in-weapon systems.

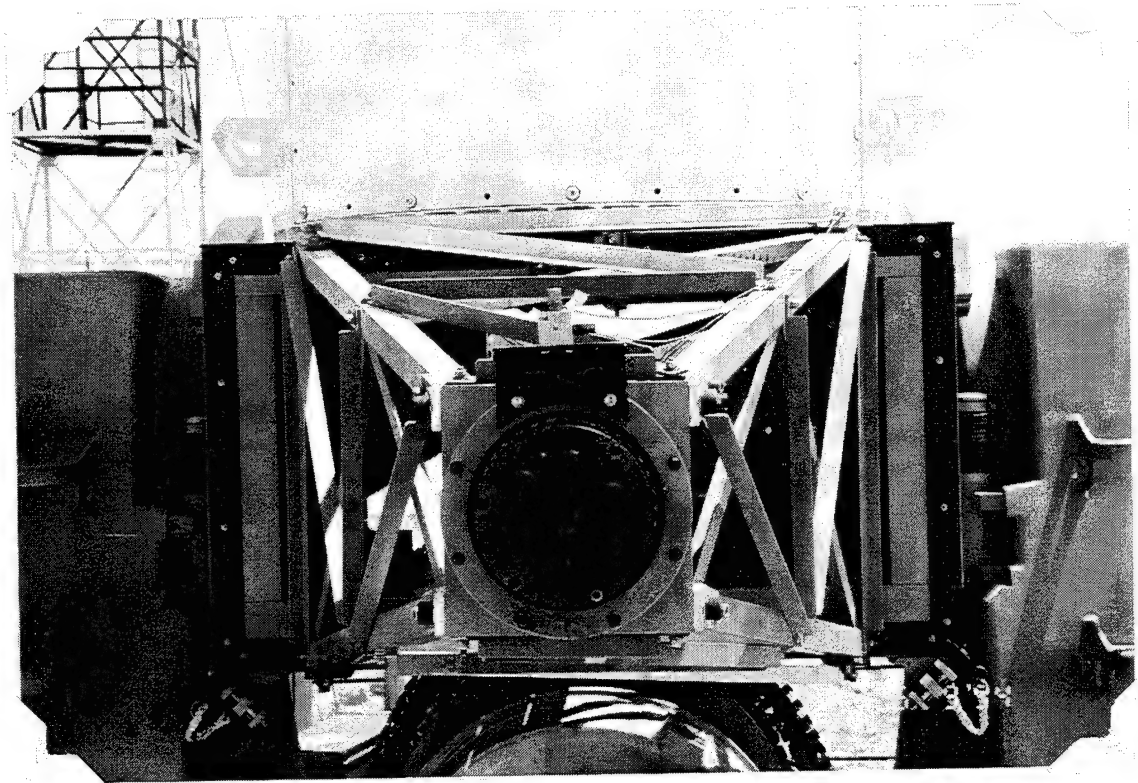


Figure 2-6 Prototype Muzzle Restraint

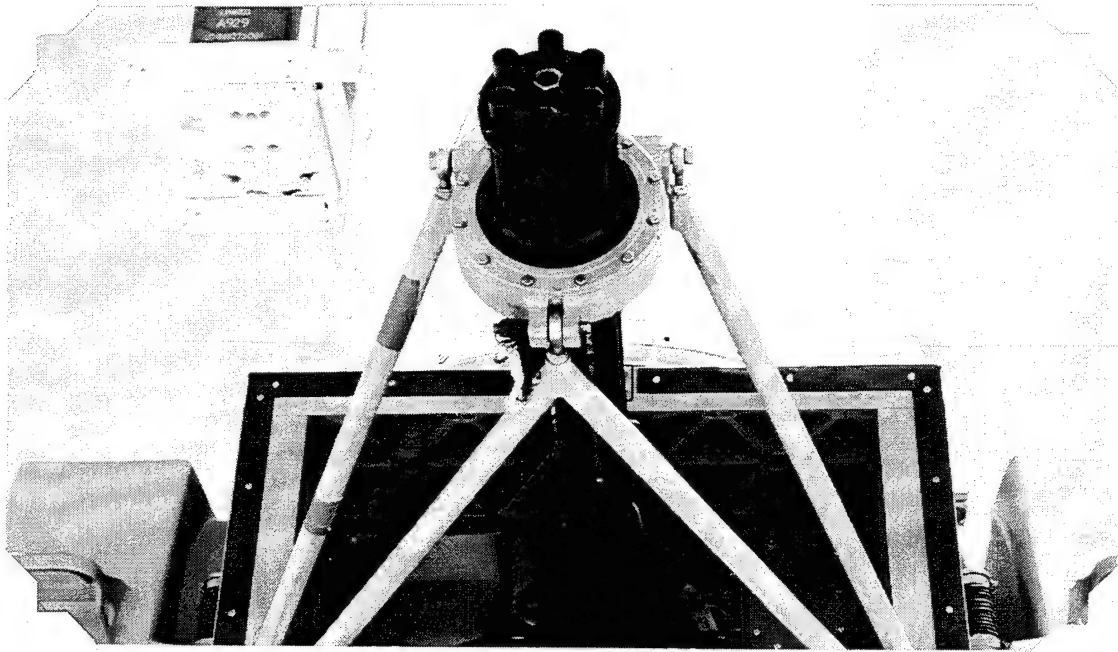


Figure 2-7 Production Muzzle Restraint

The 9 May trip to China Lake was used as a learning experience for data collection. Terrible ground loop problems were experienced while collecting data on the PHALANX gun system. This occurred because the two accelerometers used at the muzzle restraint were not ground isolated. For later data collection, this problem was corrected by using J-series (ground isolated) accelerometers. These accelerometers prevent ground loops by isolating the accelerometer case from the base.

For data collection, the intent was to use the firing signal from PHALANX gun system as a trigger for the SA 390, but as seen in Figure 2-8, the signal was very erratic and a quick solution was required. (The erratic firing signal was identified by the contractor as due to modifications in the new HOL system software.) A manual jury rigged trigger was used. The SA 390 triggers on a TTL high to low transition. A one kilohertz square wave was generated at TTL levels using a Philips Model PM 3384 DSO. [Ref 6] It was manually applied about half a second before firing. A button trigger was built for the second trip. This trigger was a voltage divider with a 9 volt battery. The voltage divider applied a TTL high to low transition when the button was pushed. The button was pushed when there was one second left in the countdown. The signal analyzer

commenced collecting data immediately prior to the gun firing. This was done in order to see and study the beginning of the gun firing.

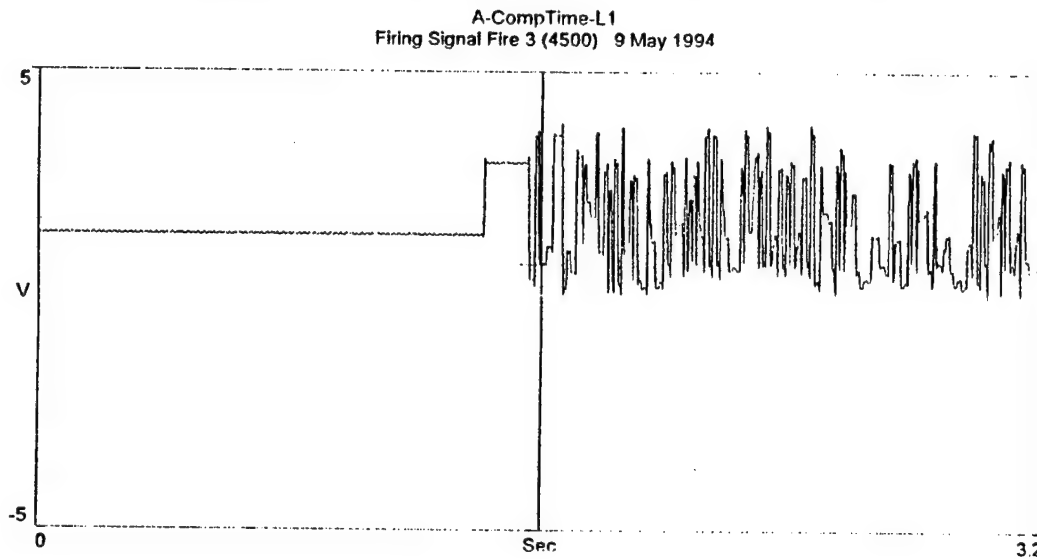


Figure 2-8 Firing Signal for the Third Firing 9 May 1994

The SA 390 sampling rate and time record can be adjusted for any need. The sampling rate is determined by the selected frequency span (4 kHz) using the equation

$$2.56 \times \text{FrequencySpan} = \text{SamplingRate}$$

$$2.56 \times 4 \text{ kHz} = 10,240 \text{ samples/channel/sec}$$

For the first trip to China Lake, it was predetermined that 3.2 seconds would be sufficient recording time. The SA 390's extended recorder time is determined by the sampling rate and memory allocated. With eight channels, the number of samples per channel was 30,768 and the total memory allocated per firing was 256k. Figure 2-9 shows that 3.2 seconds was not sufficient to collect the ramp-down after firing. For the second trip the time records were increased to four seconds, which proved to be sufficient to record a complete PAC fire. Increasing the extended recorder time increased the

number of samples per channel to 40,960. No dispersion data were collected on 9 May, therefore no correlation between the accelerometer data and dispersion data could be completed.

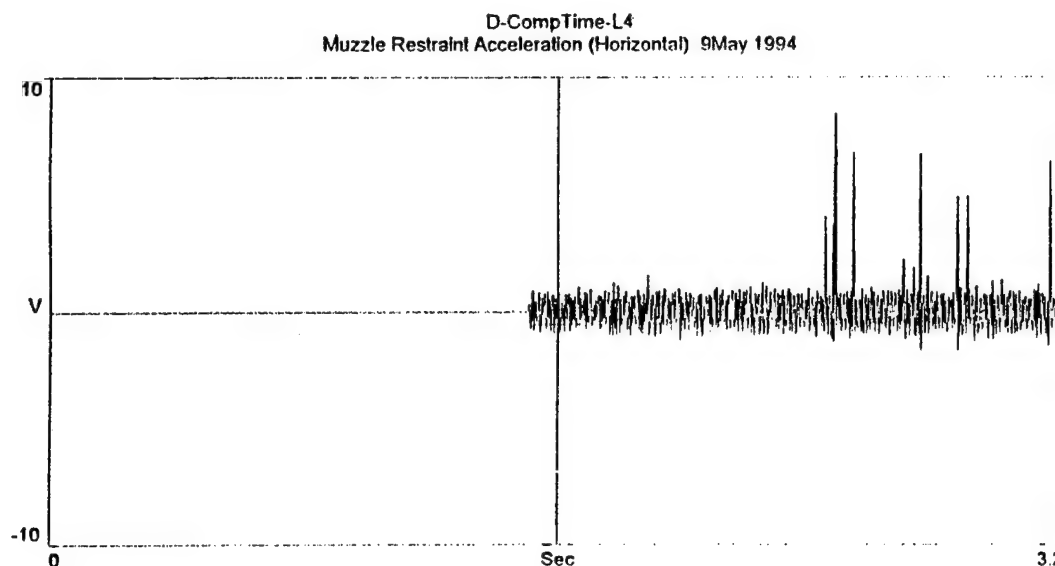


Figure 2-9 Muzzle Restraint Acceleration (Horizontal) for 9 May 1994

On 9 May, the PHALANX magazine was fully loaded with 1500 rounds. This allowed for eleven PAC-fires. The firing rate was varied between 3000 RPM and 4500 RPM. The amount of rounds fired varied between 100 and 170. Data were collected with the prototype muzzle restraint, the production muzzle restraint and without muzzle restraint. Tables 2-2, 2-3 and 2-4 summarizes the firing runs conducted on 9 May 1994.

Firing Run Number	Firing Rate RPM	Rounds Fired
1	3000	100
2	4500	170
3	4500	170

Table 2-2, 9 May Firing runs made with prototype muzzle restraint

Firing Run Number	Firing Rate RPM	Rounds Fired
4	3000	100
5	4500	160
6	3000	120
7	4500	160
8	3000	110
9	4500	No Data Available

Table 2-3, 9 May Firing runs made with production muzzle restraint

Firing Run Number	Firing Rate RPM	Rounds Fired
10	3000	No Data Available
11	4500	No Data Available

Table 2-4, 9 May Firing runs made with no muzzle restraint

From the experience learned on 9 May, it was decided that a second trip to China Lake would be extremely beneficial. This trip was conducted on 31 May 1994. This time allowed for the ordering of two additional J-series accelerometers and preparing better mounts for the tri-axial cubes.

C. EXPERIMENTAL SETUP FOR 31 MAY 1994

The same experimental set up was used for the second trip to China Lake, although accelerometer data were only obtained from the production muzzle restraint. The following changes were implemented from the first trip: bullet dispersion data were collected with the Oehler frame, a push-button trigger was used, and ground-isolated

accelerometers were used for all seven locations on the gun. Also, temperature measurements were made at the muzzle restraint before and after each firing to see if there was any variation in the dispersion with temperature. This study does not take into account the temperature effects.

The SA 390 was configured to record four seconds of data. Figure 2-10, shows that this was sufficient time to record the ramp-up and ramp-down of the gun firing. Again, eleven PAC fires were conducted. Table 2-5 provides a summary. The temperatures listed for each firing were the measured temperature before and after each firing. The data collected on 31 May 1994 were analyzed for research.

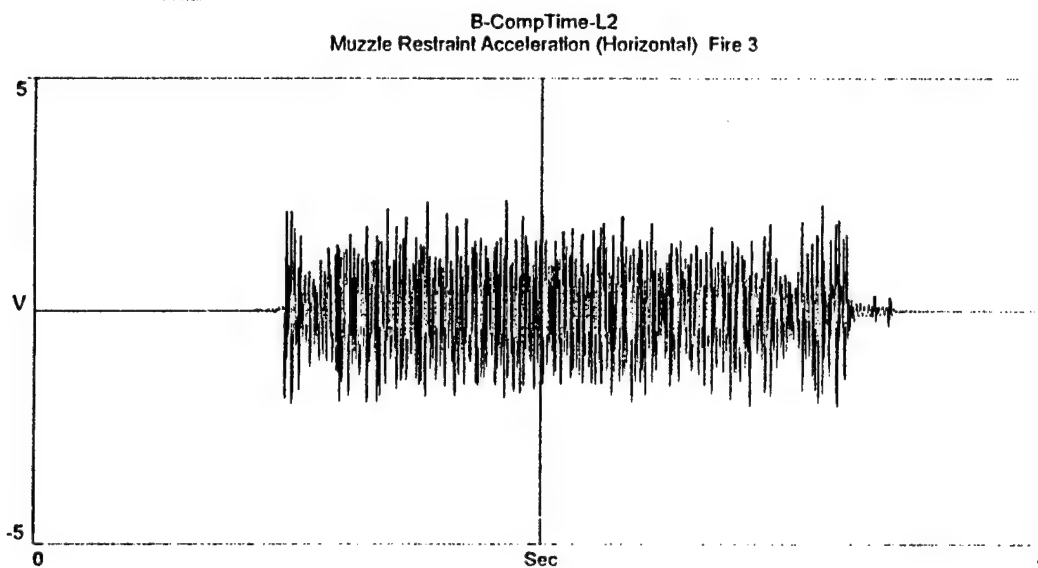


Figure 2-10 Muzzle Restraint Acceleration (Horizontal) for 31 May 1994

Firing Run	Firing Rate	Rounds Fired	Dispersion	Temperature (C)	
				Before Firing	After Firing
1	4500	170	0.93	38.8	42.8
2	3000	110	0.89	44.3	48.8
3	4500	170	0.93	50.1	55.0
4	3000	110	1.06	56.1	58.2
5	3000	120	1.06	59.6	61.9
6	4500	170	1.18	61.3	61.8
7	4500	160	0.91	62.5	64.3
8	4500	170	0.89	63.9	66.2
9	4500	170	1.14	66.2	68.7
10	4500	160	1.06	68.0	68.9
11	3000	50	N/A	57.3	58.0

Table 2-5, Firing Runs for 31 May 1994 (all made using the production muzzle restraint)

Figures 2-11 through 2-18 show the output for all eight channels of the SA 390 for firing run three. These data were used in all subsequent analyses.

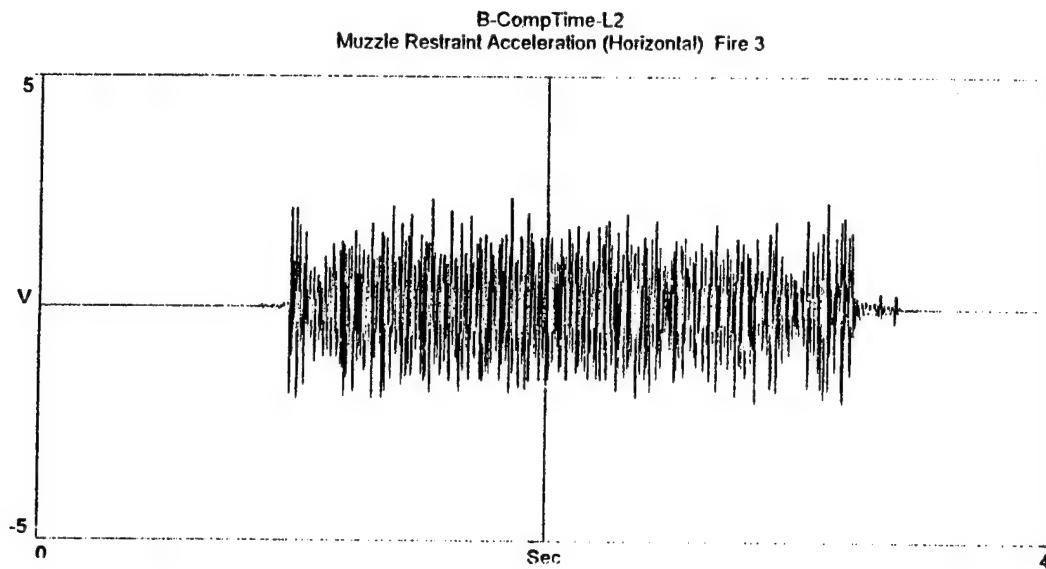


Figure 2-11 SA 390 Trace for the Muzzle Restraint Acceleration (Horizontal)

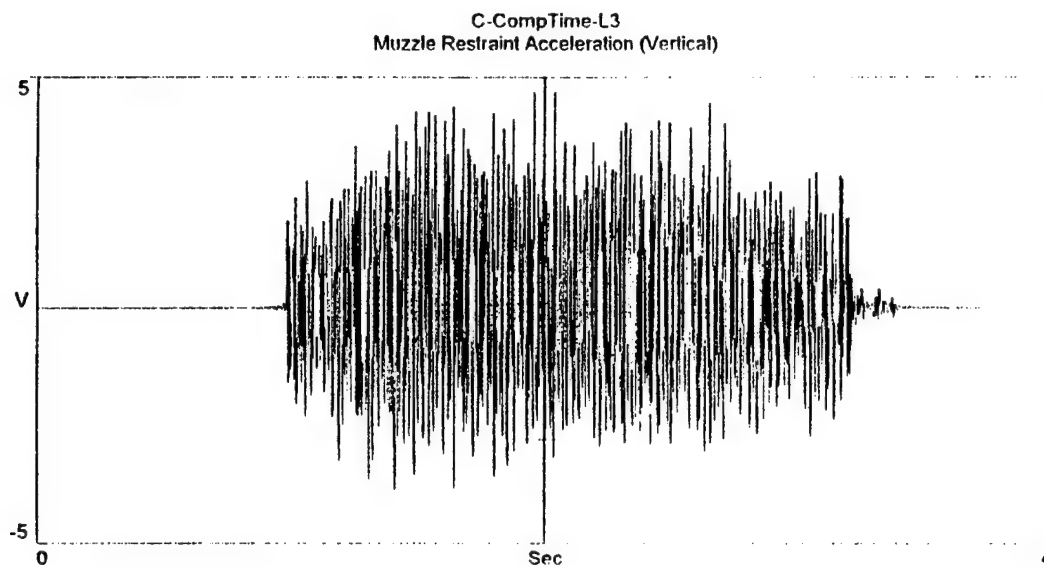


Figure 2-12 SA 390 Trace for the Muzzle Restraint Acceleration (Vertical)

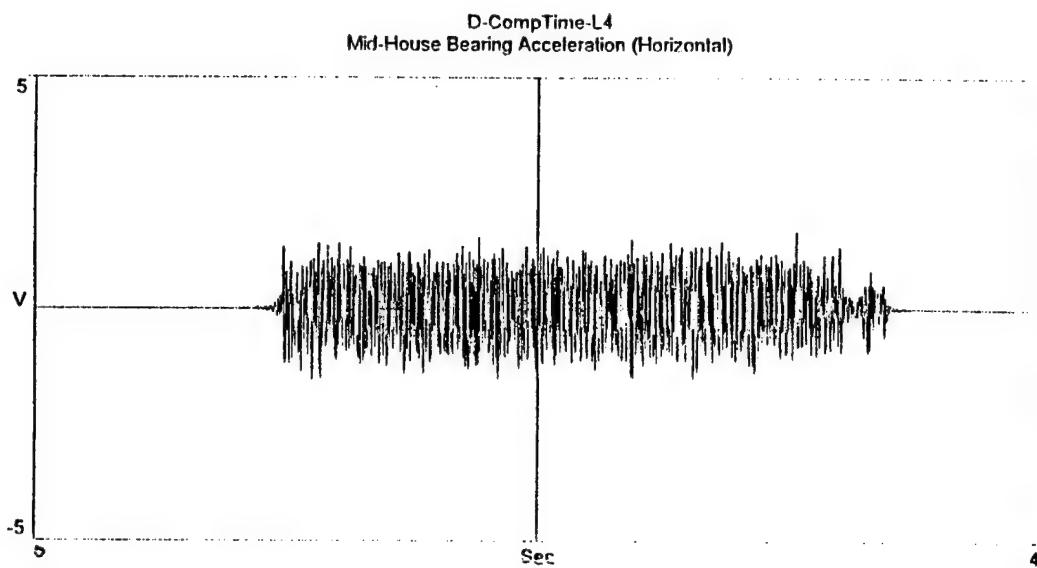


Figure 2-13 SA 390 Trace for the Mid-House Bearing Acceleration (Horizontal)

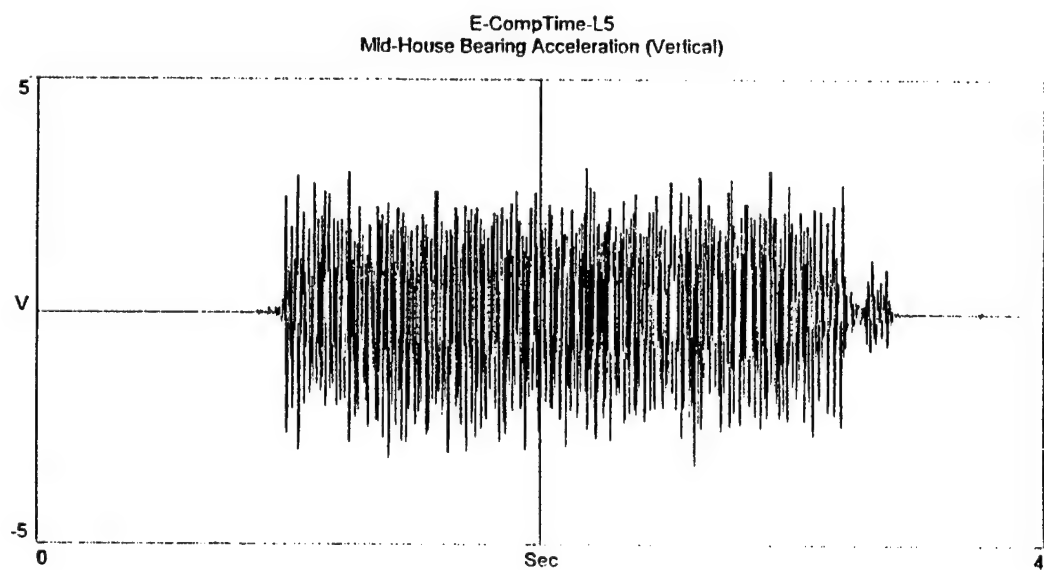


Figure 2-14 SA 390 Trace for the Mid-House Bearing Acceleration (Vertical)

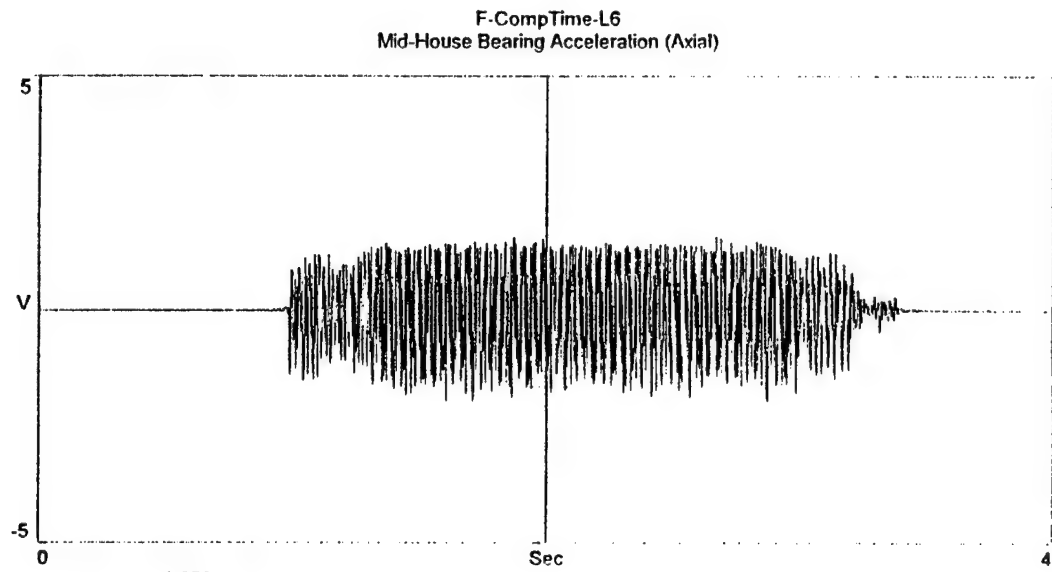


Figure 2-15 SA 390 Trace for the Mid-House Bearing Acceleration (Axial)

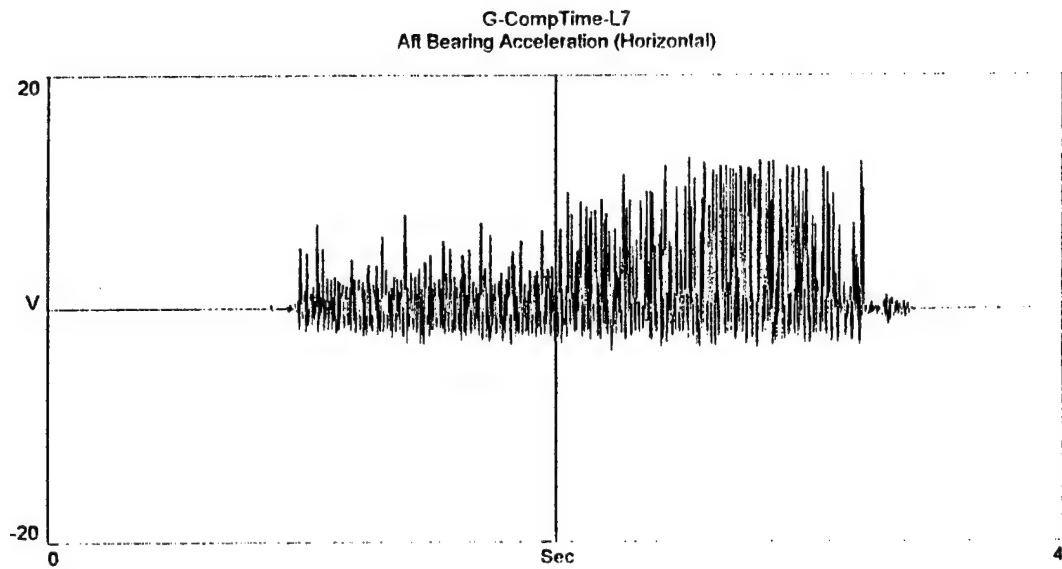


Figure 2-16 Aft Bearing Acceleration (Horizontal)

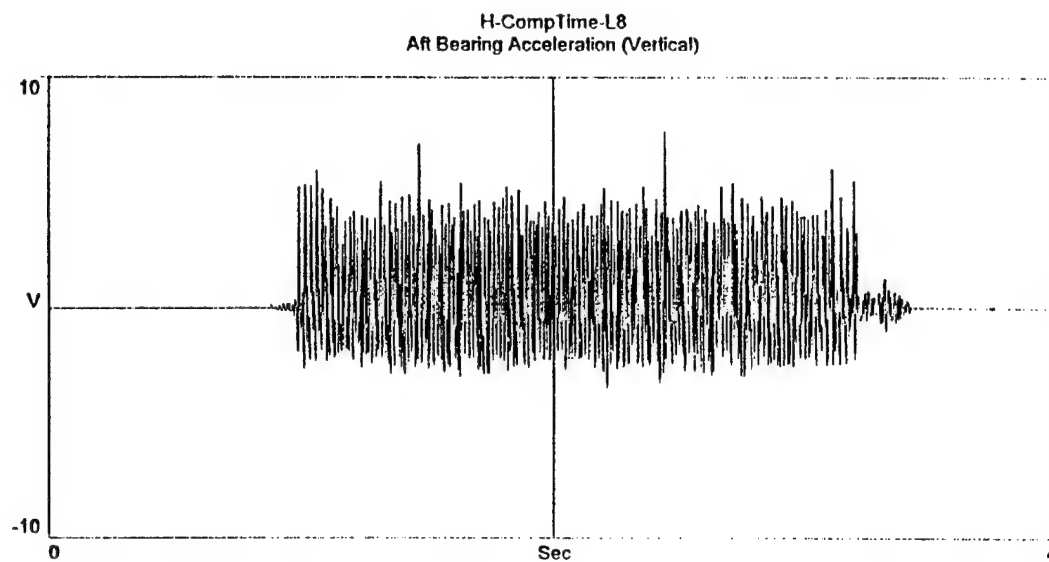


Figure 2-17 SA 390 Trace for the Aft Bearing Acceleration (Vertical)

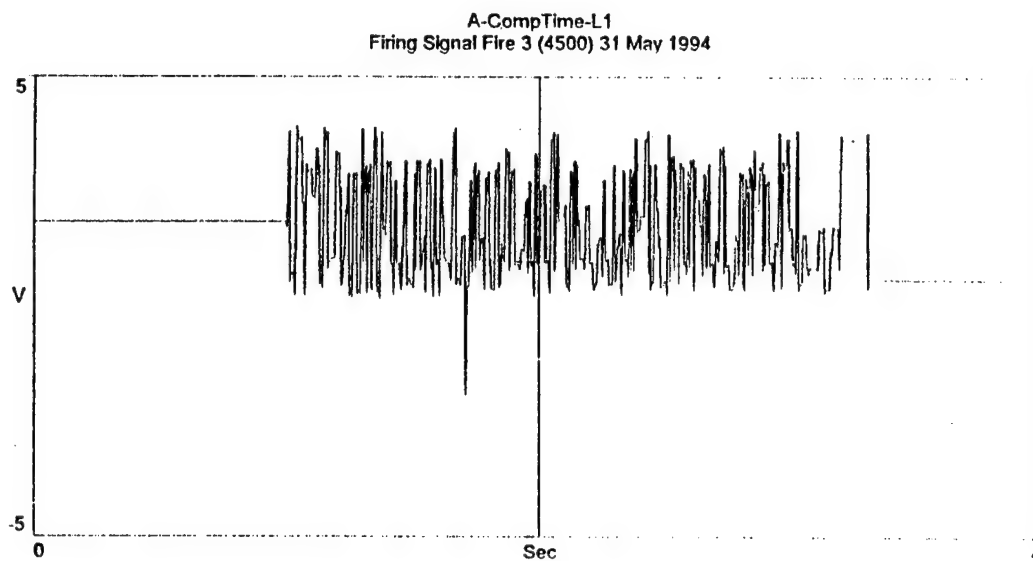


Figure 2-18 Firing Pin Signal

III. DISPERSION DATA ANALYSIS

Dispersion is directly related to the hit-probability of any gun/ammunition system. Many factors affect dispersion, but the most important are the wear on the system, the type of round fired, and the firing rate. The firing rate has a major impact on dispersion. For example, when firing at 200 rounds/minute or higher the dispersion increases by 50 per cent above the single shot figure. [Ref 7] Other factors that affect dispersion are wind, tracking errors between the sight and the gun, trunnion tilt, and recoil forces. [Ref 8] When a gun is manufactured, it will be tested for accuracy and dispersion against a test specification. A worst-case weapon, which only just passes its test specification as new, would have nearly twice the dispersion of a typical production gun. Also, since all guns wear during their life, the dispersion will increase by up to 20 per cent before refurbishment is considered necessary. [Ref 9]

The M61A1 gun was initially designed for aircraft use. When used on aircraft, high dispersion is effective. It gives the aircraft a higher probability of a kill against another fast moving target. When the gun was adopted for the Navy's close-in weapons system, it performed satisfactorily against slow sea-skimming anti-ship missiles. The radar technology was still under development, and dispersion had not been identified as a problem. As the radar improved, it began to monitor erratic dispersion patterns. These patterns cause the CIWS closed-loop spotting to pull the projectile stream off the target. Radar technology has improved dramatically and surpassed the performance of the gun. Today the anti-ship missiles are faster and smarter. Therefore, PHALANX, the last weapon in the defense in depth concept, must destroy them at the furthest possible range. The high dispersion leaves a deficiency in a ship's defensive capability.

A. DISPERSION DATA

1. Firing Rate

Dispersion data was acquired on 31 May 1994 for ten of the eleven firings. The set up was controlled by Yuji Wilson, the Project Manager and our sponsor for the PHALANX gun system. The dispersion is determined when the firing rate is steady. It takes an average of ten to twelve rounds for the gun to ramp up to the desired firing rate. The gun sometimes overshoots the desired firing rate, but it settles back down. This was seen when the firing rate was decreased from 4500 RPM to 3000 RPM. Figure 3-1 shows these features for firing run number two.

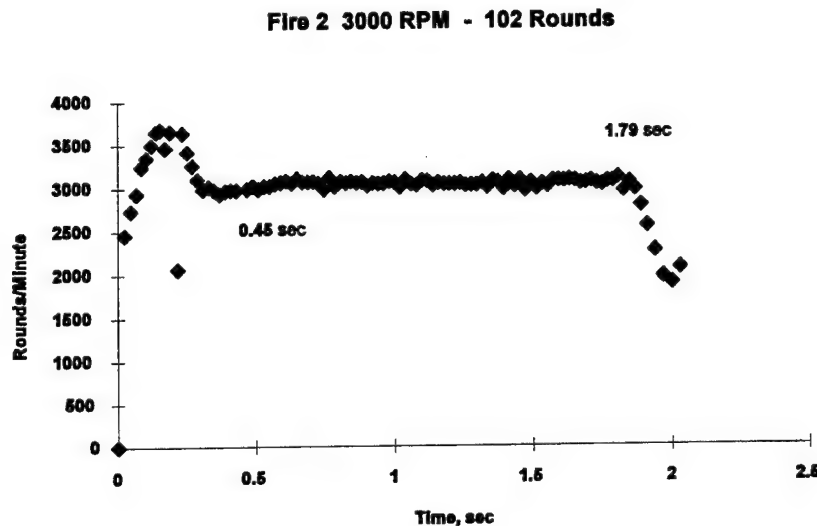


Figure 3-1 Firing Rate for the Second Firing, 31 May 1994

The Oehler 82 System records the time of each round arrival at the frame and its location. From this, it determines the gun firing rate. The two times, 0.45 s and 1.79 s, correspond to when the gun achieved steady state and when it commenced to ramp down. Figure 3-2 shows the firing rate for the third firing.

Fire 3 4500 RPM - 161 Rounds

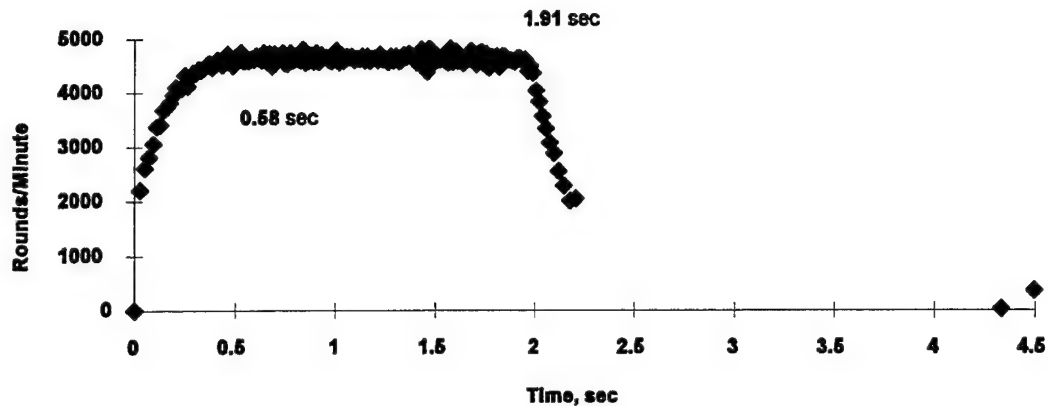


Figure 3-2 Firing Rate for the Third Firing, 31 May 1994

The marks at around 4.5 seconds are flyers. Flyers can be sabot petals or projectile debris that hits one of the microphones directly on, or a bullet that hits outside a certain radius. Flyers are disregarded when determining dispersion. In order to estimate a correct value for dispersion, the rounds with a firing rate 10 percent above and below the preset firing rate, are eliminated. These rounds account for the ramp-up and ramp-down of the gun. If there are flyers, the Oehler computer calculates a radial value for sub bursts. A sub burst includes rounds at steady firing up to the first flyer. A radial value is calculated for each sub burst. The process continues until all the rounds within the steady rate are accounted for. The radial value for each sub burst is multiplied by a factor determined by the number of rounds in the sub burst. The radial values are summed and divided by the sum of the factors. This value is multiplied by 0.707 to determine the estimated dispersion value. Table 3-1 summarizes the firing runs for 31 May 1994.

Firing Run	Firing Rate (RPM)	Rounds Fired	Dispersion (mrads)
1	4500	156	0.93
2	3000	102	0.89
3	4500	159	0.93
4	3000	101	1.06
5	3000	101	1.06
6	4500	160	1.18
7	4500	157	0.91
8	4500	156	0.89
9	4500	154	1.14
10	4500	154	1.06
11	3000	50	N/A

Table 3-1 Firing Runs for 31 May 1994

There is a disparity between Table 2-5 and Table 3-1 in the number of rounds fired. In Table 2-5, the number of rounds fired was determined by the firing pin signal. As stated earlier, this signal was extremely erratic. The number of rounds fired listed in Table 3-1 was determined by the Oehler Frame, and are the correct values.

2. Dispersion

Figure 3-3 is a plot of the dispersion pattern for firing run 3. The fact that the pattern is not centered at (0,0) is not significant. The gun barrels are aligned to the center of the Oehler Frame, which is eighty three feet away. It is difficult to get the barrels aimed at the exact center of the frame. This is easily corrected by subtracting the mean.

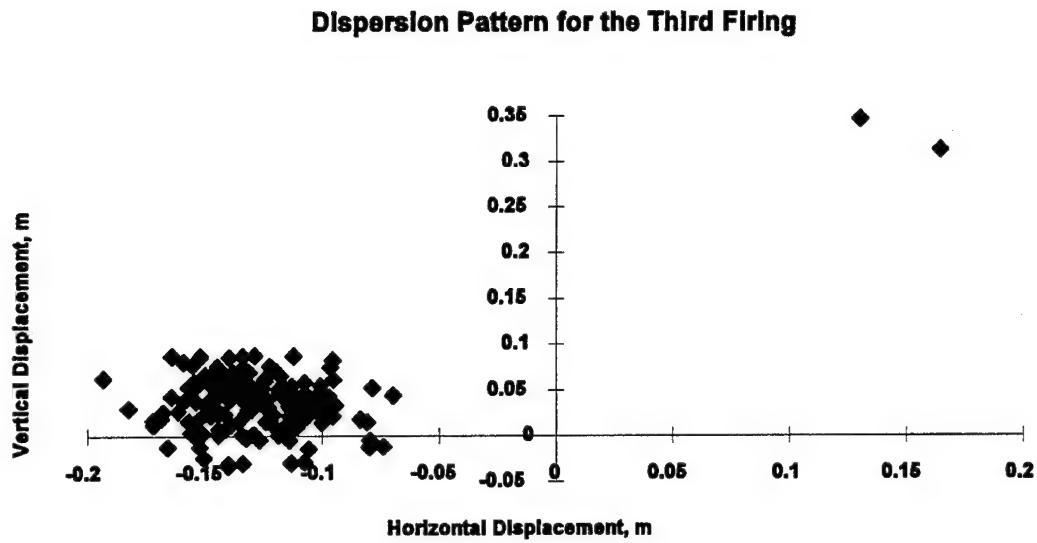


Figure 3-3 Dispersion Pattern for the Third Firing

In order to cross correlate the displacement of the muzzle restraint against the dispersion, the dispersion data was transferred into MATLAB. The array of dispersion data had to be expanded from 157 elements long to 40960 in order to match the size of the accelerometer data. The first column of the dispersion matrix contains the best estimate of the time of the first round fired. This value was determined using CROSSCORR.m (Appendix B). The procedure is detailed in the next chapter. The second and third column contain the horizontal and vertical dispersion data.

IV. ACCELEROMETER DATA ANALYSIS

Due to time constraints, it was decided to concentrate the efforts of signal analysis on one firing run. Firing run number three of 31 May 1994 was chosen for no particular reason.

The SA 390 Dynamic Signal Analyzer, although a powerful tool, is limited in its data analysis capabilities. Therefore, in order to conduct an analysis, it was necessary to transfer the data to a powerful technical computing environment for high-performance numeric computation and visualization such as MATLAB. [Ref 10]

A. DATA CONVERSION

The data stored in the SA 390 is in a raw ATT 32C DSP binary format. [Ref 11] It was required to convert the data to ASCII format for use by PC's. The SA 390 does not have the capability of exporting extended records. Initially there was no choice in the method of converting and exporting the data. The only approach was to load the extended record, and save each successive four hundred millisecond time trace as a text file. The ten text files were then reconstructed in a text editor such as Brief. Since data were collected on twenty firings, this process was tedious and long. With the help of Robert Mihata of Scientific Atlanta, an executable code, XRC2MAT, was eventually obtained. XRC2MAT extracts the data from an extended record and saves it to another file in ASCII format. When this file is loaded in MATLAB, each channel of data collected represents a column in a matrix. This resulted in a 40960 by 8 matrix.

With the data converted and imported into MATLAB, the analysis of the data began. The goal of the data analysis was to correlate the barrel tip lateral displacement with the dispersion. The first objective was to properly display the data in MATLAB and convert it from volts to meters per second². With the help of Mike Hatch, the code GTESTFFT.m, (Appendix C), was written. GTESTFFT.m originally converted the acceleration from volts to inches per second² and plots the acceleration versus time.

This procedure was modified to convert the acceleration from volts to meters per second². It creates the time scale by dividing the number of samples by the sampling rate (10,240 samples/second). Figure 4-1 shows the reconstructed record of the aft bearing accelerometers. Figure 4-2 shows the acceleration for the muzzle restraint accelerometers. Figure 4-3 shows the acceleration for the mid housing bearing accelerometers. GTESTFFT.m also computes and plots the normalized discrete-time Fourier transform (Figure 4-4) by using the following equation from the Signal Processing Toolbox in MATLAB [Ref 12, p. 2-90 2-92]

$$P_n = \text{abs}(\text{fft}(x)) \cdot 2 / \text{length}(x) \quad (1)$$

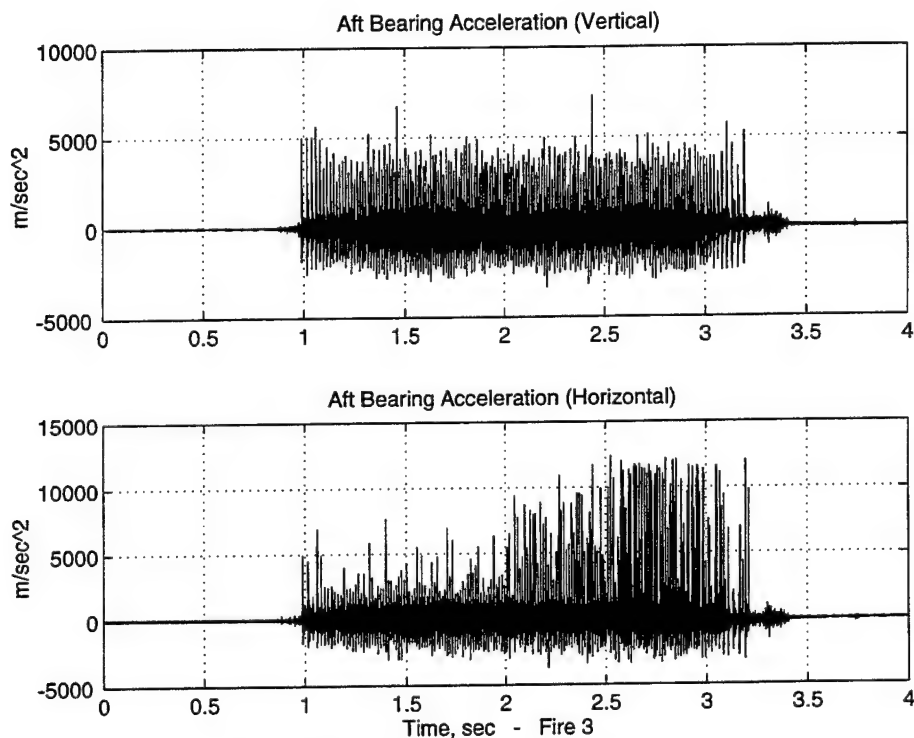


Figure 4-1 Aft Bearing Acceleration

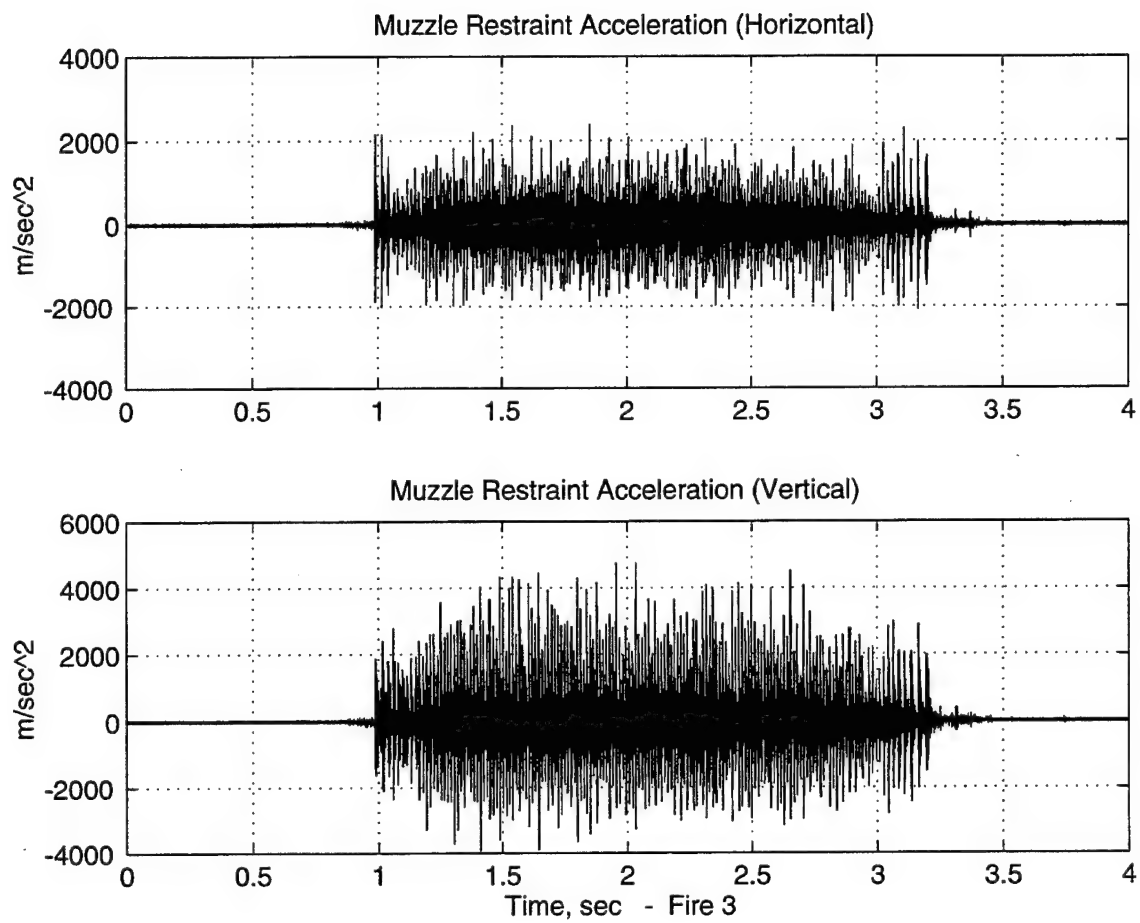


Figure 4-2 Muzzle Restraint Acceleration

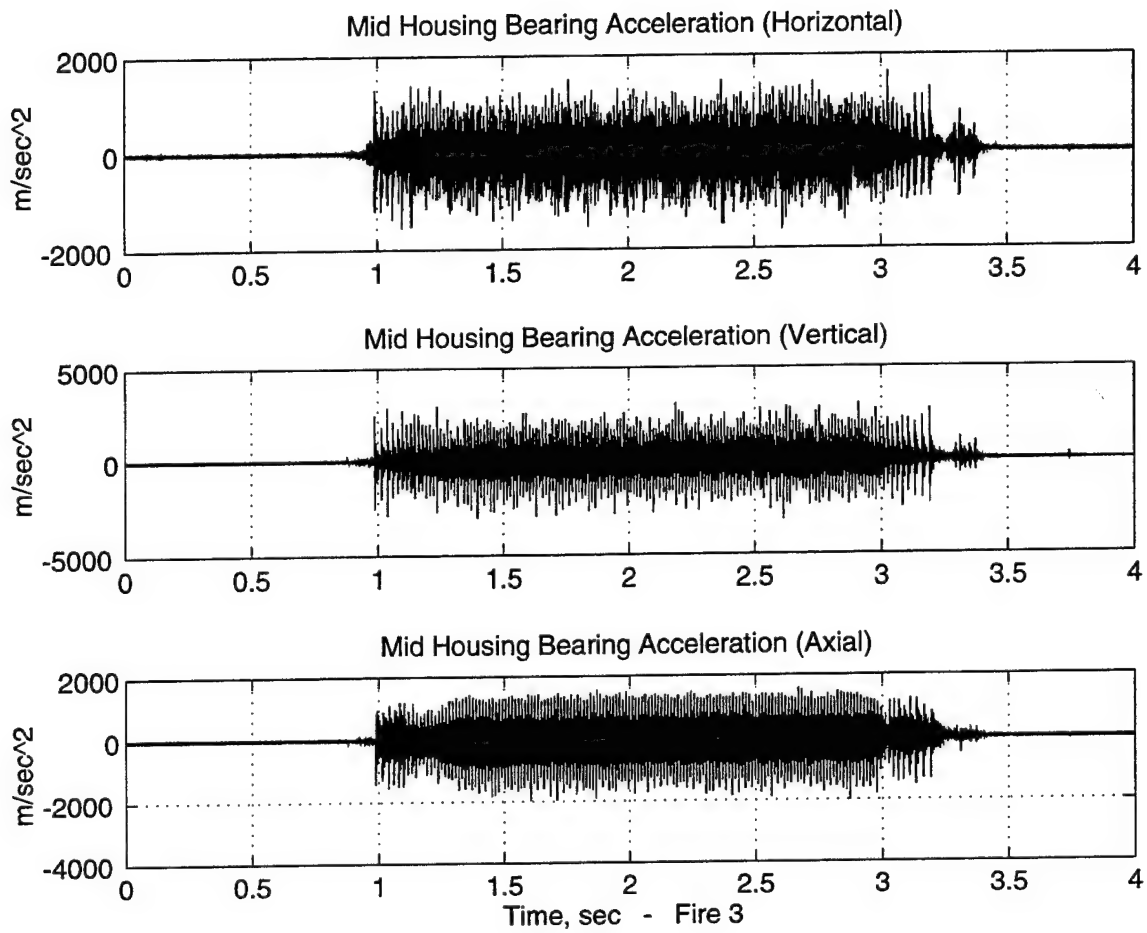


Figure 4-3 Mid Housing Bearing Acceleration

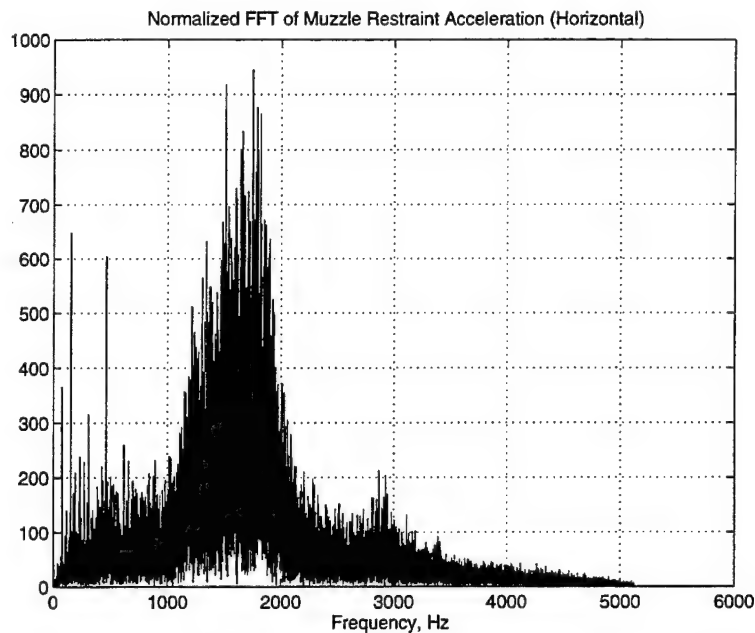


Figure 4-4 Normalized FFT of Muzzle Restraint Acceleration (Horizontal)

B. DATA ANALYSIS

1. Determining the Time of the First Round

In order to commence the correlation between measured acceleration and dispersion, it was required to time-align the dispersion data and the accelerometer data. If the firing pin signal had not been so erratic, then it would have been used for this purpose, and time alignment would have been a trivial problem. Determining the time correspondence between the acceleration and dispersion data records was completed in two steps. First, from the acceleration plots it was determined that the first round fired occurred within the first 12228 samples. Using THRESHOLD.m (Appendix D), a limit value was used to determine the first occurrence of an acceleration magnitude exceeding a threshold value. THRESHOLD.m returned the bin number when the limit was exceeded. From acceleration values around the exceeded acceleration magnitude, the threshold value was adjusted until the bin number corresponded to the maximum acceleration magnitude. For data of firing run three, this gave a time after

commencement of accelerometers data acquisition of 0.9879 seconds. Due to the process of resetting the threshold value, this time was considered a rough estimate of the first round firing time.

In order to obtain the best estimate, it was decided to cross correlate the dispersion and accelerometer data. For this step the *XCORR.m* function in the Signal Processing Toolbox [Ref 13, p. 2-226 2-228] was used. To cross correlate using *XCORR.m* the data files had to be the same size. As stated earlier, the dispersion array was increased to a 40960 element array. *XCORR.m* uses FFT's to cross correlate, and, due to the size of the files, there were memory problems. A new cross correlating function had to be created. *CROSSCORR.m* correlates for 300 values around the rough estimated time, 50 prior and 250 after. It uses the following equation to cross correlate between the dispersion data matrix $x(n,1)$ and the sum of the squares of the horizontal and vertical muzzle restraint accelerations, *batacc*.

$$xcor = \frac{1}{40,960 - |m|} \sum_{n=1}^{40960-|m|} xcor(m,1) * x(n,1) * batacc(n-m,1) \quad (2)$$

Figure 4-5 shows the cross correlation between the accelerations and dispersion. The time closest to the rough estimate with the largest correlation was used as the best estimate of when the PHALANX gun began to fire. This value was 0.9836 seconds. It is presumed that this time is more accurate.

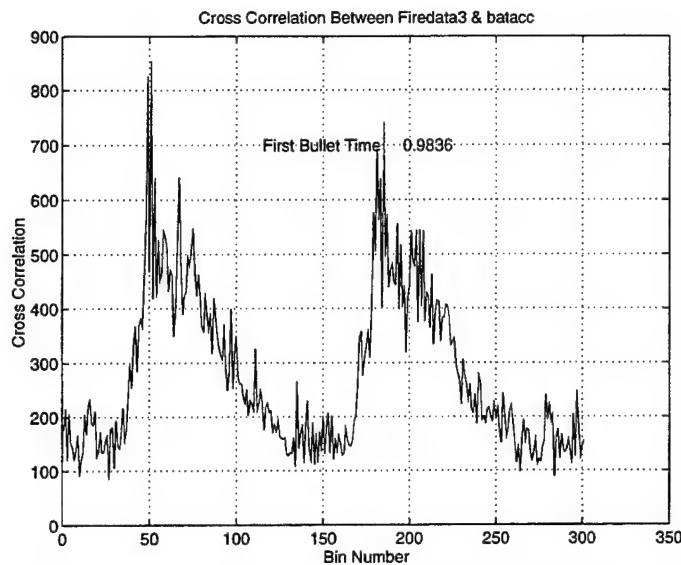


Figure 4-5 Results of Cross Correlation between acceleration and dispersion

The results from THRESHOLD.m provided some insight into the PHALANX gun movement during a firing. It was determined that the gun begins to move first at the aft bearing. This is logical, since at the start of the firing sequence, a round is loaded into the barrel. As the loaded barrel rotates to the firing position, twelve to fourteen degrees from top dead center, it induces movement at the barrel tip. The mid housing remains relatively motionless until the firing signal is applied to the round and the round commences to travel down the barrel.

Figure 4-6 shows the muzzle restraint acceleration with the best estimate of the first firing time.

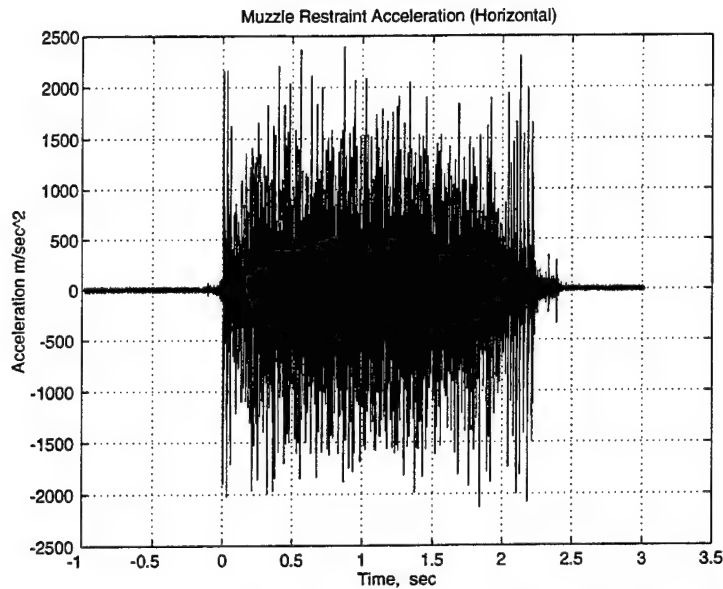


Figure 4-6 Muzzle Restraint Acceleration (Horizontal) versus the Best Estimated First Round Time

2. Barrel Tip Lateral Displacement from Acceleration

Once the time values for the accelerometer data were established, we commenced to find the muzzle restraint movement. Two methods were used to find and compare the lateral displacement at the muzzle restraint: direct time integration, and integration using the inverse FFT.

a. Displacement from Direct Time Integration

The trapezoidal numerical integration method was used. The trapezoidal rule for estimating the value of

$$\int_a^b f(x) dx \quad (3)$$

is based on approximating the region between the graph of the $f(x)$ and the x-axis with trapezoids of equal width. The trapezoids have the common base $h=(b-a)/n$ and the side of the trapezoid runs from the x-axis up (or down) to the curve. The area of the trapezoids add up to

$$\begin{aligned}
T &= \frac{1}{2}(f(x_0) + f(x_1)) h + \frac{1}{2}(f(x_1) + f(x_2)) h + \dots \\
&\quad \frac{1}{2}(f(x_{n-2}) + f(x_{n-1})) h + \frac{1}{2}(f(x_{n-1}) + f(x_n)) h \\
&= h \left(\frac{1}{2}f(x_0) + f(x_1) + f(x_2) + \dots + f(x_{n-1}) + \frac{1}{2}f(x_n) \right) \\
&= \frac{h}{2} (f(x_0) + 2f(x_1) + 2f(x_2) + \dots + 2f(x_{n-1}) + f(x_n))
\end{aligned} \tag{4}$$

where $f(x_0)=f(a)$ and $f(x_n)=f(b)$. The trapezoid rule estimates the integral from a to b. This approach was used to obtain the displacement from the acceleration in the time domain. The following equation describes the integration procedure.

$$\begin{aligned}
&a_i \text{ for } i = 1:40960 \\
v_{i+1} &= v_i + \frac{1}{2} (a_i + a_{i+1}) \Delta t \quad \text{for } i = 1:(40960-1) \\
x_{i+1} &= x_i + \frac{1}{2} (v_i + v_{i+1}) \Delta t \quad \text{for } i = 1:(40960-2)
\end{aligned} \tag{5}$$

where a_i are the accelerations values, v_i are the velocity values and x_i are the displacement values. Δt is the sampling rate, 1/10240 sec.

Figure 4-7 shows the results of double integrating the muzzle restraint acceleration data. From the figure, the muzzle restraint appears to have about a four meter displacement range. Also note that at time zero and before the muzzle restraint is moving. This is nonsense. The PHALANX gun is only displaced by millimeters. Therefore the displacement of interest is too small to even be seen in this figure. The displacement shown is dominated by a large, low frequency drift. Figure 4-8 shows the velocity obtained by singly integrating the accelerometer data. The actual velocity is seen in this figure as the "noise" added to the large, low frequency trend.

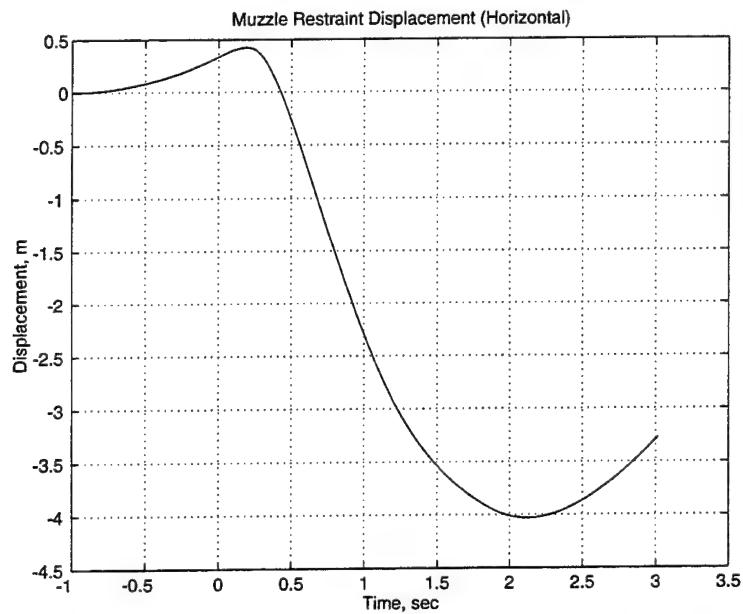


Figure 4-7 Muzzle Restraint Displacement (Horizontal) from Direct Time Integration

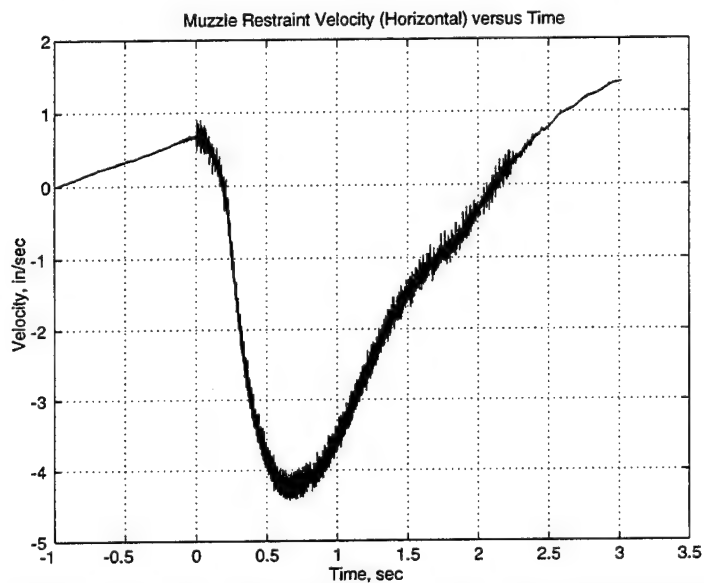


Figure 4-8 Muzzle Restraint Velocity (Horizontal) from Direct Time Integration

It is speculated that the large, low frequency drift is due to temperatures effects. Under its high firing rate, the PHALANX barrels tend to increase rapidly in temperature. When using an air gun to heat and cool an accelerometer to recreate this effect, there was

a drift of approximately 2 millivolts per degree per second. As seen in the calibration charts in Appendix E, the accelerometers have a very low sensitivity to temperature, but are sensitive to high gradient temperature changes. Other sources of the low frequency drift could be the high impact environment of the firing gun, or possibly wind effects or the electronics (accelerometers and signal analyzer).

It was necessary to remove the large, low frequency drift. The first attempt was to use the DETREND.m function in the Signal Processing Toolbox. [Ref 14, p. 2-77] Using DETREND.m, the linear trend and mean were removed from the acceleration. The linear trend was also removed from the velocity and from the displacement. Note that the displacement no longer begins at zero, and that now the muzzle restraint appears to have a displacement range of two and one-half meters. (Figure 4-9) This is a step in the right direction, but is not sufficient.

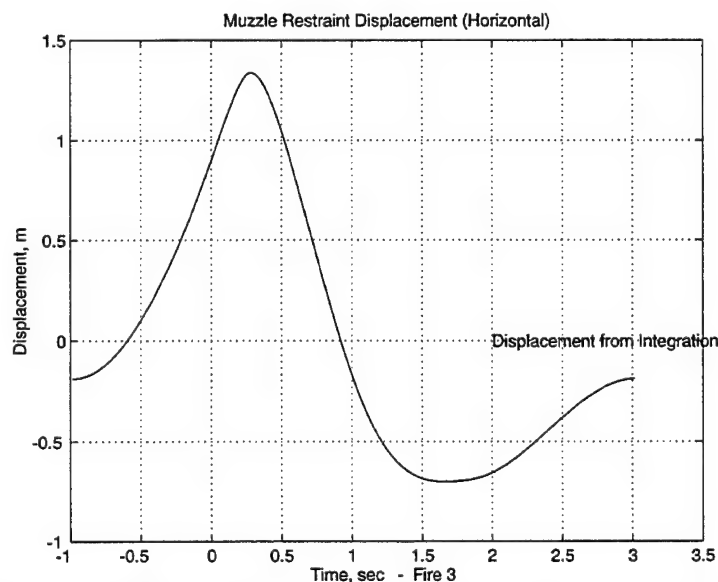


Figure 4-9 Detrended Muzzle Restraint Displacement (Horizontal) from Direct Time Integration

b. Displacement from the FFT of the Acceleration

The displacement can be obtained from the Fast Fourier Transform of the acceleration. Dividing the FFT of the acceleration by the minus frequency squared gives the FFT of the displacement. Applying the Inverse FFT function to the FFT of the displacement gives the displacement in the time domain. Equation (6) gives the expressions for acceleration, velocity and displacement in terms of the coefficients of their fourier transforms.

$$\begin{aligned}a(t) &= \sum_0^{\infty} \tilde{a}_i e^{j\omega t} \\v(t) &= \sum_0^{\infty} \tilde{v}_i e^{j\omega t} \\\xi(t) &= \sum_0^{\infty} \tilde{\xi}_i e^{j\omega t}\end{aligned}\tag{6}$$

Equation (7) shows the relationship between the coefficients of the displacement transform to the coefficients of the acceleration transform.

$$\begin{aligned}v(t) &= \frac{d\xi(t)}{dt} = \sum_0^{\infty} \tilde{\xi}_i j\omega e^{j\omega t} \\a(t) &= \frac{dv(t)}{dt} = -\sum_0^{\infty} \tilde{\xi}_i \omega^2 e^{j\omega t} \\\therefore \tilde{\xi}_i &= -\frac{\tilde{a}_i}{\omega^2}\end{aligned}\tag{7}$$

In applying this relation to obtain the fourier coefficients of the displacement, the fourier coefficient corresponding to zero frequency was set to zero. Figure 4-10 shows the FFT of the displacement for the muzzle restraint in the vertical axis. The peak of 77.29 Hertz in the FFT of the displacement is the average firing rate.

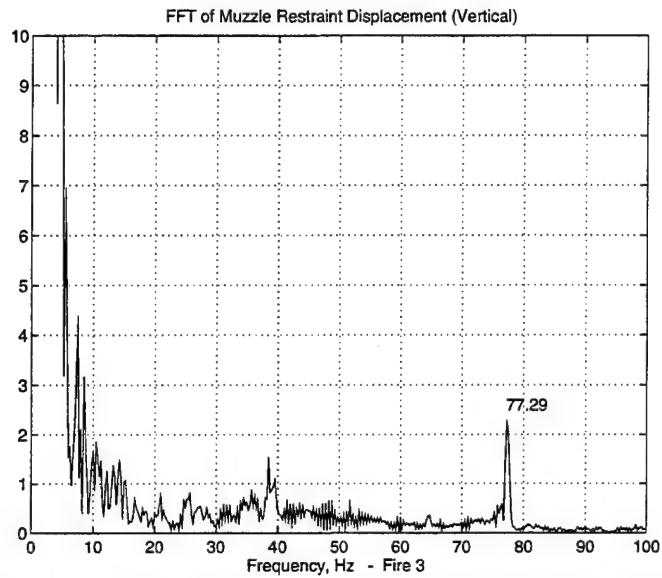


Figure 4-10 FFT of Muzzle Restraint Displacement (Vertical)

Figure 4-11 shows the muzzle restraint displacement obtained using this method.

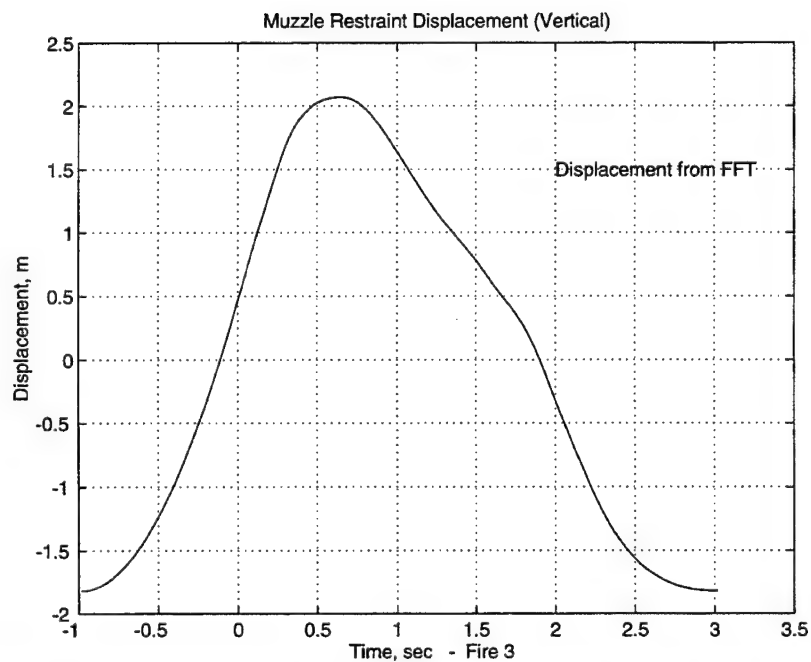


Figure 4-11 Muzzle Restraint Displacement (Vertical) from the Inverse FFT

c. Comparison of Two Integration Methods

Figure 4-12 shows the displacement curves obtained from the accelerometer data by the methods described in the preceding sections. Clearly there is a disparity between the two results. Several procedures to improve the agreement between the two were investigated. First, the acceleration was detrended prior to time integration. This was not sufficient, however. Further the mean was removed from the velocity and displacement curves for the direct time integration. This procedure resulted in excellent agreement between the two integration methods, and therefore either one could be used for further evaluation. Figure 4-13 shows these results.

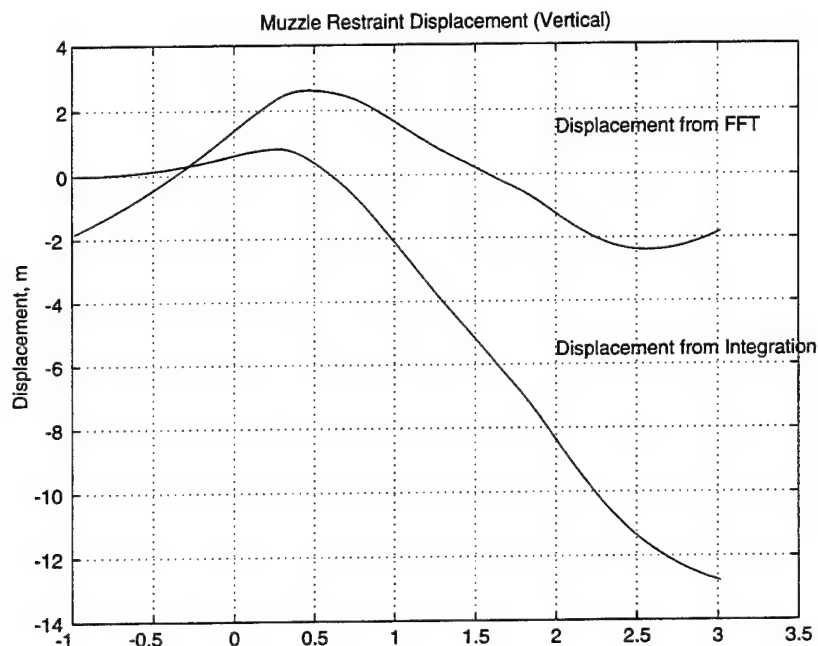


Figure 4-12 Comparison of the Two Integration Methods without Detrending

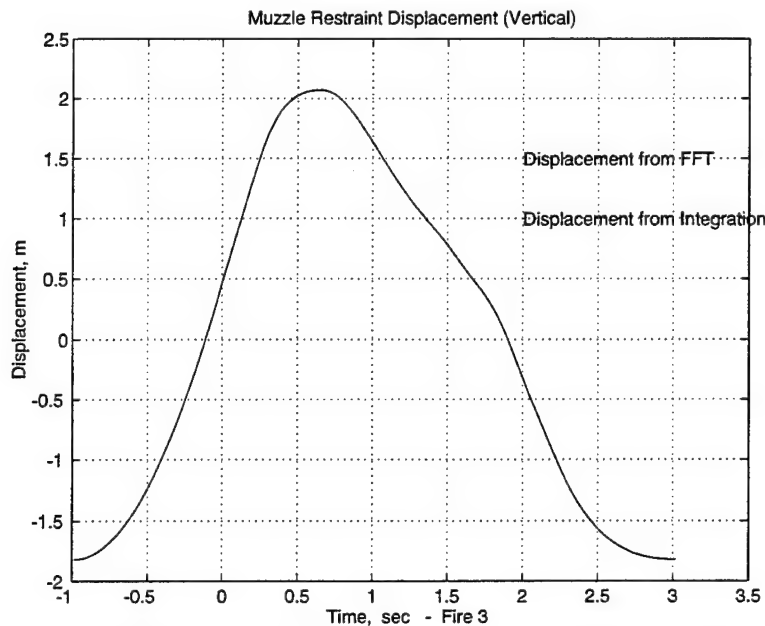


Figure 4-13 Comparison of the Two Integration Methods with Detrending.

d. Removing the Low Frequency Trend

In order to derive the "true" barrel tip displacement from the acceleration data, a means of removing the large, low frequency in the measurements was required. Initially it was thought that removing the trend from a small section of data would prove most effective.

Figure 4-14 shows the detrended displacement from 1.216 seconds to 1.413 seconds. The displacement has a range of 0.03 inches or 0.762 millimeters. These values are much closer to the actual movement of the gun. The integration of the entire record does not show the true displacement. By forcing the integration on a small section when the gun was at steady firing rate, the displacement can be obtained. Three methods were investigated in order to obtain the "true" displacement for the entire record: time and frequency windowing, global polynomial approximation and cubic spline smoothing.

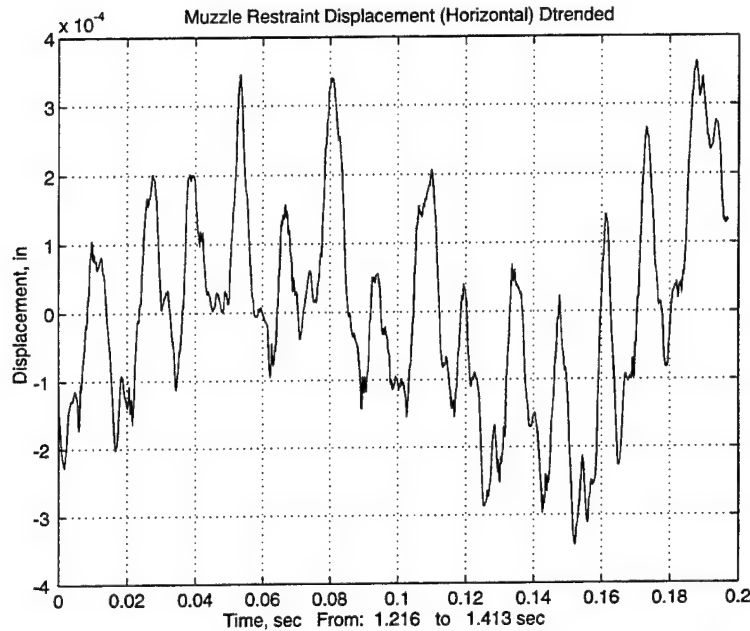


Figure 4-14 Detrended Displacement from 1.216 to 1.413 Seconds

(1) Time and Frequency Windowing. The possibility of removing the trend from a time windowed record by a high pass filter in the frequency domain was investigated. Two window functions were created, one in the time domain, TIMWIN.m (Appendix F) and one in the frequency domain, FREQWIN.m (Appendix G). They allowed for a smooth transition from zero to a desired value. These window functions are composed of a half cosine and half sine. Figure 4-15 is an example of a normalized half cosine and half sine window functions. This function was applied to the acceleration data in the time domain to effect a time window or to FFT data in the frequency domain to effect a high-pass filter. (In MATLAB, the FFT includes negative frequencies; small negative frequencies occur at the end of the FFT record). [Ref 15]

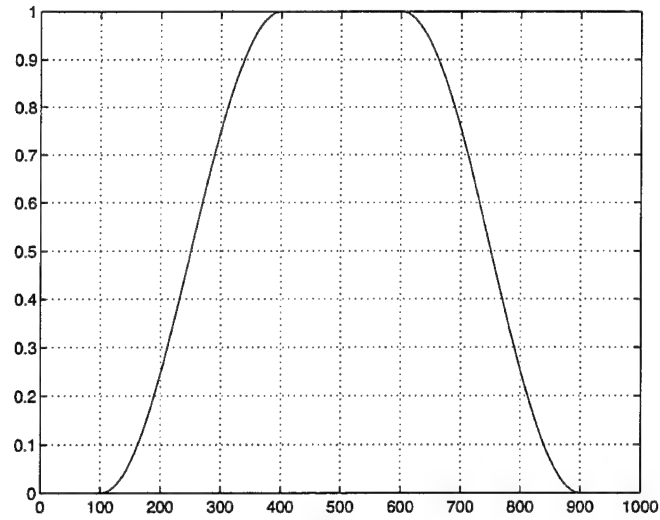


Figure 4-15 Window Function

Figure 4-16 shows the time domain window function applied to the muzzle restraint acceleration for 1.5 to 2 seconds.

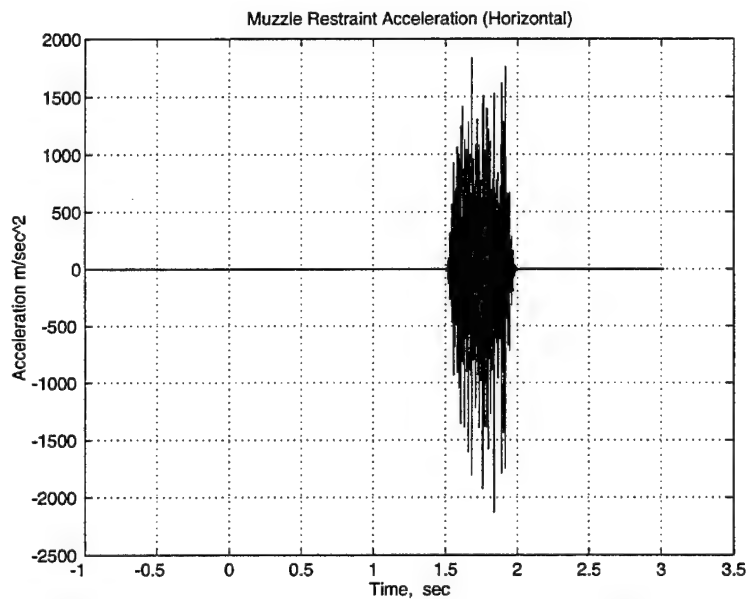


Figure 4-16 Time-Windowed Muzzle Restraint Acceleration (Horizontal) From 1.5 to 2 Seconds

In Figure 4-17 the frequency domain window was applied to the FFT of the acceleration, then it was divided by omega squared, the result is the windowed FFT of the displacement. The FREQWIN.m function could not be used above three hertz since the

first mode of vibration is 3.4 Hz as identified in the Finite Element Model. [Ref 16] The use of these functions, although helpful in concentrating on one region, could not be applied to the entire record. Windowing had to be abandoned because in order to remove the low frequency drift, a lot of the data had to be excluded. It was not the right approach.

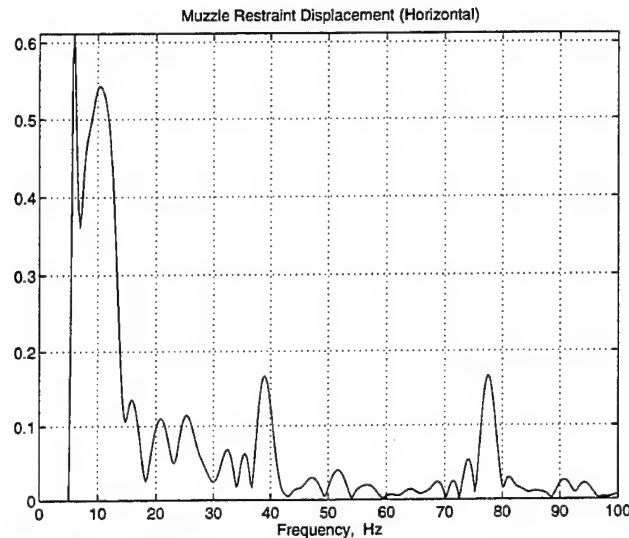


Figure 4-17 Frequency-Windowed FFT of the Muzzle Restraint Displacement (Horizontal)

(2) Global Polynomial Approximation. The second method used to remove the low frequency drift was polynomial approximation. Polynomials are the approximating functions of choice when a smooth function is to be approximated locally. [Ref 17, p. 1-3] A relatively small data set can be approximated smoothly but as the interval gets larger, the degree of the approximating polynomial may be unacceptably large. For the muzzle restraint acceleration, a twelfth order polynomial did not provide a good enough approximation. It was not possible to fit polynomials of higher order to the displacement curve due to memory problems. Figure 4-18 shows a twelfth order polynomial fit of the displacement curve and the difference between the two on the same scale.

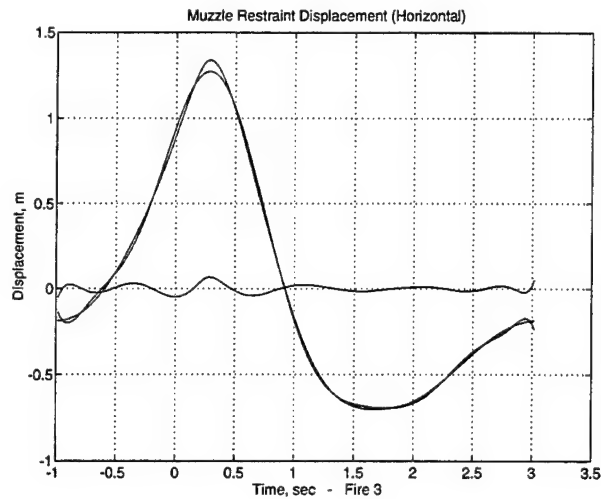


Figure 4-18 Twelfth Order Polynomial Fit to the Displacement Data

Figure 4-19 is the difference from the fitted polynomial and the displacement curve. A twelfth order polynomial is not a good approximation, since the barrel tip does not move over a one centimeter range.

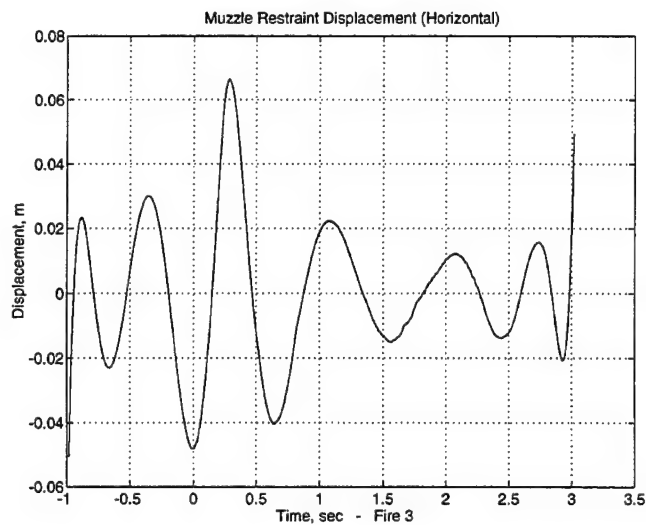


Figure 4-19 Barrel Tip Displacement Extracted from Twelfth Order Polynomial Fit to the Displacement Data

(3) Cubic Spline Approximation. An alternative to a polynomial approximation is to subdivide the interval of approximation into sufficiently small intervals. On each such interval, a polynomial of relatively low degree can provide a good approximation. A cubic spline is a smooth piecewise polynomial, where the derivatives of each polynomial pieces blend smoothly. I.J. Schoenberg coined this term since a twice continuously differentiable cubic spline (with a sufficiently small first derivative) approximates the shape of a draftsman's spline. [Ref 18, p. 1-3]

The CSAPS.m command in the Spline Toolbox [Ref 19, p. 2-13], constructs a cubic smoothing spline s to a given data x, y . It is constructed for the specified smoothing parameter p . For $p=0$, this is a least-squares straight line fit to the data, while on the other extreme, i.e., for $p=1$, this the "natural" cubic spline interpolant. [Ref 20, p.2-13] As p moves from 0 to 1, the smoothing spline changes from one extreme to the other. The interesting range of p is often near $1/(1+h^3/16)$, with h the average spacing of the data abscissae. For the accelerometer data $h=1/10240$, or the sampling rate. Since the data are uniformly spaced, the smoothing spline is expected to follow the data closely for $p=1/(1+h^3/16*10)$ and to provide satisfactory smoothing when $p=1/(1+h^3/16/10)$.

CSAPSTXY.m, Appendix H, is code that applies the CSAPS.m command to the muzzle restraint displacement curves for the horizontal and vertical directions. It plots the displacement curve obtained from direct integration along with the cubic spline approximation. Figure 4-20 shows the results with a smoothing parameter $p=1/(1+h^3/16/10)=0.999...$. The two curves are on top of each other.

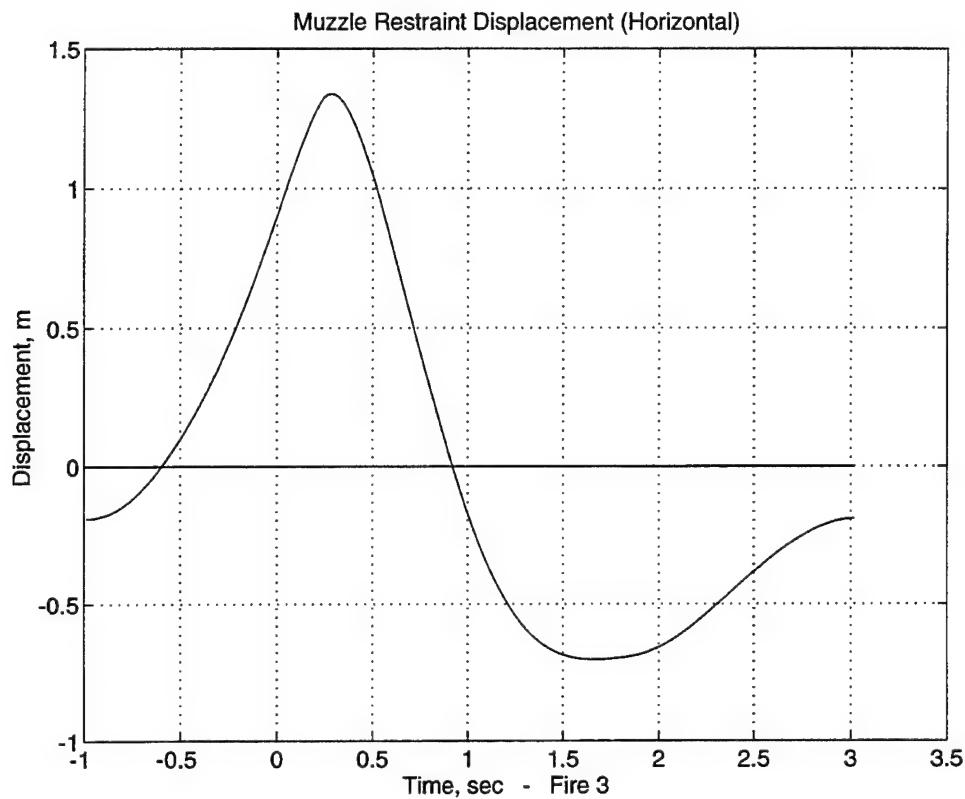


Figure 4-20 Cubic Spline Smoothing of the Displacement Data

Figure 4-21 shows a small section of the curve with an expanded vertical scale, and it shows how this cubic approximation is not smooth enough. Figure 4-22 shows the difference between the displacement curve and the cubic smoothing. It shows a displacement range of four microns. Since the barrel tip is displaced about a millimeter, the cubic smoothing parameter was too large, and the data followed too closely. The smoothing parameter needed to be adjusted.

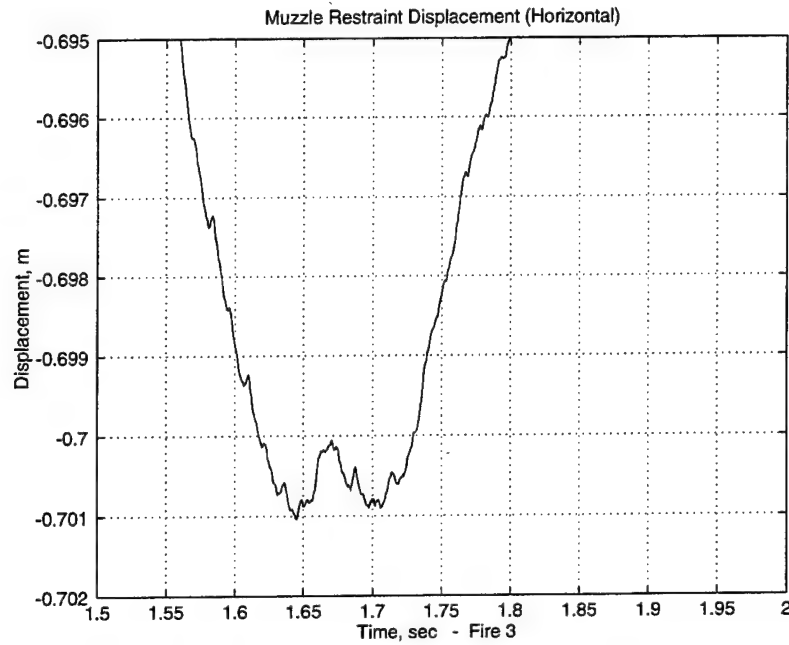


Figure 4-21 Zoom of the Cubic Smoothing Approximation. Obtained using CSAPS.m
The Smoothing Parameter $p=0.999999999999418$

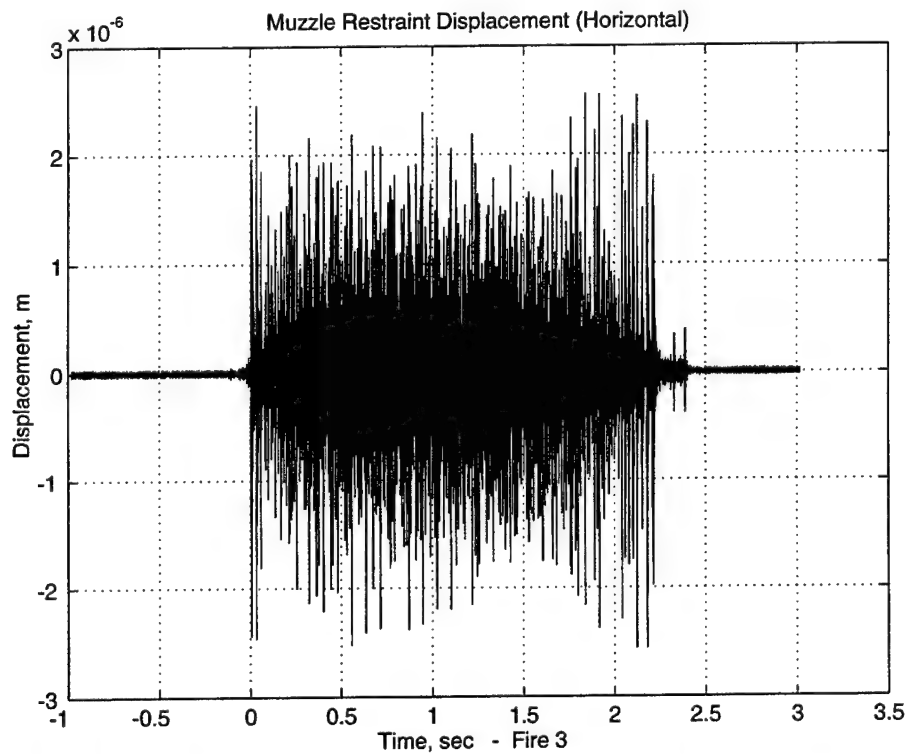


Figure 4-22 Muzzle Restraint Displacement (Horizontal) Extracted Using Cubic Smoothing of the Displacement Data

Through trial and error the smoothing parameter was decreased in order to achieve a "more" smooth approximation. The smoothing parameter needed to be decreased by a factor of one billion, for an appropriate smoothing. The final smoothing parameter chosen was equal to 0.9999417957270211. Figure 4-23 shows a section of the cubic smoothing spline approximation on the displacement curve.

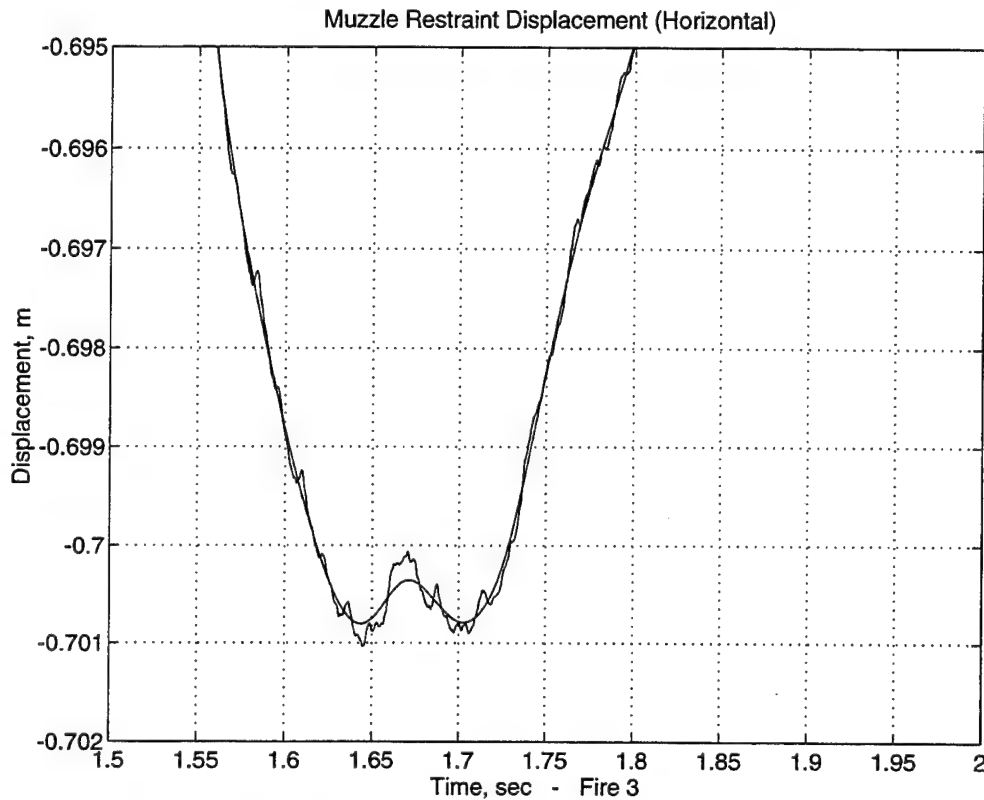


Figure 4-23 Zoom of the Cubic Smoothing Approximation. Obtained using CSAPS.m. The smoothing parameter $p=0.9999417957270211$.

Figures 4-24 and 4-25 show the difference between the cubic smoothing approximation and the displacement curves for the horizontal and vertical direction at the muzzle restraint. The range of displacement obtained is very reasonable. It is expected for the vertical direction to have a larger range in the displacement than in the horizontal direction

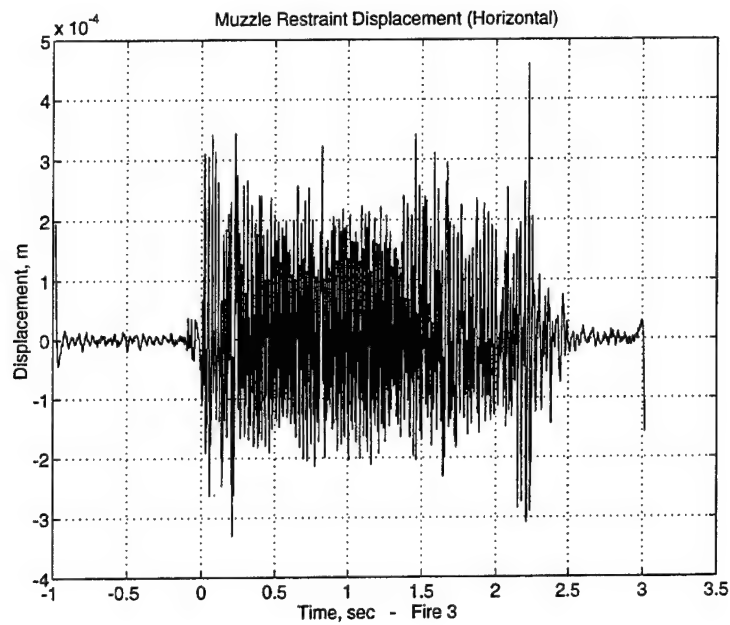


Figure 4-24 Muzzle Restraint Displacement (Horizontal) Extracted Using Cubic Smoothing on the Displacement Data

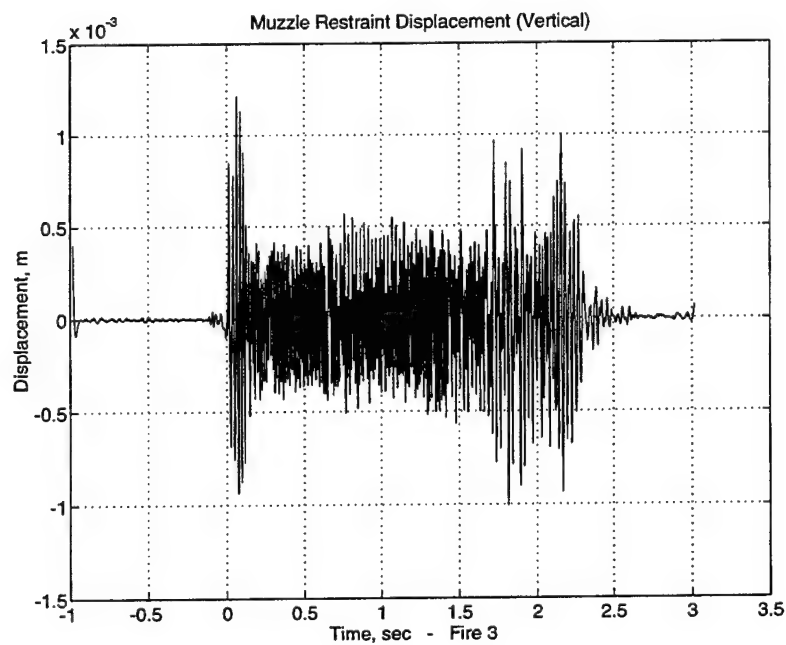


Figure 4-25 Muzzle Restraint Displacement (Vertical) Extracted Using Cubic Smoothing on the Displacement Data

Examination of a small section of the time line reveals some details about the PHALANX while firing. Figure 4-26 is a plot of the horizontal displacement for one tenth of a second. It shows each round firing and the subsequent ringing. Figure 4-27 shows the vertical displacement for the same period of time. The shots are not as clear as in the horizontal direction, but the curve gives a rough indication of the number of rounds fired in one tenth of second or an average firing rate of 77 rounds per minute.

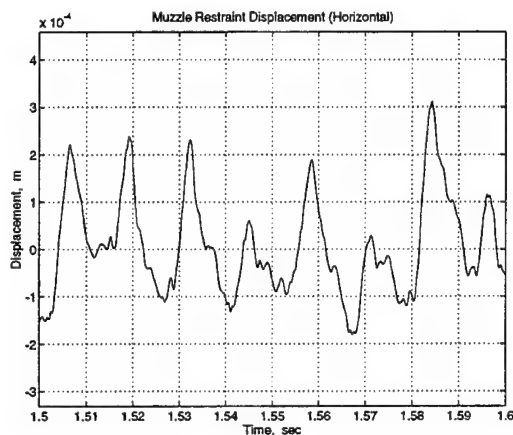


Figure 4-26 Muzzle Restraint Displacement (Horizontal) From 1.5 to 2 Seconds

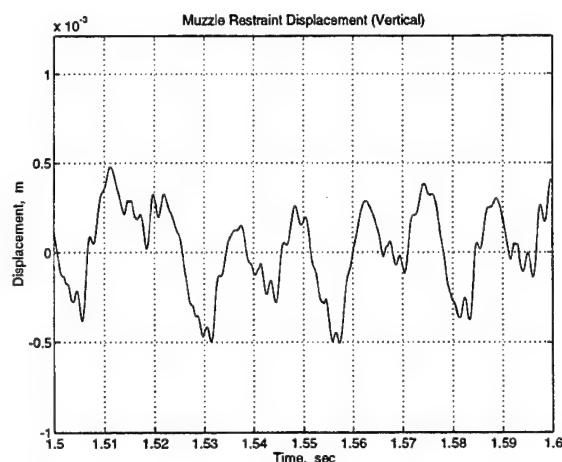


Figure 4-27 Muzzle Restraint Displacement (Vertical) From 1.5 to 2 Seconds

Figure 4-28 gives an insight on the movement of the gun while its firing. Besides the displacement being larger in the vertical direction, it leads the horizontal movement. This can be explained by the firing action of PHALANX. The firing sequence begins about twelve to fourteen degrees before top dead center creating an imbalance, thus the smaller horizontal displacement.

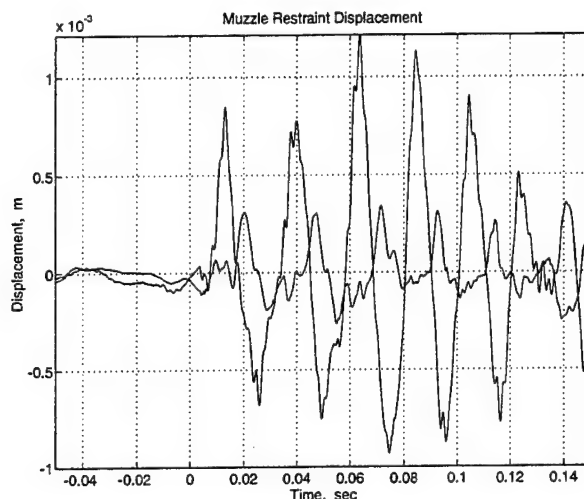


Figure 4-28 Difference Between the Horizontal and Vertical Displacement

C. CORRELATION OF DISPERSION DATA AND BARREL TIP LATERAL DISPLACEMENT

Figure 4-29 shows the time of each round fired obtained from the dispersion data shown as vertical lines. Also shown is the derived vertical barrel tip displacement. It is evident from the figure that there is good correspondence between firing time and maximum vertical displacement. Figure 4-30 shows the time of each round superimposed over the horizontal barrel tip displacement. Note the lag in the maximum displacement after each firing. From these figures it is evident that when a round is fired most of the force is in the vertical direction. But due to the construction of the gun system, horizontal vibration is later excited. Also note the best estimated time of bullet firing obtained from CROSSCORR.m does not quite coincide with the time of the maximum vertical displacement. For future work it would be necessary to recalculate the time of the first round using the vertical displacement instead of the acceleration.

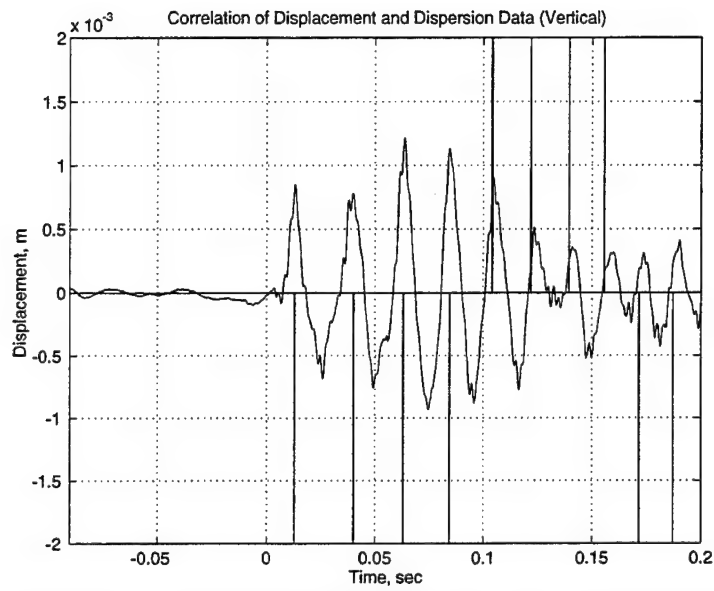


Figure 4-29 Correlation of Barrel Tip Displacement and Dispersion Data (Vertical)

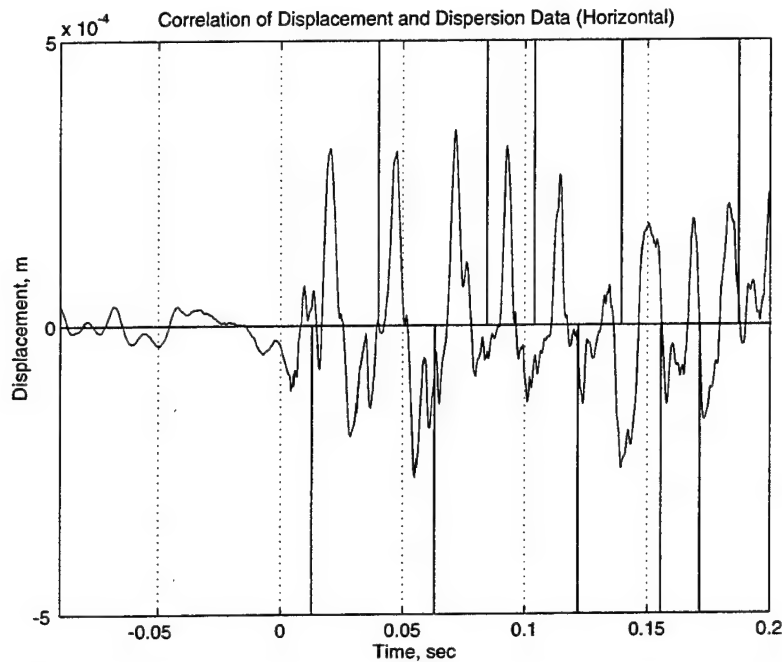


Figure 4-30 Correlation of Barrel Tip Displacement and Dispersion (Horizontal)

Figures 4-31 and 4-32 were made to investigate further the correlation of barrel tip motion with bullet dispersion. In figure 4-31 is plotted the vertical dispersion, in radians, against the vertical barrel tip displacement occurring at the estimated time of bullet firing, also in radians. Figure 4-32 shows the same for the horizontal direction. If there were good correlation between the two displacements plotted, one would expect the data points to lie close to a line of slope one. There is no such correlation agreement in Figures 4-31 and 4-32. This suggests that further refinement of the procedure to extract the barrel tip displacement from the accelerometer data is needed. This will be the subject to follow-on investigation.

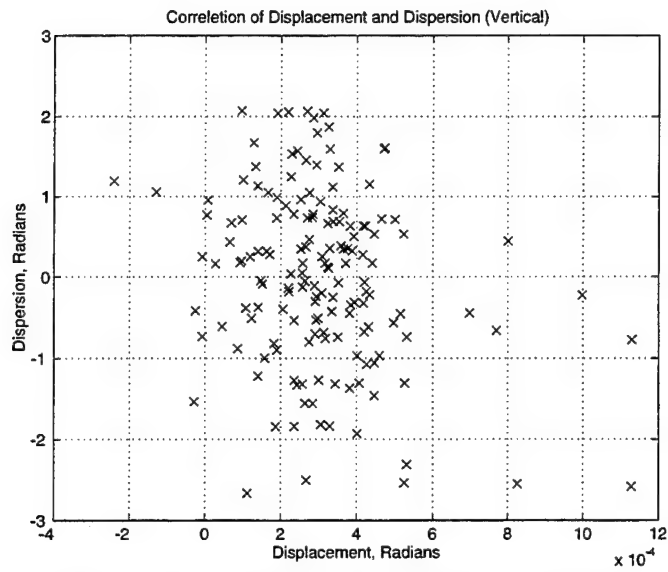


Figure 4-31 Dispersion Correlation (Vertical)

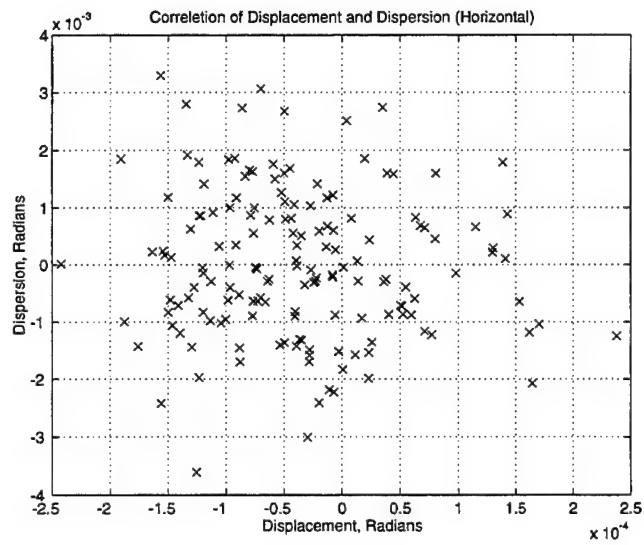


Figure 4-32 Dispersion Correlation (Horizontal)

V. CONCLUSIONS

The objective of this body of work was to correlate the barrel tip transverse displacement with bullet dispersion. The displacement was derived from accelerometer data obtained from a firing PHALANX gun system with the production muzzle restraint installed. From the data collection and analysis, many difficulties were uncovered in measuring the motion of the gun and its influence on dispersion. In order to correlate dispersion with displacement, it was necessary to time-align the measured dispersion with the measured acceleration. This study also gave an insight into the PHALANX gun motion while firing.

Due to a large, low frequency drift in displacement caused by a combination of electronics, environment and temperature, the "true" displacement of the barrel tip was best estimated by subtracting out a smooth trend using cubic splines. Although there was a good correlation between the time of firing obtained from the dispersion and the time of maximum vertical displacement, correlation between dispersion data and extracted lateral barrel tip displacement was disappointing.

While the results of the present investigation did not show the correlation that was hoped for, it is still expected that good correlation can be found between bullet dispersion and properly extracted lateral barrel tip displacement. To that end, the following suggestions are made for further investigation. One, a potentially significant source of error is the correspondence between the times of bullet firings and accelerometer time data. What is needed most is a reliable firing pin signal. It is suggested that repairing this signal be given high priority. Two, further investigation of the best way to subtract the large, low frequency trend in the displacement obtained from the accelerometer data is needed. Cubic spline smoothing appears to be the best method, as was demonstrated in the present investigation. However, more investigation is needed of how to optimally choose the smoothing parameter. Third, if some means could be found to measure lateral barrel tip motion using non-contacting transducers, such as a proximity probe or a laser vibrometer, then the problem of the large low frequency drift, if it is related to

temperature, might be lessened.

APPENDIX A. DISPERSION DATA

This appendix contains the dispersion data obtained at Naval Air Weapons Station, China Lake, CA. The Oehler System 82, was used to collect the dispersion data from a firing PHALANX gun system.

"OEHLER SYSTEM 82, VERSION 4.3, PHONE 512-327-6900"

DATE = 94-05-31 11:45H O.K. ? _

ENTER ID (LESS THAN 80 CHARACTERS)

"053194d3, 4500spm, 100rds, prod muz rest, h7-h12_"

O.K. ? _

SLOW FIRE ? N

MACHINE GUN ? _

DISTANCE = 10 ? _

MINIMUM VELOCITY = 2000 ? 3300_

MINIMUM VELOCITY = 3300 ? _

MAX RATE OF FIRE = 6000 ? 5000_

MAX RATE OF FIRE = 5000 ? _

TARGET SIZE = 72.6 IN ? _

TEMPERATURE = 70 DEG F ? 86_

TEMPERATURE = 86 DEG F ? _

RANGE = 600 FT ? 83_

RANGE = 83 FT ? _

IMPACT VELOCITY = 2800 FT/SEC ? 3600_

IMPACT VELOCITY = 3600 FT/SEC ? _

SIGNAL LEVEL = 30 ? 60_

SIGNAL LEVEL = 60 ? _

"053194d3, 4500spm, 100rds, prod muz rest, h7-h12"

OEHLER SYSTEM 82 94-05-31 11:45H MACHINE GUN CHRONOGRAPH

DISTANCE = 10 MIN VEL = 3300 MAX ROF = 5000 TGT TEMP = 86

FRAME = 72.6 IN SIGNAL = 60 TGT VEL = 3600 RANGE = 83

11:45H COMMENT: 053194d3_

-

FIRE BURST...THEN TYPE A SPACE

ROUND	EPOCH	A.TIME	VEL	RND/M	HORIZ	VERT	TIME2
1	0	0	0	0	-5.272	-1.176	0
2	0.02722	0	0	2204	-3.29	0.716	0
3	0.05019	0	0	2611	-5.512	-1.21	0
4	0.07153	0	0	2811	-3.175	0.602	0
5	0.09116	0	0	3055	-4.004	1.817	0
6	0.10893	0	0	3377	-5.267	3.413	0
7	0.12652	0	0	3411	-5.05	1.422	0
8	0.1428	0	0	3686	-5.244	2.506	0
9	0.15882	0	0	3744	-5.992	-0.465	0
10	0.17451	0	0	3823	-3.933	0.839	0
11	0.18966	0	0	3959	-3.911	1.326	0
12	0.20427	0	0	4107	-6.067	2.08	0
13	0.21899	0	0	4076	-5.897	0.989	0
14	0.23366	0	0	4090	-5.165	1.807	0

15	0.24752	0	0	4329	-5.516	-1.29	0
16	0.26206	0	0	4126	-4.235	-1.131	0
17	0.27604	0	0	4290	-4.487	0.864	0
18	0.28977	0	0	4371	-5.506	2.205	0
19	0.30349	0	0	4371	-4.478	1.194	0
20	0.31702	0	0	4433	-3.97	2.165	0
21	0.33057	0	0	4428	-4.436	1.177	0
22	0.34402	0	0	4460	-3.089	2.06	0
23	0.35732	0	0	4512	-3.755	3.244	0
24	0.37052	0	0	4544	-4.418	3.437	0
25	0.38394	0	0	4471	-4.973	1.727	0
26	0.39723	0	0	4514	-3.752	2.424	0
27	0.41025	0	0	4608	-3.942	0.576	0
28	0.42332	0	0	4592	-2.741	1.747	0
29	0.43658	0	0	4524	-5.015	1.727	0
30	0.44972	0	0	4565	-5.903	2.623	0
31	0.46244	0	0	4719	-6.064	1.543	0
32	0.47552	0	0	4587	-5.641	2.831	0
33	0.48884	0	0	4504	-4.316	1.262	0
34	0.50171	0	0	4660	-3.711	1.322	0
35	0.51469	0	0	4623	-4.5	1.3	0
36	0.5273	0	0	4756	-5.981	3.415	0
37	0.54036	0	0	4595	-5.749	2.42	0
38	0.55341	0	0	4594	-5.692	2.907	0
39	0.56648	0	0	4593	-5.282	0.059	0
40	0.57944	0	0	4626	-3.767	1.25	0
41	0.59242	0	0	4623	-4.282	1.542	0
42	0.60521	0	0	4692	-6.261	3.172	0
43	0.61812	0	0	4647	-5.499	1.544	0
44	0.63114	0	0	4608	-5.268	1.536	0
45	0.64378	0	0	4745	-4.743	0.406	0
46	0.65687	0	0	4584	-4.622	2.007	0
47	0.66955	0	0	4730	-4.88	0.635	0
48	0.6829	0	0	4495	-4.895	2.363	0
49	0.6956	0	0	4724	-6.051	1.48	0
50	0.70858	0	0	4621	-4.942	2.045	0
51	0.72152	0	0	4636	-4.606	1.761	0
52	0.73416	0	0	4747	-4.451	2.152	0
53	0.74735	0	0	4549	-3.933	0.635	0
54	0.76055	0	0	4546	-5.469	1.625	0
55	0.77319	0	0	4746	-5.114	1.155	0
56	0.7862	0	0	4609	-5.067	3.444	0
57	0.79917	0	0	4628	-5.923	-0.939	0
58	0.81213	0	0	4629	-4.065	1.41	0
59	0.82514	0	0	4610	-4.457	0.758	0
60	0.83762	0	0	4809	-6.111	3.05	0
61	0.85074	0	0	4570	-5.738	1.544	0
62	0.8638	0	0	4597	-3.873	1	0
63	0.87656	0	0	4702	-4.756	0.919	0

64	0.88965	0	0	4582	-3.798	2.946	0
65	0.90228	0	0	4748	-4.333	1.05	0
66	0.91539	0	0	4576	-5.647	2.259	0
67	0.92812	0	0	4714	-5.011	2.002	0
68	0.94097	0	0	4669	-5.101	1.693	0
69	0.95385	0	0	4659	-5.479	2.527	0
70	0.96685	0	0	4613	-4.23	1.838	0
71	0.97993	0	0	4588	-4.584	1.647	0
72	0.99282	0	0	4655	-5.494	3.357	0
73	1.00535	0	0	4788	-7.181	1.195	0
74	1.01849	0	0	4565	-5.163	2.748	0
75	1.03124	0	0	4705	-5.56	0.317	0
76	1.04429	0	0	4598	-4.904	1.651	0
77	1.05712	0	0	4675	-5.126	1.905	0
78	1.07	0	0	4659	-6.769	0.672	0
79	1.08283	0	0	4675	-5.309	2.086	0
80	1.09583	0	0	4613	-5.808	0.867	0
81	1.10876	0	0	4639	-5.68	0.3	0
82	1.12171	0	0	4635	6.474	12.329	0
83	1.13452	0	0	4684	-4.201	0.809	0
84	1.14755	0	0	4604	-5.763	2.153	0
85	1.16036	0	0	4682	-5.344	1.875	0
86	1.17342	0	0	4594	-5.562	1.718	0
87	1.18634	0	0	4641	-5.67	1.062	0
88	1.19924	0	0	4654	-3.758	0.843	0
89	1.21225	0	0	4611	-4.824	0.698	0
90	1.22496	0	0	4719	-5.78	2.111	0
91	1.23794	0	0	4624	-4.065	1.309	0
92	1.2509	0	0	4627	-4.673	2.007	0
93	1.26402	0	0	4575	-4.837	1.236	0
94	1.27682	0	0	4684	-3.821	1.695	0
95	1.28986	0	0	4601	-4.509	0.106	0
96	1.30268	0	0	4681	-5.096	2.061	0
97	1.31576	0	0	4585	-6.078	0.008	0
98	1.32881	0	0	4600	-5.341	0.618	0
99	1.34154	0	0	4711	-4.671	0.047	0
100	1.3544	0	0	4665	-4.358	1.626	0
101	1.36708	0	0	4734	-4.841	1.122	0
102	1.37985	0	0	4698	-5.696	2.971	0
103	1.39286	0	0	4611	-5.52	1.718	0
104	1.40601	0	0	4563	-6.452	3.43	0
105	1.41905	0	0	4598	-5.094	0.068	0
106	1.43151	0	0	4815	-7.604	2.491	0
107	1.44458	0	0	4592	-6.462	1.69	0
108	1.45823	0	0	4395	-5.264	2.968	0
109	1.47066	0	0	4827	-5.88	1.285	0
110	1.48355	0	0	4653	-6.023	2.335	0
111	1.49666	0	0	4577	-5.572	0.947	0
112	1.50948	0	0	4681	-5.187	1.134	0

113	1.52248	0	0	4614	-5.263	1.549	0
114	1.53527	0	0	4689	5.118	13.656	0
115	1.54833	0	0	4596	-6.146	0.558	0
116	1.56149	0	0	4558	-5.226	0.927	0
117	1.57391	0	0	4831	-6.524	-0.465	0
118	1.58703	0	0	4571	-4.168	-0.555	0
119	1.59959	0	0	4778	-5.338	2.582	0
120	1.61268	0	0	4585	-6.601	1.031	0
121	1.62558	0	0	4650	-6.631	0.765	0
122	1.63876	0	0	4552	-5.647	2.107	0
123	1.65169	0	0	4638	-5.941	0.101	0
124	1.66465	0	0	4631	-4.648	1.905	0
125	1.67718	0	0	4785	-6.172	0.642	0
126	1.69019	0	0	4613	-6.178	2.106	0
127	1.70343	0	0	4530	-5.675	0.059	0
128	1.71609	0	0	4740	-4.82	2.986	0
129	1.7287	0	0	4758	-5.794	1.624	0
130	1.7419	0	0	4544	-2.903	-0.441	0
131	1.75461	0	0	4722	-4.911	2.43	0
132	1.76804	0	0	4465	-6.352	1.073	0
133	1.78088	0	0	4672	-6.018	0.693	0
134	1.79375	0	0	4664	-4.706	2.77	0
135	1.80654	0	0	4691	-4.596	2.143	0
136	1.81993	0	0	4480	-4.234	2.309	0
137	1.83273	0	0	4687	-4.638	2.567	0
138	1.84554	0	0	4684	-5.72	2.094	0
139	1.8585	0	0	4629	-4.487	-0.178	0
140	1.87149	0	0	4618	-6.088	2.33	0
141	1.88452	0	0	4604	-4.577	0.377	0
142	1.89762	0	0	4579	-5.077	0.068	0
143	1.91051	0	0	4656	-3.933	0.957	0
144	1.9234	0	0	4654	-6.257	1.496	0
145	1.93645	0	0	4597	-6.134	0.156	0
146	1.94943	0	0	4622	-5.241	2.036	0
147	1.96305	0	0	4405	-4.987	-0.157	0
148	1.97636	0	0	4505	-4.359	0.406	0
149	1.9901	0	0	4369	-4.858	1.57	0
150	2.00493	0	0	4045	-5.432	2.743	0
151	2.02053	0	0	3845	-6.76	0.477	0
152	2.03734	0	0	3567	-5.466	0.495	0
153	2.05527	0	0	3347	-3.137	-0.462	0
154	2.07477	0	0	3077	-3.895	0.978	0
155	2.09557	0	0	2884	-4.457	-1.164	0
156	2.11907	0	0	2553	-5.683	0.93	0
157	2.14536	0	0	2282	-3.801	1.148	0
158	2.17518	0	0	2011	-3.129	-0.182	0
159	2.2044	0	0	2053	-5.213	-0.085	0
160	4.3306	0	0	28	20000	20000	0
161	4.49671	0	0	361	20000	20000	0

SUMMARY: RNDS 1 - 161 2134 RND/M
MEAN STD DEV MAX MIN RANGE
VELOCITY 0 0 0 0
HORIZONTAL -4.925 1.512 6.474 -7.604 14.078
VERTICAL 1.52 1.684 13.656 -1.29 14.946
RADIAL 2.263

RNDS 1 - 159 4300
RNDS 160 - 161 361

"ENTER SUB-BURST START AND END ROUND NUMBERS SEPARATED BY A COMMA 12,81_"

SUMMARY: RNDS 12 - 81 4577 RND/M
MEAN STD DEV MAX MIN RANGE
VELOCITY 0 0 0 0
HORIZONTAL -4.975 0.854 -2.741 -7.181 4.44
VERTICAL 1.632 1.015 3.444 -1.29 4.734
RADIAL 1.327

"ENTER SUB-BURST START AND END ROUND NUMBERS SEPARATED BY A COMMA 83,113_"

SUMMARY: RNDS 83 - 113 4639 RND/M
MEAN STD DEV MAX MIN RANGE
VELOCITY 0 0 0 0
HORIZONTAL -5.265 0.831 -3.758 -7.604 3.845
VERTICAL 1.474 0.875 3.43 0.008 3.422
RADIAL 1.207

"ENTER SUB-BURST START AND END ROUND NUMBERS SEPARATED BY A COMMA 115,150_"

SUMMARY: RNDS 115 - 150 4599 RND/M
MEAN STD DEV MAX MIN RANGE
VELOCITY 0 0 0 0
HORIZONTAL -5.306 0.874 -2.903 -6.631 3.728
VERTICAL 1.217 1.077 2.986 -0.555 3.541
RADIAL 1.387

ENTER SUB-BURST START AND END ROUND NUMBERS SEPARATED BY A COMMA _

"11:45H COMMENT: dispersion 0.93, 2 flyers_"

APPENDIX B. CROSS CORRELATION CODE

This appendix contains the cross correlation code used to better estimate the time of the first round. The intent was to use the XCORR.m function in the Signal Processing Toolbox. XCORR.m cross correlates two files using the following equation.

$$C_{\text{unc}}(m) = \frac{1}{N - |m|} \sum_{n=0}^{N-|m|} x(n) y^*(n+m) \quad (1)$$

Due to the size of the files there were memory problems, and the command function XCORR.m had to be modified. CROSSCORR.m, is a modified version of the function. The purpose of CROSSCORR.m is to obtain a better estimate of the time of the first round fired. CROSSCORR.m uses the rough estimated from THRESHOLD.m as a bench mark to cross correlate the times between the accelerometers and dispersion. For cross correlation two files are used. One is the sum of the squares of the horizontal and vertical muzzle restraint accelerations. The second contains the time of each round and its horizontal and vertical dispersion. CROSSCORR.m cross correlates for three hundred values around the rough estimate, fifty prior and two hundred and fifty after. It uses the following equation to cross correlate

$$xcor = \frac{1}{40,960 - |m|} \sum_{n=1}^{40960-|m|} xcor(m,1) + x(n,1) * batacc(n+m,1) \quad (2)$$

where m is the value for the bin around the rough estimate, and batacc is the sum of the squares. The correlated time is used as the best estimate of when the PHALANX gun began to fire.

```

% crosscorr.m
% Calculate when the first bullet is fired by using the xcorr function in the Signal Processing Toolbox

clear all;
plt;

load batx
xsense=9.73/1000;    % V/g
xscale=1/(xsense/386); % in/sec^2 per V
batx=xscale*batx;
tinc=1/10240;
ttotal=(length(batx)-1)*tinc;
tx=0:tinc:ttotal;

load baty;
ysense=9.63/1000;    % V/g
yscale=1/(ysense/386); % in/sec^2 per V
baty=yscale*baty;
tinc=1/10240;
ttotal=(length(baty)-1)*tinc;
ty=0:tinc:ttotal;
t=tx;

batacc=(batx.^2 + baty.^2); % Sum of the Squares
plot(t,batacc)
title('Sum of the Squares (Muzzle Restraint)')
xlabel(['Time, sec ',num2str(date)])
ylabel('Acceleration ^2, (in/sec^2)^2')
grid
pause

load firedata3;
for i=1:159
    firedata3(i,1)=firedata3(i,1)*10240+10117;
end
shott=zeros(40960,3);
for i=1:159
    j=round(firedata3(i,1));
    shott(j,1)=firedata3(i,1);

```

```

shott(j,2)=firedata3(i,2);
shott(j,3)=firedata3(i,3);
end

```

```

x=zeros(size(batx));

```

```

for i=1:40960
    if abs(shott(i,2)) > 0;
        x(i)=1;
    end
end
plot(t,x)
title('Normalized Dispersion Displacement')
xlabel(['Time, sec ',num2str(date)])
ylabel('Normalized Displacement')
grid
pause

```

```

clear batx batx1 batx2 batx3 batx4 batx5 batx6 batx7 batx8 batx9 batx10
clear baty baty1 baty2 baty3 baty4 baty5 baty6 baty7 baty8 baty9 baty10
clear xsense ysense xscale yscale tx ty ttotal firedata3 shott

```

```

% Estimate the cross-correlation between the firedata3 and the sum of the squares of the muzzle restraint acceleration
(vertical and horizontal)

```

```

tinput=input('Enter the estimated time of the first bullet firing ');

```

```

bin=round(tinput/tinc);

```

```

bin

```

```

for m=bin-50:bin+250

```

```

    m

```

```

        xcor(m,1)=0.0;

```

```

        for n=1:40960-abs(m)

```

```

            xcor(m,1)=xcor(m,1)+x(n,1)*batacc(n+m,1);

```

```

        end

```

```

xcor(m,1)=xcor(m,1)/(40960-abs(m));

```

```

end

```

```

xcor(bin-50:bin+250)*tinc;

```

```

[maxcor,mmaxcor]=max(xcor)

```

```

bullet=(mmaxcor+1)/10240

```

```
plot(xcor(bin-50:bin+250)*tinc)
title('Cross Correlation Between Firedata3 & batacc')
xlabel('Bin Number')
ylabel('Cross Correlation')
text(115,700, ['First Bullet Time ',num2str(bullet)])
grid
```

APPENDIX C. GTESTFFT.M

This appendix contains the modified code written by Mike Hatch. GTESTFFT.M converts the acceleration from volts to meters/second². It also computes the normalized FFT. It plots the acceleration versus time and the normalized FFT versus frequency.

```

% gtestfft.m calculate the fft of forcing function
clear all;
plt;

load afty.mat;
ysense = 10.25/1000;      % V/g
yscale = 1/(0.102);      % m/sec^2/g
ysense=yscale/ysense;
afty=ysense*afty;
tinc = 1/10240;
ttotal = (length(afty)-1)*tinc;
ty = 0:tinc:ttotal;
plot(ty,afty)
title('AFT BEARING ACCELERATION (VERTICAL) ')
xlabel(['Time, sec - Fire 3 ',num2str(date)])
ylabel('Acceleration, in/sec^2')
grid

f = 10240*(1:20480)/40960;
pn = abs(fft(afty))*2/length(afty);
plot(f,pn(1:20480))
title('PSD OF AFT BEARING ACCELERATION (VERTICAL)')
xlabel(['Frequency, Hz ',num2str(date)])
ylabel('Acceleration, in/sec^2')
grid

% load and plot x direction
load afty.mat;
xsense = 10.24/1000;      % V/g
xscale = 1/(0.102);      % m/sec^2/g
xsense=xscale/xsense;
afty = xsense*afty;
tinc = 1/10240;
ttotal = (length(afty)-1)*tinc;
tx = 0:tinc:ttotal;

plot(tx,afty)
title('AFT BEARING ACCELERATION (HORIZONTAL) ')
xlabel(['Time, sec - Fire 3 ',num2str(date)])

```

```

ylabel('Acceleration, in/sec^2')
grid

f = 10240*(1:20480)/40960;
pn = abs(fft(aftx))*2/length(aftx);
plot(f,pn(1:20480))
title('PSD OF AFT BEARING ACCELERATION (HORIZONTAL)')
xlabel(['Frequency, Hz ',num2str(date)])
ylabel('Acceleration, in/sec^2')
grid

```

% load and plot x direction

```

load batx.mat;
xsense = 9.73/1000;      % V/g
xscale = 1/(0.102);      % m/sec^2/g
xsense=xscale/xsense;
batx = xsense*batx;
tinc = 1/10240;
ttotal = (length(batx)-1)*tinc;
tx = 0:tinc:ttotal;

plot(tx,batx)
title('MUZZLE RESTRAINT ACCELERATION (HORIZONTAL) ')
xlabel(['Time, sec - Fire 3 ',num2str(date)])
ylabel('Acceleration, in/sec^2')
grid

```

```

f = 10240*(1:20480)/40960;
pn = abs(fft(batx))*2/length(batx);
plot(f,pn(1:20480))
title('PSD OF MUZZLE RESTRAINT ACCELERATION (HORIZONTAL)')
xlabel(['Frequency, Hz ',num2str(date)])
ylabel('Acceleration, in/sec^2')
grid

```

% load and plot y direction

```

load baty.mat;
ysense = 9.63/1000;      % V/g

```

```

yscale = 1/(0.102);      % m/sec^2/g
ysense=yscale/ysense;
baty = ysense*baty;
tinc = 1/10240;
ttotal = (length(baty)-1)*tinc;
ty = 0:tinc:ttotal;

plot(ty,baty)
title('MUZZLE RESTRAINT ACCELERATION (VERTICAL) ')
xlabel(['Time, sec - Fire 3 ',num2str(date)])
ylabel('Acceleration, in/sec^2')
grid

f = 10240*(1:20480)/40960;
pn = abs(fft(baty))*2/length(baty);
plot(f,pn(1:20480))
title('PSD OF MUZZLE RESTRAINT ACCELERATION (VERTICAL)')
xlabel(['Frequency, Hz ',num2str(date)])
ylabel('Acceleration, in/sec^2')
grid

% load and plot x direction
load midx.mat;
xsense = 10.09/1000;      % V/g
xscale = 1/(0.102);      % m/sec^2/g
xsense=xsense/xsense;
midx = xsense*midx;
tinc = 1/10240;
ttotal = (length(midx)-1)*tinc;
tx = 0:tinc:ttotal;

plot(tx,midx)
title('MID HOUSING ACCELERATION (HORIZONTAL) ')
xlabel(['Time, sec - Fire 3 ',num2str(date)])
ylabel('Acceleration, in/sec^2')
grid

f = 10240*(1:20480)/40960;
pn = abs(fft(midx))*2/length(midx);

```

```

plot(f,pn(1:20480))
title('PSD OF MID HOUSING ACCELERATION (HORIZONTAL)')
xlabel(['Frequency, Hz ',num2str(date)])
ylabel('Acceleration, in/sec^2')
grid

% load and plot y direction
load midy.mat;
ysense = 10.02/1000;    % V/g
yscale = 1/(0.102);    % m/sec^2/g
ysense=yscale/ysense;
midy = ysense*midy;
tinc = 1/10240;
ttotal = (length(midy)-1)*tinc;
ty = 0:tinc:ttotal;

plot(ty,midy)
title('MID HOUSING ACCELERATION (VERTICAL) ')
xlabel(['Time, sec - Fire 3 ',num2str(date)])
ylabel('Acceleration, in/sec^2')
grid

f = 10240*(1:20480)/40960;
pn = abs(fft(midy))*2/length(midy);
plot(f,pn(1:20480))
title('PSD OF MID HOUSING ACCELERATION (VERTICAL)')
xlabel(['Frequency, Hz ',num2str(date)])
ylabel('Acceleration, in/sec^2')
grid

% load and plot z direction
load midz.mat;
zsense = 10.05/1000;    % V/g
zscale = 1/(0.102);    % m/sec^2/g
zsense=zscale/zsense;
midz = zsense*midz;
tinc = 1/10240;
ttotal = (length(midz)-1)*tinc;
tz = 0:tinc:ttotal;

```

```

plot(tz,midz)
title('MID HOUSING ACCELERATION (AXIAL) ')
xlabel(['Time, sec - Fire 3 ',num2str(date)])
ylabel('Acceleration, in/sec^2')
grid

```

```

f = 10240*(1:20480)/40960;
pn = abs(fft(midz))*2/length(midz);
plot(f,pn(1:20480))
title('PSD OF MID HOUSING ACCELERATION (AXIAL)')
xlabel(['Frequency, Hz ',num2str(date)])
ylabel('Acceleration, in/sec^2')
grid

```

```

% load and plot signal

```

```

load sig.mat;
tinc = 1/10240;
ttotal = (length(sig)-1)*tinc;
ts = 0:tinc:ttotal;

```

```

plot(ts,sig)
title('FIRING SIGNAL ')
xlabel(['Time, sec - Fire 3 ',num2str(date)])
ylabel('Acceleration, in/sec^2')
grid

```

APPENDIX D. THRESHOLD.M

This appendix contains the MATLAB code, THRESHOLD.m. It sets a limit value to determine the first occurrence of an acceleration magnitude. THRESHOLD.m returns the bin number when the limit is exceeded. This gives a rough estimate of the time of the first round fired. This estimate is used to calculate a better initial firing time with CROSSCORR.m.

```
% Determine when the first bullet is fired.
```

```
% threshold.m
```

```
clear ;
```

```
plt;
```

```
load batx3.txt;
```

```
threshold=0.25;
```

```
for i=1:12288
```

```
if batx3(i) > abs(threshold)
```

```
bx=i;
```

```
break
```

```
end
```

```
end
```

```
load baty3.txt;
```

```
for i=1:12288
```

```
if baty3(i)> abs(threshold)
```

```
by=i;
```

```
break
```

```
end
```

```
end
```

```
load aftx3.txt;
```

```
for i=1:12288
```

```
if aftx3(i)> abs(threshold)
```

```
ax=i;
```

```
break
```

```
end
```

```
end
```

```
load afty3.txt;
```

```
for i=1:12288
```

```
if afty3(i)> abs(threshold)
```

```
ay=i;
```

```
break
```

```
end
```

```
end
```

```
load midx3.txt;
```

```
for i=1:12288
```

```
if midx3(i)> abs(threshold)
```

```
mx=i;
```

```
break
```

```
end
```

```
end
load midy3.txt;
for i=1:12288
if midy3(i)> abs(threshold)
my=i;
break
end
end
load midz3.txt;
for i=1:12288
if midz3(i)> abs(threshold)
mz=i;
break
end
end
```


**APPENDIX E. CALIBRATION CERTIFICATES FOR THE QUARTZ SHEAR
MODE ICP ACCELEROMETERS USED FOR DATA COLLECTION ON THE
PHALANX GUN SYSTEM.**

This appendix contains the calibration charts for the Series 353 accelerometers.

Table E-1 summarizes the accelerometer set up for 31 May 1994.

Accelerometer			
Model	Serial Number	Location	Direction
J353B03	SN 5966	Mid Housing	Axial
J353B03	SN 5967	Mid Housing	Vertical
J353B03	SN 5968	Mid Housing	Horizontal
J353B03	SN 9319	Aft Bearing	Horizontal
J353B03	SN 5969	Aft Bearing	Vertical
353B03	SN11851	Muzzle Restraint	Horizontal
353B03	SN11850	Muzzle Restraint	Vertical

Table E-1, 31 May 1994 Accelerometer Set Up

Calibration Certificate

Excluded Period

Per ISA-RP37.2

Model No. J353B03

Serial No. 5966

PO No. _____ Customer _____

Calibration traceable to NIST thru Project No. 822/251101-93

ICP® ACCELEROMETER

with built-in electronics

Calibration procedure is in compliance with MIL-STD-45662A and traceable to NIST.

CALIBRATION DATA

Voltage Sensitivity **10.09** mV/g
 Transverse Sensitivity **1.4** %
 Resonant Frequency **49** kHz
 Time Constant **0.5** s
 Output Bias Level **8.9** V

KEY SPECIFICATIONS

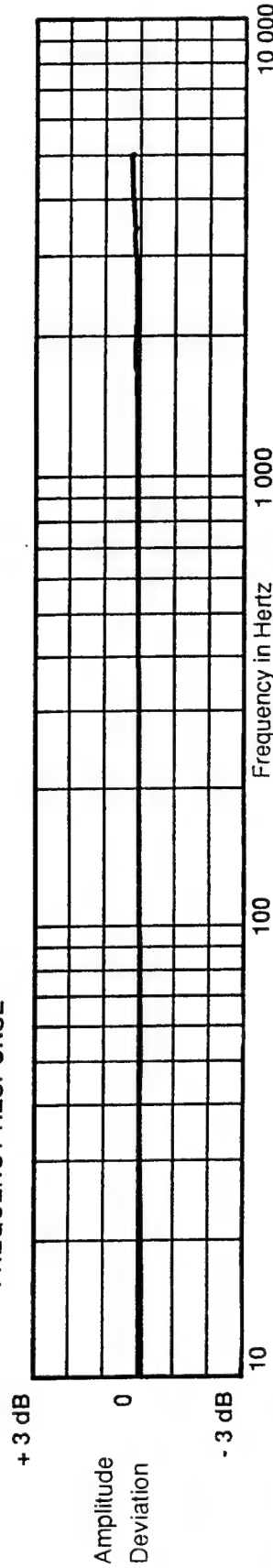
Range **500** ± g
 Resolution **0.01** g
 Temp. Range **-65/+250** °F

METRIC CONVERSIONS:
 $\text{ms}^{-2} = 0.102 \text{ g}$
 $^{\circ}\text{C} = 5/9 \times (^{\circ}\text{F} - 32)$

Reference Freq.

Frequency	Hz	10	15	30	50	100	300	500	1000	3000	5000	
Amplitude Deviation	%	-1.3	-1.2	-1.2	-1.2	-1.2	-1.2	-1.2	-1.2	-1.2	-1.2	

FREQUENCY RESPONSE



PCB

Piezotronics, Inc. 3425 Walden Avenue Depew, NY 14043-2495 USA

716-684-0001

Date 2/8/94

Calibrated by Di. Hoyle

CODE: CC-ENG

Calibration Certificate

Model No. **J353B03**

Serial No. **5967**

PO No. _____ Customer _____

Calibration traceable to NIST thru Project No. **822/251101-93**

Per ISA-RP37.2

ICP® ACCELEROMETER

with built-in electronics

Calibration procedure is in compliance with MIL-STD-45662A and traceable to NIST.

CALIBRATION DATA

Voltage Sensitivity **10.02** mV/g
 Transverse Sensitivity **0.9** %
 Resonant Frequency **47** kHz
 Time Constant **0.7** s
 Output Bias Level **8.8** V

KEY SPECIFICATIONS

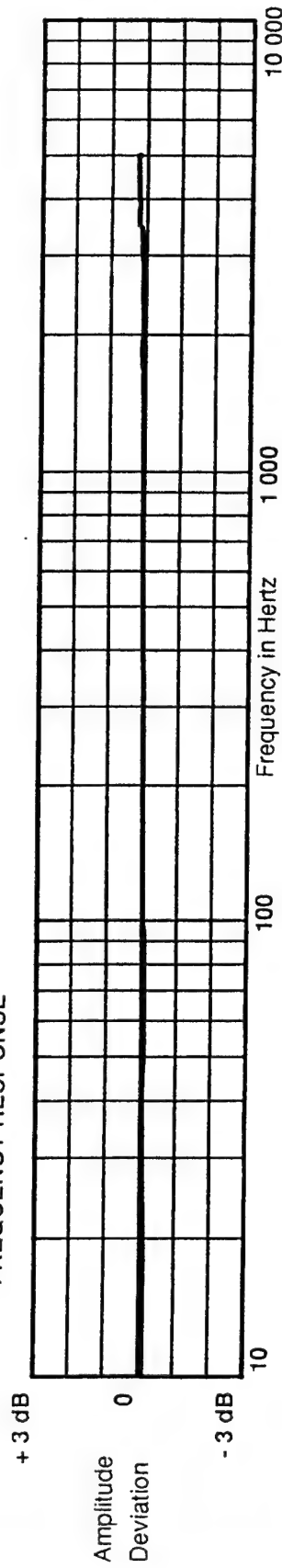
Range **500** ± g
 Resolution **0.01** g
 Temp. Range **-65/+250** °F

METRIC CONVERSIONS:
 ms⁻² = 0.102 g
 °C = 5/9 x (°F - 32)

Reference Freq.

Frequency	Hz	10	15	30	50	100	300	500	1000	3000	5000	
Amplitude Deviation	%	-1.0	-1.1	-1.5	-1.7	0.0	.3	.6	.9	1.7	3.0	

FREQUENCY RESPONSE



PCB

Piezotronics, Inc. 3425 Walden Avenue Depew, NY 14043-2495 USA

716-684-0001

Date **2/8/94**

Calibrated by _____

CODE CC-ENG

Calibration Certificate

Per ISA-RP37.2

Model No. **J353803**

Serial No. **5968**

PO No. _____ Customer _____

Calibration traceable to NIST thru Project No. **822/251101-93**

ICP® ACCELEROMETER

with built-in electronics

Calibration procedure is in compliance with MIL-STD-45662A and traceable to NIST.

CALIBRATION DATA

Voltage Sensitivity **10.05** mV/g
 Transverse Sensitivity **1.3** %
 Resonant Frequency **43.5** kHz
 Time Constant **0.7** s
 Output Bias Level **8.4** V

KEY SPECIFICATIONS

Range **500** ± g
 Resolution **0.01** g
 Temp. Range **-65/+250** °F

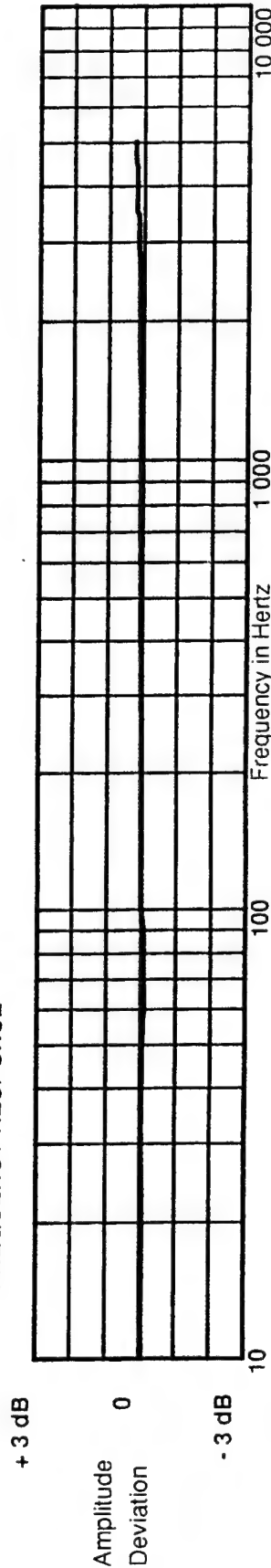
METRIC CONVERSIONS:

ms⁻² = 0.102 g
 °C = 5/9 x (°F - 32)

Reference Freq.

Frequency	10	15	30	50	100	300	500	1000	3000	5000	
Amplitude Deviation %	-0.9	-1.1	-0.5	-0.7	0.0	0.3	0.7	0.9	1.8	2.8	

FREQUENCY RESPONSE



PCB

Piezotronics, Inc. 3425 Walden Avenue Depew, NY 14043-2495 USA

716-684-0001

Date **2/21/94**

Calibrated by *M. Ruchalski*

CODE: CC-ENG

Calibration Certificate

Per ISA-RP37.2

Model No. J353B03

Serial No. 5969

PO No. _____ Customer _____

Calibration traceable to NIST thru Project No. 822/251101-93

ICP® ACCELEROMETER

with built-in electronics

Calibration procedure is in compliance with
MIL-STD-45662A and traceable to NIST.

CALIBRATION DATA

Voltage Sensitivity 10.25 mV/g

Transverse Sensitivity 0.8 %

Resonant Frequency 48 kHz

Time Constant 1.3 s

Output Bias Level 8.3 V

KEY SPECIFICATIONS

Range 500 ±g

Resolution 0.01 g

Temp. Range -65/+250 °F

METRIC CONVERSIONS:

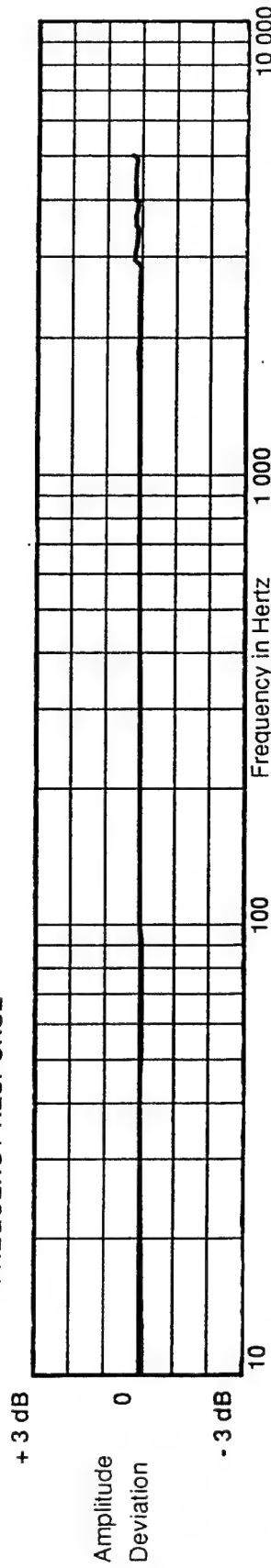
ms⁻² = 0.102 g

°C = 5/9 x (°F -32)

Reference Freq.

Frequency	Hz	10	15	30	50	100	300	500	1000	3000	5000
Amplitude Deviation	%	-1.3	-1.0	-0.4	-0.8	0.0	0.0	0.3	0.5	2.4	3.1

FREQUENCY RESPONSE



PCB

Piezotronics, Inc. 3425 Walden Avenue Depew, NY 14043-2495 USA

716-684-0001

Date 2/23/94

Calibrated by Ron Burke

CODE: CC-ENG

Calibration Certificate

Per ISA-RP37.2

Model No. **J353B03**

Serial No. **9319**

PO No. _____ Customer _____

Calibration traceable to NIST thru Project No. **822/251101-93**

ICP® ACCELEROMETER
with built-in electronics

Calibration procedure is in compliance with
MIL-STD-45662A and traceable to NIST.

CALIBRATION DATA

Voltage Sensitivity **10.24** mV/g
Transverse Sensitivity **1.5** %
Resonant Frequency **49.5** kHz
Time Constant **0.9** s
Output Bias Level **8.4** V

KEY SPECIFICATIONS

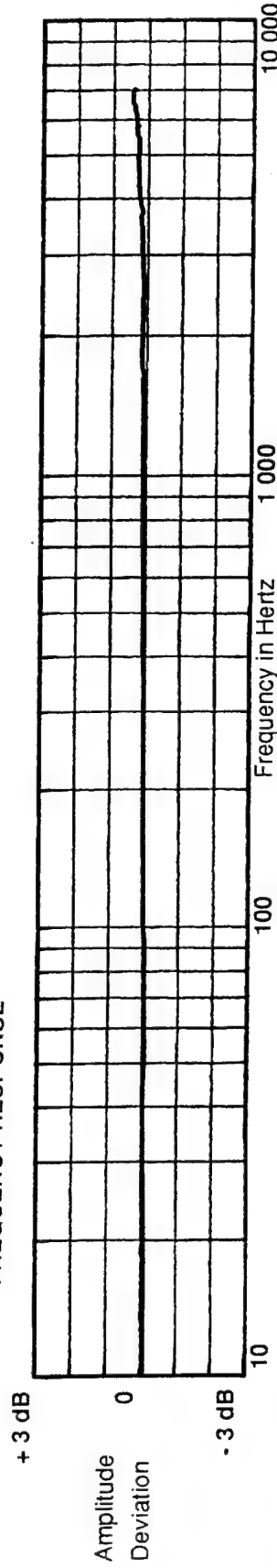
Range **500** ± g
Resolution **0.01** g
Temp. Range **-65/+250** °F

METRIC CONVERSIONS:
ms⁻² = 0.102 g
°C = 5/9 x (°F - 32)

Reference Freq.

Frequency	Hz	10	15	30	50	100	300	500	1000	3000	5000	
Amplitude Deviation	%	-0.9	-1.2	-0.5	-0.8	0.0	0.0	0.5	0.9	1.7	3.0	

FREQUENCY RESPONSE



PCB

Piezotronics, Inc. 3425 Walden Avenue Depew, NY 14043-2495 USA

716-684-0001

Calibrated by J. Redmond Date **1/25/94**

CODE CC-ENG

Calibration Certificate

3.20-32004

Model No. J353B04
 Serial No. 11850
 PO No. _____ Customer _____
 Calibration traceable to NIST thru Project No. 822/253168

ICP® ACCELEROMETER
 with built-in electronics

Calibration procedure is in compliance with
 MIL-STD-45662A and traceable to NIST.

CALIBRATION DATA

Voltage Sensitivity **9.63** mV/g
 Transverse Sensitivity **1.4** %
 Resonant Frequency **51.5** kHz
 Time Constant **0.8** s
 Output Bias Level **8.6** V

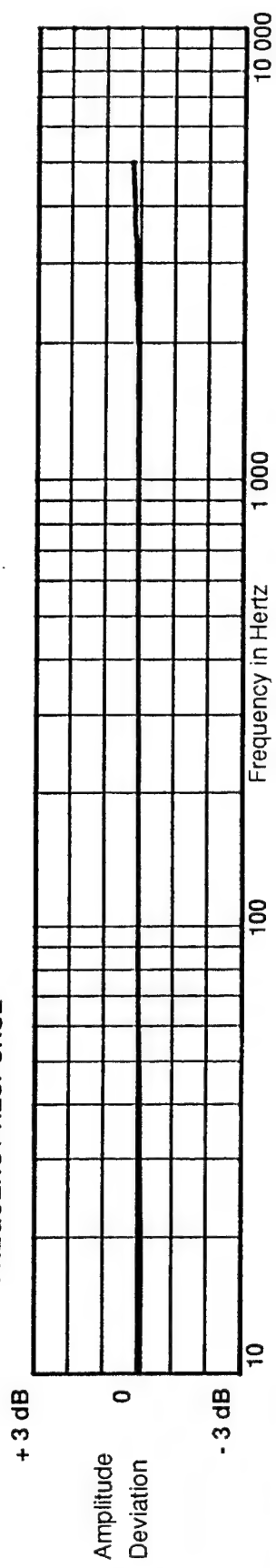
KEY SPECIFICATIONS

Range **500** ± g
 Resolution **0.01** g
 Temp. Range **-65/+250** °F
 METRIC CONVERSIONS:
 ms⁻² = 0.102 g
 °C = 5/9 x (°F -32)

91 Reference Freq.

Frequency	Hz	10	15	30	50	100	300	500	1000	3000	5000	
Amplitude Deviation	%	-0.9	-1.1	-0.7	-0.3	0.0	0.4	0.6	0.8	1.5	2.8	

FREQUENCY RESPONSE



Piezotronics, Inc. 3425 Walden Avenue Depew, NY 14043-2495 USA
 716-684-0001

Calibrated by J. Chadwick
 Date 5/20/94
 CODE: CC-ENG

Calibration Certificate

Per ISA-RP37.2

Model No. **J353B04**

Serial No. **11851**

PO No. _____ Customer _____

Calibration traceable to NIST thru Project No. **822/253168**

ICP® ACCELEROMETER

with built-in electronics

Calibration procedure is in compliance with MIL-STD-45662A and traceable to NIST.

CALIBRATION DATA

Voltage Sensitivity **9.73** mV/g
 Transverse Sensitivity **3.7** %
 Resonant Frequency **51** kHz
 Time Constant **0.5** s
 Output Bias Level **8.7** V

KEY SPECIFICATIONS

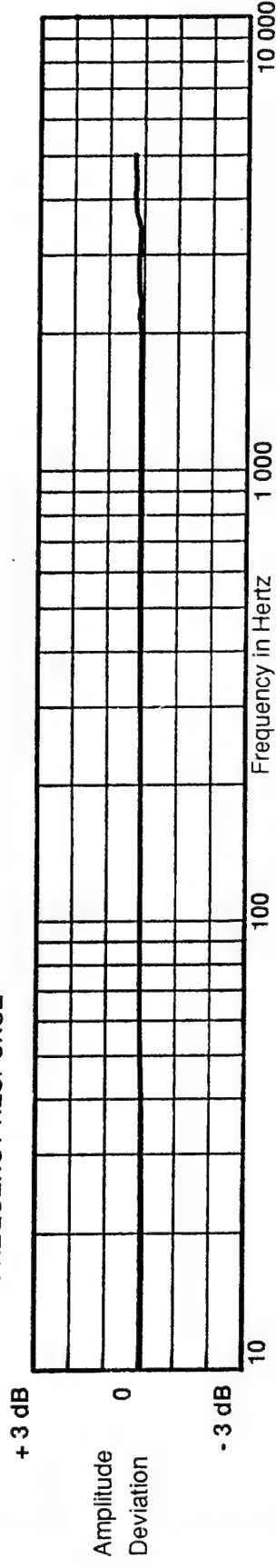
Range **500** ± g
 Resolution **0.01** g
 Temp. Range **-65/+250** °F
 METRIC CONVERSIONS:
 ms⁻² = 0.102 g
 °C = 5/9 x (°F - 32)

92

Reference Freq.

Frequency	Hz	10	15	30	50	100	300	500	1000	3000	5000	
Amplitude Deviation	%	-0.8	-1.0	-0.7	-0.2	0.0	0.4	0.7	0.6	1.3	3.1	

FREQUENCY RESPONSE



PCB

Piezotronics, Inc. 3425 Walden Avenue Depew, NY 14043-2495 USA

716-684-0001

Calibrated by *J. Chadwick* Date **5/20/94**

CODE: CC-ENG

APPENDIX F. TIME DOMAIN WINDOW

This appendix contains the MATLAB code used to apply a time domain window to the acceleration. The function uses a normalized half cosine and half sine and multiplies it by the acceleration in the time domain.

```

function y = timwin(t1,t2,t3,t4,timdat,xdat);
% timwin.m
% Create a window that when applied to a data it will set zeros up
% to an initial time, then apply half a cosine and increase the
% value from zero to one then stay at one until a certain time
% then decrease back to zero with half a cosine wave.

y=zeros(size(xdat));
ndx1=timndx(t1,timdat);
ndx2=timndx(t2,timdat);
ndx3=timndx(t3,timdat);
ndx4=timndx(t4,timdat);

y(ndx2:ndx3,1) = ones(ndx3-ndx2+1,1);

denom=ndx2-ndx1;
for i=ndx1:ndx2
    y(i,1)=0.5*(1-cos(pi*(i-ndx1)/denom));
end

denom=ndx4-ndx3;
for i=ndx3:ndx4
    y(i,1)=0.5*(1+cos(pi*(i-ndx3)/denom));
end

y = y .* xdat;

```

APPENDIX G. FREQUENCY DOMAIN WINDOW

This appendix contains the MATLAB code used to apply a frequency domain window to the FFT. The function uses a normalized half cosine and half sine and multiplies it by the FFT in the frequency domain.

```

function y = freqwin(f1,f2,fdat,fftdat);
% freqwin.m
% Create a window that when applied to fft data it will set zeros
% up to an initial time, then apply half a cosine and increase the
% value from zero to one then stay at one until a certain time
% then decrease back to zero with half a cosine wave.

y=zeros(size(fftdat));
lenfdat=length(fdat);
finc=0.25;
ndx1=round(f1/finc)+1;
ndx2=round(f2/finc)+1;
ndx3=lenfdat-ndx2+2;
ndx4=lenfdat-ndx1+2;

y(ndx2:ndx3,1) = ones(ndx3-ndx2+1,1);

denom=ndx2-ndx1;
for i=ndx1:ndx2
    y(i,1)=0.5*(1-cos(pi*(i-ndx1)/denom));
end

denom=ndx4-ndx3;
for i=ndx3:ndx4
    y(i,1)=0.5*(1+cos(pi*(i-ndx3)/denom));
end

y = y .* fftdat;

```

APPENDIX H. CUBIC SMOOTHING SPLINES CODE

CSAPSXY.m is code that applies the CSAPS.m command of the Splines Toolbox, to the muzzle restraint displacement curves for the horizontal and vertical directions. It plots the displacement curve obtained from direct integration along with the cubic spline approximation.

```

% Calculate the Cubic Smoothing of the Muzzle Restraint Displacement
% (Horizontal) obtained from the integration algorithm.
% Using MatLab csaps function
% Repeat for a third p value

clear all;
plt;

load time;
load disintx;

t0=cputime;

% Plot the Muzzle Restraint Displacement (Horizontal) vs Time

figure(1)
plot(time,disx)
title('Muzzle Restraint Displacement (Horizontal)')
xlabel(['Time, sec - Fire 3 ',num2str(date)])
ylabel('Displacement, m')
grid
hold on

% Calculate and plot the Cubic Spline for the third p value
% Plot and compare to the Displacement curve obtained from the integration
% Increase the Cubic Spline Parameter by 1000000000

epsilon=max(diff(time))^3/16;
p3x=1/(1+epsilon*1000000000);
p3x

fdix12=csaps(time,disx,p3x,time);
ddix12=disx-fdix12;
save fdix12 fdix12;
save ddix12 ddix12;

% Plot the Cubic Smoothing Spline and print
plot(time,fdix12,'r')
text(1,1.1, 'Cubic Spline Parameter epsilon*10000000')

```

```

plot(time,ddisx12,'g')
print

figure (2)
plot(time,ddisx12)
title('Muzzle Restraint Displacement (Horizontal)')
xlabel(['Time, sec - Fire 3 ',num2str(date)])
ylabel('Displacement, m')
grid

e1=(cputime-t0)/3600

% Calculate the Cubic Smoothing of the Muzzle Restraint Displacement
% (Vertical) obtained from the integration algorithm.
% Using MatLab csaps function
% Repeat for a third p value

t3=cputime;

load disinty;

% Plot the Muzzle Restraint Displacement (Vertical) vs Time
figure (3)
plot(time,disy)
title('Muzzle Restraint Displacement (Vertical)')
xlabel(['Time, sec - Fire 3 ',num2str(date)])
ylabel('Displacement, m')
grid
hold on

% Calculate and plot the Cubic Spline for the third p value
% Plot and compare to the Displacement curve obtained from the integration
% Increase the Cubic Spline Parameter by 1000000000

epsilon=max(diff(time))^3/16;
p3y=1/(1+epsilon*1000000000);
p3y

fdisy12=csaps(time,disy,p3y,time);

```

```

ddisy12=disy-fdisy12;
save fdisy12 fdisy12;
save ddisy12 ddisy12;

% Plot the Cubic Smoothing Spline and print
plot(time,fdisy12,'r')
text(1,2.1, 'Cubic Spline Parameter epsilon*10000000')
plot(time,ddisy12,'g')

figure (4)
plot(time,ddisy12)
title('Muzzle Restraint Displacement (Vertical)')
xlabel(['Time, sec - Fire 3 ',num2str(date)])
ylabel('Displacement, m')
grid

e3=(cputime-t3)/3600
ttotal=(cputime-t0)

```

LIST OF REFERENCES

1. Telephone conversation between Yuji Wilson, Port Hueneme, Naval Surface Warfare Center, Code 4121, and LT David Cela, Naval Postgraduate School, September 1994.
2. Wilson, Yuji, Port Hueneme Division, Naval Surface Warfare Center, Code 4121, Port Hueneme, California, 93043.
3. SA 390 Dynamic Signal Analyzer Specifications, Scientific Atlanta, San Diego, California, (619) 679- 6000.
4. Quartz Shear Mode ICP Accelerometer, Series 353, Operator's Manual, PCB Piezotronics, Inc, Depew, New York, (716) 684-0001.
5. Oehler System 82 Instructions, Oehler Reserach, Inc, Austin, Texas, (512) 327-6900.
6. Philips Model PM3384 DSO Service Manual, Fluke and Philips, Holland.
7. Garner, F. , "Hit Probability for Small and Medium Calibre Belt-Fed Cannon", *International Review*, pp. 1244-1249, November 1991.
8. Garner, F. , "Hit Probability for Small and Medium Calibre Belt-Fed Cannon", *International Review*, pp. 1244-1249, November 1991.
9. Garner, F. , "Hit Probability for Small and Medium Calibre Belt-Fed Cannon", *International Review*, pp. 1244-1249, November 1991.
10. MATLAB User's Guide for Macintosh Computers, The Math Works, Inc, Natick, Massachusetts, (508) 653-2297
11. Memorandum from Robert Mihata, Instrumentation Group, Signal Processing System, 29 July 1994, Scientific Atlanta, San Diego, California, (619) 679-6000.
12. MATLAB Signal Processing Toolbox, p. 2-90 2-92, The Math Works, Inc, Natick, Massachusetts, (508) 653-2297
13. MATLAB Signal Processing Toolbox, p. 2-226 2-228, The Math Works, Inc, Natick, Massachusetts, (508) 653-2297
14. MATLAB Signal Processing Toolbox, p. 2-77, The Math Works, Inc, Natick, Massachusetts, (508) 653-2297

15. MATLAB Signal Processing Toolbox, p. 2-90, The Math Works, Inc, Natick, Massachusetts, (508) 653-2297
16. MacNeil, Donald P., *Normal Modes of Oscillation of the Vulcan PHALANX Close-In Weapon Syatem*, Naval Postgraduate School, Master's Thesis, June 1993.
17. MATLAB, Spline Toolbox, p. 1-3, The Math Works, Inc, Natick, Massachusetts, (508) 653-2297.
18. MATLAB, Spline Toolbox, p. 1-3, The Math Works, Inc, Natick, Massachusetts, (508) 653-2297.
19. MATLAB, Spline Toolbox, p. 2-13, The Math Works, Inc, Natick, Massachusetts, (508) 653-2297
20. MATLAB, Spline Toolbox, p.2-13, The Math Works, Inc, Natick, Massachusetts, (508) 653-2297

INITIAL DISTRIBUTION LIST

		No. Copies
1.	Defense Technical Information Center Cameron Station Alexandria, Virginia 22304-6145	2
2.	Library, Code 52 Naval Postgraduate School Monterey, California 93943-5002	2
3.	Professor William B. Colson Code PH/Cw Chairman, Department of Physics Naval Postgraduate School Monterey, California 93943-5000	2
4.	Professor Steven R. Baker Code PH/Ba Department of Physics Naval Postgraduate School Monterey, California 93943-5000	2
5.	Yuji Wilson Port Hueneme Division Naval Surface Warfare Center Code 4121 Port Hueneme, California 93043	1
6.	Mike Hatch 2163 Woodleaf Way Mountain View, California 94040	1
7.	LT David Cela 29 Fairlawn Street Ho-Ho-Kus, New Jersey 07431	2
8.	Capt Robert J. Hansberry 215 Robinson Avenue Newburgh, New York 12550	1